AD-A284 890

**US Army Corps
of Engineers**
Waterways Experiment
Station

Water Quality Research Program

Self-Aerated Flow on Corps
of Engineers Spillways

by   *Steven C. Wilhelms*

John S. Gulliver
University of Minnesota

DTIC
ELECTE
SEP 2 7 1994
S G D

Approved For Public Release; Distribution Is Unlimited

94 9 2   073

94-30766

Water Quality
Research Program

Self-Aerated Flow on Corps of Engineers Spillways

by Steven C. Wilhelms

U.S. Army Corps of Engineers
Waterways Experiment Station
3909 Halls Ferry Road
Vicksburg, MS   39180-6199

John S. Gulliver

St. Anthony Falls Hydraulic Laboratory
Department of Civil and Mineral Engineering
University of Minnesota
Minneapolis, MN   55455

Accesion For		
NTIS CRA&I		☒
DTIC TAB		☐
Unannounced		☐
Justification		
By		
Distribution /		
Availability Codes		
Dist	Avail and / or Special	
A-1		

Final Report

DTIC QUALITY INSPECTED 3

US Army Corps
of Engineers
Waterways Experiment
Station

Contents

List of Figures

Preface

The work reported herein was conducted as part of the Water Quality Research Program (WQRP), Work Unit 32369. The WQRP is sponsored by the Headquarters, U.S. Army Corps of Engineers (HQUSACE), and is assigned to the U.S. Army Engineer Waterways Experiment Station (WES) under the purview of the Environmental Laboratory (EL). Funding was provided under Department of the Army Appropriation No. 96X3121, General Investigation. The WQRP is managed under the Environmental Resources Research and Assistance Programs (ERRAP), Mr. J. L. Decell, Manager. Mr. Robert C. Gunkel was Assistant Manager, ERRAP, for the WQRP. Technical Monitors during this study were Mr. Frederick B. Juhle, Mr. Rixie Hardy, and Dr. John Bushman, HQUSACE.

The research reported herein was conducted by the Hydraulics Laboratory (HL), WES, and the St. Anthony Falls Hydraulic Laboratory (SAFHL) of the Department of Civil and Mineral Engineering, University of Minnesota. This report summarizes results of an investigation into the area of air entrainment at Corps of Engineers hydraulic structures.

This report was prepared by Mr. Steven C. Wilhelms of the Reservoir Water Quality Branch (RWQB), HL, and Dr. John S. Gulliver, SAFHL. Assistance in data analysis and report preparation was provided by Ms. Laurin I. Yates, RWQB, and Ms. Barbara A. Parsons, Hydraulic Structures Division (HSD). Special gratitude is expressed to Dr. John M. Killen, SAFHL, whose efforts formed a basis for the analysis presented herein. The effort was under the general direction of Messrs. Frank A. Herrmann, Jr., Director, HL, and Glenn A. Pickering, Chief, HSD, HL.

At the time of publication of this report, Director of WES was Dr. Robert W. Whalin. Commander was COL Bruce K. Howard, EN. Dr. Roger L. A. Arndt was Director, SAFHL.

This report should be cited as follows:

> Wilhelms, S. C., and Gulliver, J. S. (1994). "Self-aerated flow on Corps of Engineers spillways," Technical Report W-94-2, U.S. Army Engineer Waterways Experiment Station, Vicksburg, MS.

vi

Conversion Factors, Non-SI to SI Units of Measurement

Non-SI units of measurement used in this report can be converted to SI units as follows:

Multiply	By	To Obtain
cubic feet	0.02831685	cubic meters
degrees (angle)	0.01745329	radians
feet	0.3048	meters

1 Introduction

Background

Self-aeration is a phenomenon seen in high-velocity flows on a spillway or in a channel. The flow on the spillway turns frothy and white when self-aeration is initiated (Figure 1) because of entrained air. From studies of self-aerated spillway flows, it was concluded that the turbulent boundary layer, caused by the spillway surface, initiated air entrainment when its thickness was approximately the depth of flow. Keller, Lai, and Wood (1974) presented the definitions used today for the developing regions of aerated flow (Figure 2). The "point of inception" is the location where aeration starts, which is also where the turbulent boundary layer intersects the water surface. For some distance, the flow is developing, i.e., there is a net flux of air into the water. When the air bubbles are transported to their maximum depth in the water, the flow is considered fully aerated, but may continue to entrain more air and thus would be still developing. At some long distance along the spillway, uniform conditions are established. Thereafter, there is no change in the hydraulic or air transport characteristics.

The process of self-aeration in spillways and steep chutes has historically been of interest to hydraulic engineers because of the effects the entrained air has on the depth of flow. The amount of "bulking" of the flow is a necessary design parameter in determining the height of spillway or chute sidewalls. Engineers have also been interested in eliminating or minimizing cavitation damage to high-velocity spillways, chutes, and channels. To accomplish this, aerators have been designed to aspirate air into the flow. The location on the spillway where sufficient air from the self-aeration process becomes available to prevent or reduce the damage caused by cavitation is required by the design engineer when siting these aerators or determining if aerators are required. More recently, this highly aerated flow has been recognized for its gas transfer characteristics with the transfer of atmospheric gases (oxygen and nitrogen) into the water and the volatilization of toxic pollutants.

Many hydraulicians and experimentalists have examined the phenomenon of self-aerating flows on spillways and in high-velocity channels over the last six decades. Ehrenberger (1926) was the first to investigate the concentration

Figure 1. Self-aerated flow on an OGEE crest

and distribution of air in self-aerated flow. Straub and Anderson (1958) performed an award-winning experimental study of the distribution of air in self-aerated flow. More recently, Cain and Wood (1981) measured air concentration in the flow on the Aviemore Spillway in New Zealand. As recently as 1988, Ruze (1988) conducted laboratory experiments on self-aerated flow. Falvey and Ervine (1988) recently reviewed past work, discussed the hydrodynamic processes affecting aeration, and identified areas where understanding must be improved. It is hoped that the effort reported herein will aid in describing self-aeration.

Objective and Scope

The objective of this effort was to improve the description of self-aerated flow. Because entrained air contributes greatly to absorption of oxygen and the transfer of other gases and can significantly reduce cavitation damage, being able to estimate the amount of air entrained in spillway flows is important. To achieve this objective, the conceptual descriptions of the aeration process, proffered by past researchers,
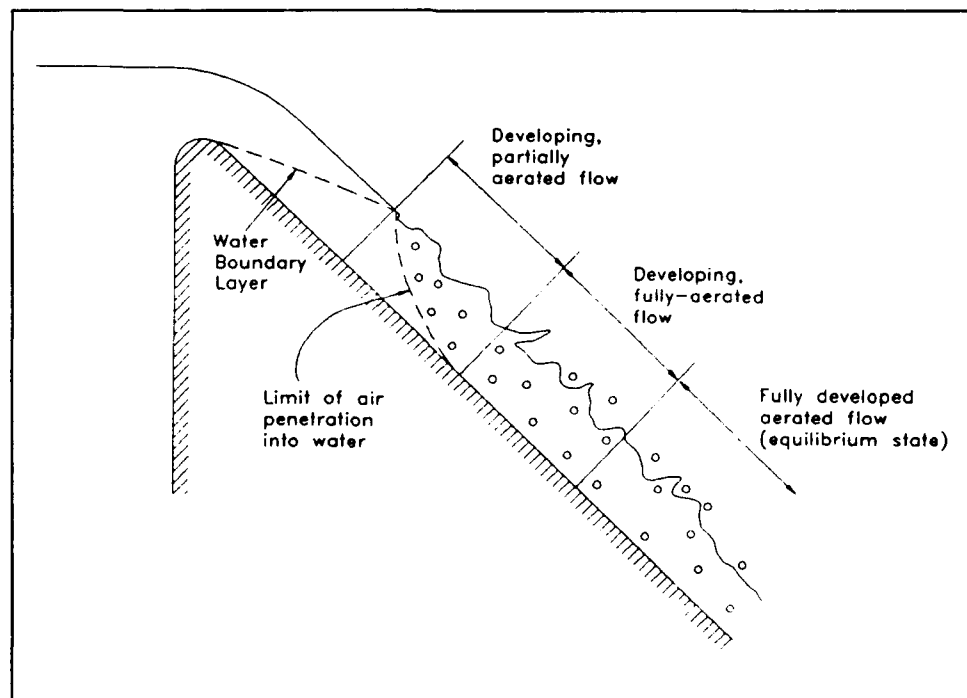
Figure 2. Region of developing flow (after Keller, Lai, and Wood 1974)

were closely examined. New concepts were proposed regarding the conceptual definition of entrained air. Data from selected past efforts were analyzed within this new framework to estimate the air entrainment at Corps of Engineers (CE) spillways.

Concepts and Theory

Historical perspective

Ehrenberger (1926) is usually cited as the first study of self-aeration in open-channel flow. Although not described in his paper, the hydraulic performance of the Rutz Works high-velocity chute was apparently unacceptable. It is presumed that the problem was related to the self-aeration phenomenon, where the entrained air caused the flow depth to be greater than expected and the side walls were too low. At that time, knowledge about self-aerated flow was essentially nonexistent, as Ehrenberger described the "...science of flow in steep chutes..." as "...an almost unexplored field...." The major contributions of Ehrenberger's effort were (a) recognition of the significant influence that entrained air has on hydraulic characteristics and (b) although not completely correct, the physical description of highly aerated flow, which was as follows: "At the top, droplets of water interspersed through air are first noticed. Below this layer, there is a layer consisting of a mixture of air and water, which in turn covers a layer of water containing individual air bubbles, and finally there is a layer of unaerated water adjacent to the bottom" (Figure 3). This "layered" description ultimately developed into the concept of a continuum of air/water from the bottom to the surface.

In a benchmark article on self-aerated flow, Straub and Anderson (1958) showed measurements of air concentration (Figure 4) that seemed to indicate that this was the case inasmuch as the air concentration varied in a continuous fashion over the depth of flow. They conducted extensive tests in a laboratory flume at slopes from 7.5 to 75 deg with unit discharges from 1.47 to 10.0 cfs.[1] In agreement with Ehrenberger's (1926) description, they conceptualized air-entrained flow as having an upper region, where water is transported with air, and a lower region, where air is transported with water.

Killen (1968), however, showed in high-speed photos taken during flume experiments in the midfifties, that the water surface remained "intact but very contorted" (Figure 5) with a very small quantity of flying droplets over the surface. Hence, a well-mixed continuum of increasing air and decreasing water over the depth did not appear to exist. This was in contrast to the entrainment concept proposed by Ehrenberger (1926) and Straub and Anderson (1958).

---

[1] A table of factors for converting non-SI units of measurement to SI units is presented on page vii.
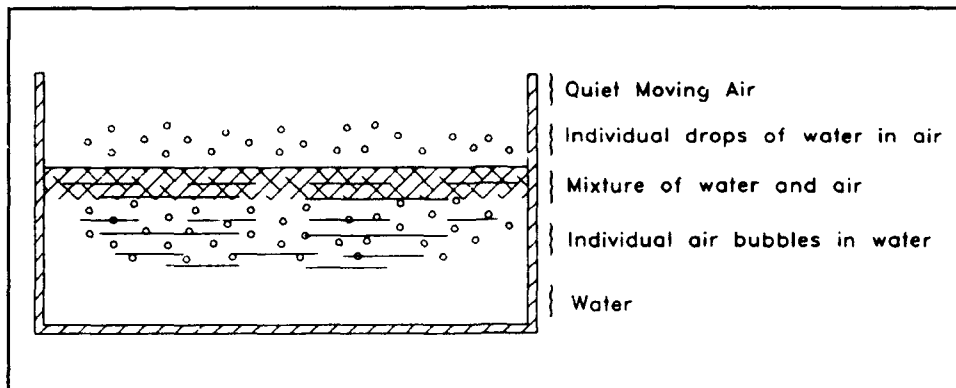
Figure 3. Ehrenberger's (1926) concept of air transport
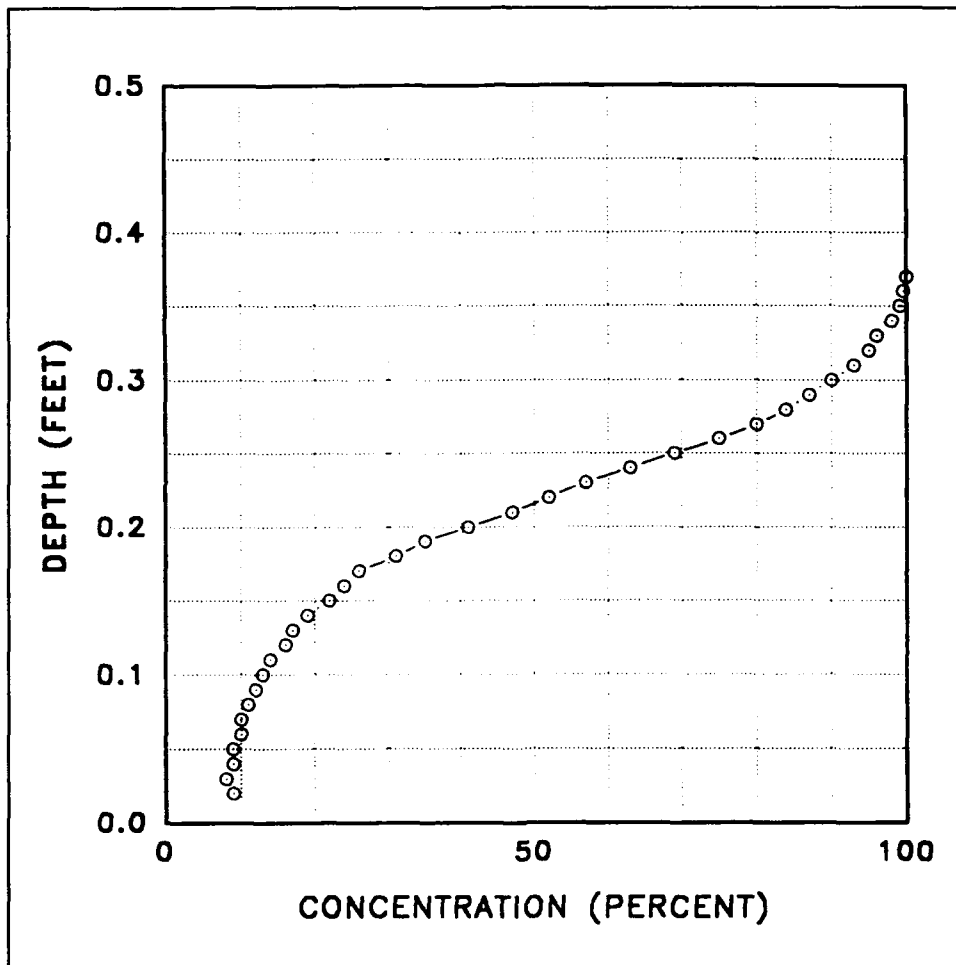
Figure 4. Air concentration distribution measured by Straub and Anderson (1958)
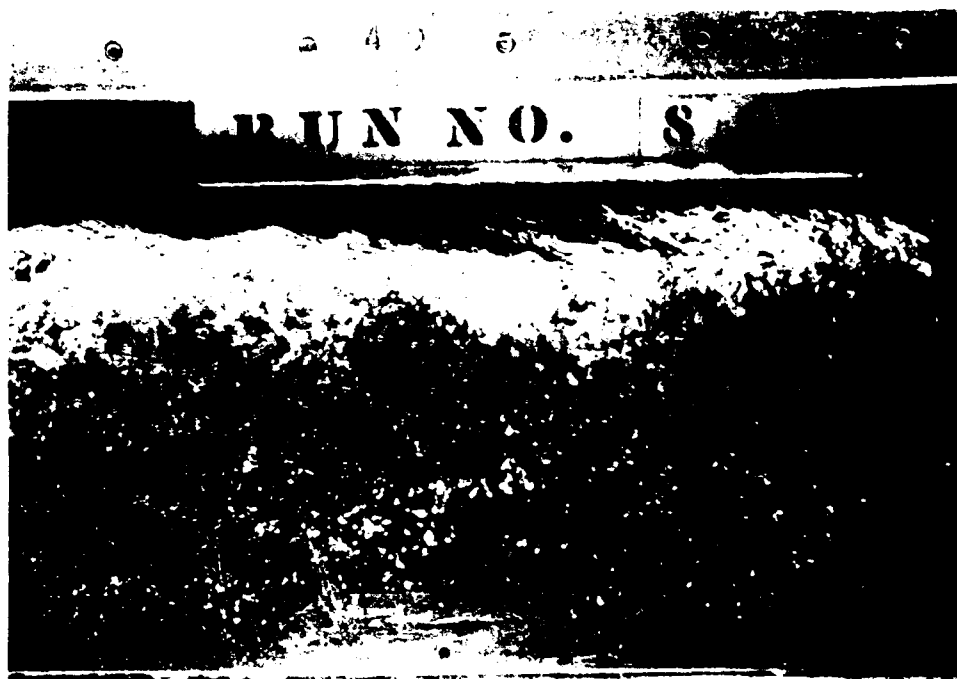
Figure 5. Water surface of self-aerated flow (Courtesy of St. Anthony Falls
Hydraulic Laboratory, University of Minnesota)

New concepts

Based upon Killen's (1968) observations, the concepts of "entrained" and
"entrapped" air (Figure 6) are introduced. Entrained air is being transported
along with the flow in the form of air bubbles that, at some point, have been
pulled into the flowing water through the process of air entrainment.
Entrapped air is the air above the water surface that is being transported
along with the flow because it is trapped in the surface roughness. Entrained
and entrapped air together are the "total conveyed air" being transported with
the flow, which, for past researchers, was defined as entrained air.

Obviously, for bulking interests, total conveyed air is of prime impor-
tance, and the differentiation of entrained and entrapped air is of no conse-
quence. However, for cavitation prevention, entrained air, i.e., air bubbles,
must be present at the spillway surface. Thus, in evaluating the potential for
cavitation prevention, entrained air must receive stronger consideration than
total conveyed air or entrapped air. For characterizing gas transfer on the
spillway face, the entrained air is of more significance than the entrapped air
because of the tremendous surface area available for transfer in a bubble
flow. When the flow plunges into a pool below the spillway, then the total
conveyed air will be important since most of the entrapped air will become
entrained at the spillway/pool plunge point.
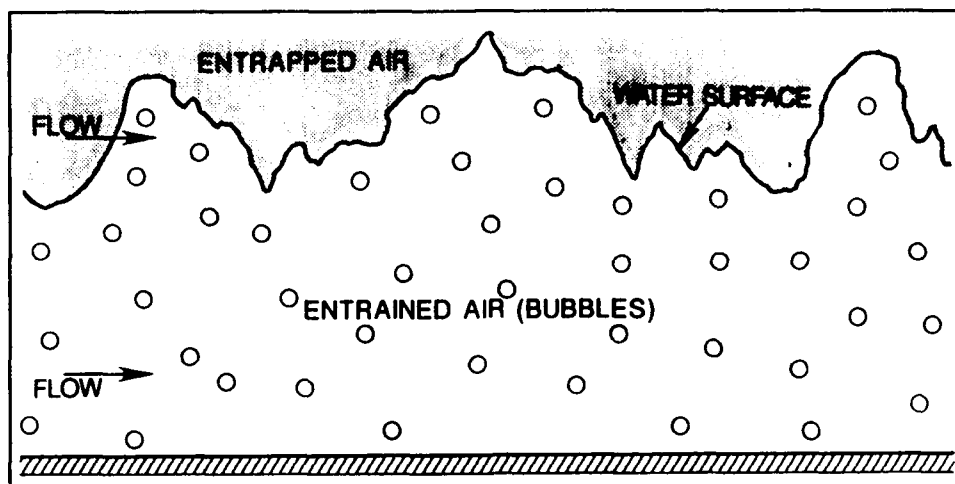
Figure 6. Concepts of entrained and entrapped air

Entrained air and gas transfer

The flux of a volatile gas, such as oxygen and nitrogen, across the airwater interface should be written as

$$J = k_L \left(C_s - C \right) = k_L D \tag{1}$$

where

J = mass flux rate per unit area

k_L = liquid film coefficient

C_s = saturation concentration[1]

C = ambient concentration in water

D = saturation deficit

---

[1]Henry's Law defines a "saturation concentration" as

$$C_s = H \, p$$

where

C_s = saturation concentration for gas

H = proportionality or equilibrium constant for gas

p = partial pressure of gas in the atmosphere

Henry's Law states that at a given temperature, a liquid can absorb an amount of gas that is proportional to the partial pressure of that gas in the overlying atmosphere. Thus, there exists an "equilibrated" state at the saturation concentration where the partial pressure of the gas in the water is equal to the partial pressure of the gas in the atmosphere.

Examination of this equation shows that if the water is undersaturated $(C < C_s)$, then gas will be absorbed across the interface. If the water is supersaturated $(C > C_s)$, there will be a net movement of gas out of the water. The liquid film coefficient is a measure of the ease with which dissolved gases move across the air-water interface. This transfer coefficient is dependent on the internal structure or ordering of water molecules and the breakdown of that structure by turbulent mixing.

The rate of change in concentration for a volume of water can be determined by calculating the total rate of mass flux into a water body. The mass flux per unit area (Equation 1) must be multiplied by the surface area and divided by the volume of water giving the following:

$$\frac{dC}{dt} = \frac{JA}{V} = k_L \frac{A}{V}(C_s - C) = -\frac{dD}{dt} \tag{2}$$

where

$\dfrac{dC}{dt}$ = rate of change of concentration

A = surface area over which transfer occurs

V = volume of the water body

$\dfrac{dD}{dt}$ = rate of change of the saturation deficit

Over the travel time through the structure from upstream to downstream, Equation 2 can be integrated to the following mathematical model of gas transfer:

$$\frac{D_f}{D_i} = \exp\left(-k_L \frac{A}{V} t\right) = \exp\left(-K_2 t\right) \tag{3}$$

where

D_f, D_i = final and initial oxygen deficits, respectively

t = elapsed time from initial to final deficits

K_2 = reaeration or oxygen transfer coefficient

From the perspective of flow in a stream reach or through some control volume, the initial and final deficits would be the upstream and downstream deficits, respectively, and the elapsed time would be the time of flow from the upstream to downstream locations.

Several physical processes or effects are described by the mathematical formulation presented above. The impacts of these processes are governed mainly by the fluid mechanics and flow conditions. The following provides a general description of these processes and their effect on gas transfer.

a. *Increased mass transfer because of increased interfacial area resulting from air that has been entrained into the flow.* When air is entrained into the flow either from the surface or at a plunge point, the surface area available for gas transfer can increase dramatically. Gulliver, Thene, and Rindels (1990) estimated that entrained air because of free surface aeration increased the air-water surface area by a factor of nearly 500 compared with the unit area of surface exposed to the atmosphere in a 0.3-ft-deep spillway flow. Thus, if air is entrained, gas transfer will increase significantly for a given flow condition.

b. *Turbulent mixing at the water surface and within the body of the flowing water.* It would seem logical that the rate of turbulent mixing would significantly affect gas transfer because of the concept of water-surface renewal (water surface that is swept away from the surface and "renewed" with water from below) (Danckwerts 1951) causing increased gas transfer.

c. *Mass transfer enhancement by pressure resulting from the hydrostatic pressure of tailwater.* In addition to the contribution that air bubbles make to the air-water surface area, absorption of atmospheric gases from the air bubbles can be increased because of the increased pressure that the bubbles experience as they are transported into the depth of the structure's stilling basin. Increased hydrostatic pressure on entrained air causes an increase in the saturation concentration (see Equations 1 and 2) and thereby increases the saturation deficit (Wilhelms et al. 1987; Wilhelms and Gulliver 1990).

Each of the above is included either directly or indirectly in Equation 3. Turbulent mixing is characterized by the liquid film coefficient k_L. The effects of pressure on mass transfer results in an increased saturation concentration and thus, an increased saturation deficit D. The increase in mass transfer because of greater interfacial area because of entrained air bubbles is included in the interfacial area term A.

Entrained air and cavitation

The damaging effects of cavitation can be minimized or eliminated if sufficient air can be introduced to the flow upstream of and near the cavitating surface. For spillways, this problem has led to the design and installation of aerators on the spillway slope. These aerators may be sited more effectively if the location can be estimated where sufficient air from self-aeration reaches the spillway face to prevent cavitation damage. In addition, oversizing aerators (designing the aerator to introduce more air than the flow can carry) will not

result in more entrained air being transported, because the carrying capacity of the flow would be exceeded and excess air would be lost to the atmosphere.

Peterka (1953) conducted water tunnel experiments and determined that damage caused by cavitation could be minimized if an air concentration of at least 8 percent was introduced upstream of and near the cavitating surface. Thus, in developing aerated flow on a spillway, once the entrained air near the spillway surface reaches 8 percent, then the placement of an aerator is unwarranted. However, if cavitation is occurring upstream of this location, then aerators may be needed to help decrease cavitation damage.

2   Data and Analysis

Analysis of Killen's Observations

Separation of entrained and entrapped air

Most data collected in experimental studies of aerated flow consist of
concentration profiles of total conveyed air (Straub and Anderson 1958; Killen
1968). To make use of the entrained or entrapped air concepts, each must be
separated from total conveyed air. Killen (1968) was interested in the surface
characteristics of aerated flow and measured "surface roughness" in addition
to the total conveyed air concentration profile. He measured the total
conveyed air (entrapped and entrained air) content with an air concentration
probe (Lamb and Killen 1950). He characterized the surface with a
conduction probe that dipped in and out of the surface roughness as flow
passed the probe. The signal from the probe was maximum when it was in
the water and at zero when out of the water. At a given elevation above the
flume bottom, the signal from the probe showed that it was in the water (in
contact with a wave on the rough surface) some portion of time and out of the
water (between the roughness of the surface) for the remainder of time spent
at that elevation. Further analysis of these observations showed that the
time-average of this signal was, in reality, the concentration of air that was
trapped within the surface roughness and transported along with the flow, i.e.,
the entrapped air. The difference between the total conveyed air concentration
and the entrapped air concentration is the entrained air concentration.

Killen collected these data at several locations along the length of a
1.5-ft-wide flume for several flow rates and two slopes. An example of his
observations is shown in Figure 7 for a unit discharge q of 4.3 ft^3/sec per ft,
channel slope θ of 30 deg, and a distance X along the flume of 34 ft. All of
Killen's observed profiles are presented in graphical form in Appendix A;
corresponding digital profile data are presented in Appendix B. The total
conveyed air at the channel bottom represents the concentration of entrained
air, since the water surface roughness does not extend to the bottom. At the
lower limit of roughness penetration, the total conveyed air consists only of
entrained air bubbles. However, above this limit, entrapped and entrained air
contribute to total conveyed air. Entrained air gradually decreases in
proportion to entrapped air until the entrapped air and total conveyed air

10
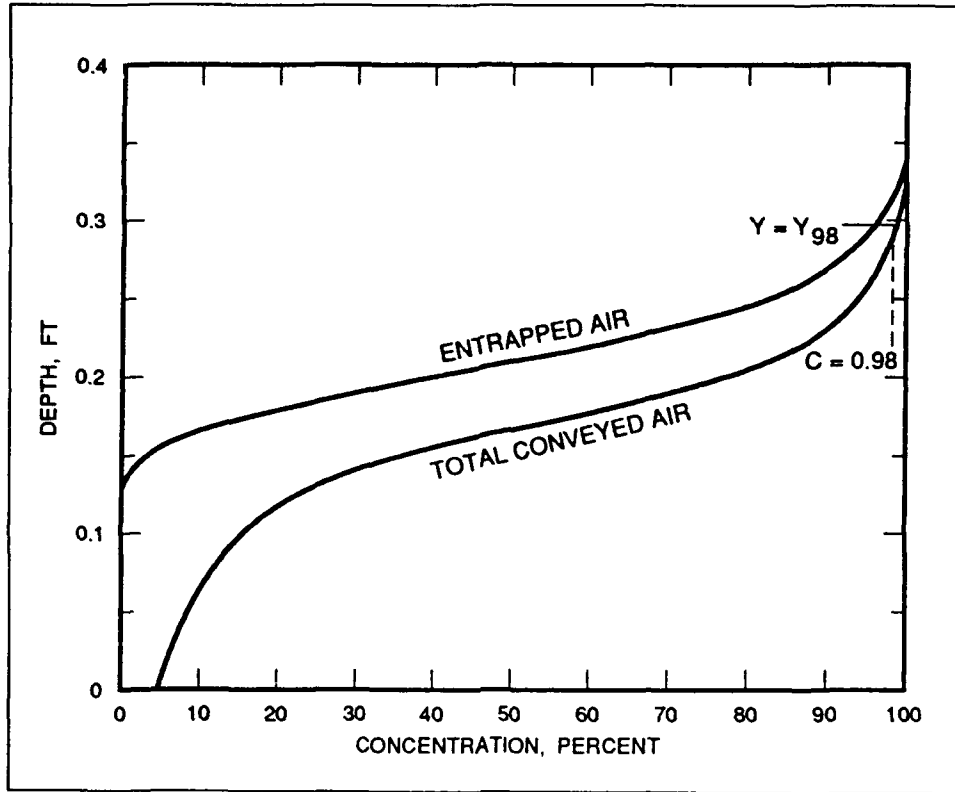
Figure 7. Air concentration profile (percent by volume) (after Killen (1968))

concentrations are equal to 100 percent, where the probe is completely out of the water.

Mean concentrations

The mean concentration of entrapped and total conveyed air can be determined by integrating these two profiles over depth and dividing by depth

$$\bar{C} = \frac{\int_0^{Y_c} c(y)\ dY}{\int_0^{Y_c} dy} \tag{4}$$

where

$\bar{C}$ = mean concentration of entrapped or total conveyed air

$c(y)$ = concentration profile of the entrapped or total conveyed air, respectively, as a function of depth y

Y_c = the integration limit

The mean concentration of entrained air is the difference between entrapped and total conveyed air.

Because of difficulty in defining the upper limit of flow, which should be the upper limit of integration, Straub and Anderson (1958) suggested integrating the profiles to a depth where the total conveyed air concentration was 0.95 or 0.99. Cain and Wood (1981) adopted an integration limit where total conveyed air is 0.95. In a later analysis, Wood (1985) used the depth where total conveyed air concentration was 0.90. The mean entrapped air concentration was determined for several integration limits and is presented in Appendix C. It was observed that there was less variability in the entrapped air concentrations as the integration limit increased. The depth, denoted by Y_{98} (Figure 7), where total conveyed air equals 0.98 was easily identifiable on concentration profiles and was selected for use in calculating mean values.

Mean concentrations for total conveyed air and entrapped air were calculated for all of Killen's observed profiles with Equation 4. Mean entrained air concentration was the difference between total conveyed air and entrapped air. The results of integrating these profiles are given in Table 1 and shown in Figure 8. This figure shows mean concentration as a function of distance along the flume for Killen's slopes and discharges. As one might expect, in the developing flow region, the total conveyed air concentration gradually increased, approaching an "equilibrium" concentration. Entrained air concentration followed a similar trend. It was anticipated that the entrapped air concentration would do likewise. However, the data show essentially a constant value for entrapped air concentration, suggesting that the mean entrapped air concentration is constant over a relatively wide range of discharges and slopes.

Constant entrapped air concentration

The question of why the entrapped air concentration should be constant immediately arises. Killen (1968) experimentally found that a Gaussian error function (cumulative normal distribution) described the surface roughness characteristics and, thus, also described the shape of the entrapped air profile. The difference between the depths d_{02} and d_{98} (Figure 9), where the entrapped air concentrations are 0.02 and 0.98, respectively, represents 4.1 $\sigma_{Entrapped}$, where $\sigma_{Entrapped}$ is the standard deviation of the cumulative normal distribution. With much difficulty, it can be shown that since the entrapped air concentration distribution is cumulative normal, then the entrapped air (numerator of Equation 4) is equal to a constant K^* times $\sigma_{Entrapped}$. Through Equation 4, this results in a mean entrapped air concentration $\bar{C}_{Entrapped}$ of

$$\bar{C}_{Entrapped} = \frac{K^* \sigma}{d_{98}} = \frac{K^* \left(d_{98} - d_{02} \right)}{4.1 \, d_{98}} \tag{5}$$

Table 1
Mean Concentrations of Entrapped, Entrained, and Total Conveyed Air for Killen's 1968 Observations

Profile	Entrapped	Entrained	Total	X ft
Test No. 1, $\Theta = 30$ deg, q = 4.3 ft³/sec-ft				
1-1	0.253	0.036	0.209	12
1-2	0.262	0.093	0.355	18
1-3	0.246	0.094	0.340	20
1-4	0.243	0.118	0.361	24
1-5	0.236	0.196	0.432	34
Test No. 2, $\Theta = 30$ deg, q = 8.5 ft³/sec-ft				
2-1	0.179	0.052	0.230	20
2-2	0.187	0.100	0.287	24
2-3	0.215	0.134	0.349	30
2-4	0.232	0.151	0.348	38
Test No. 3, $\Theta = 52.5$ deg, q = 4.3 ft³/sec-ft				
3-1	0.241	0.078	0.319	7
3-2	0.247	0.150	0.396	9
3-3	0.212	0.269	0.480	12
3-4	0.223	0.255	0.478	14
3-5	0.174	0.372	0.546	20
3-6	0.224	0.374	0.598	25
3-7	0.294	0.349	0.643	30
3-8	0.256	0.390	0.646	35
Test No. 4, $\Theta = 30$ deg, q = 2.1 ft³/sec-ft				
4-1	0.203	0.265	0.468	12
4-2	0.258	0.292	0.550	18
4-3	0.217	0.267	0.484	35
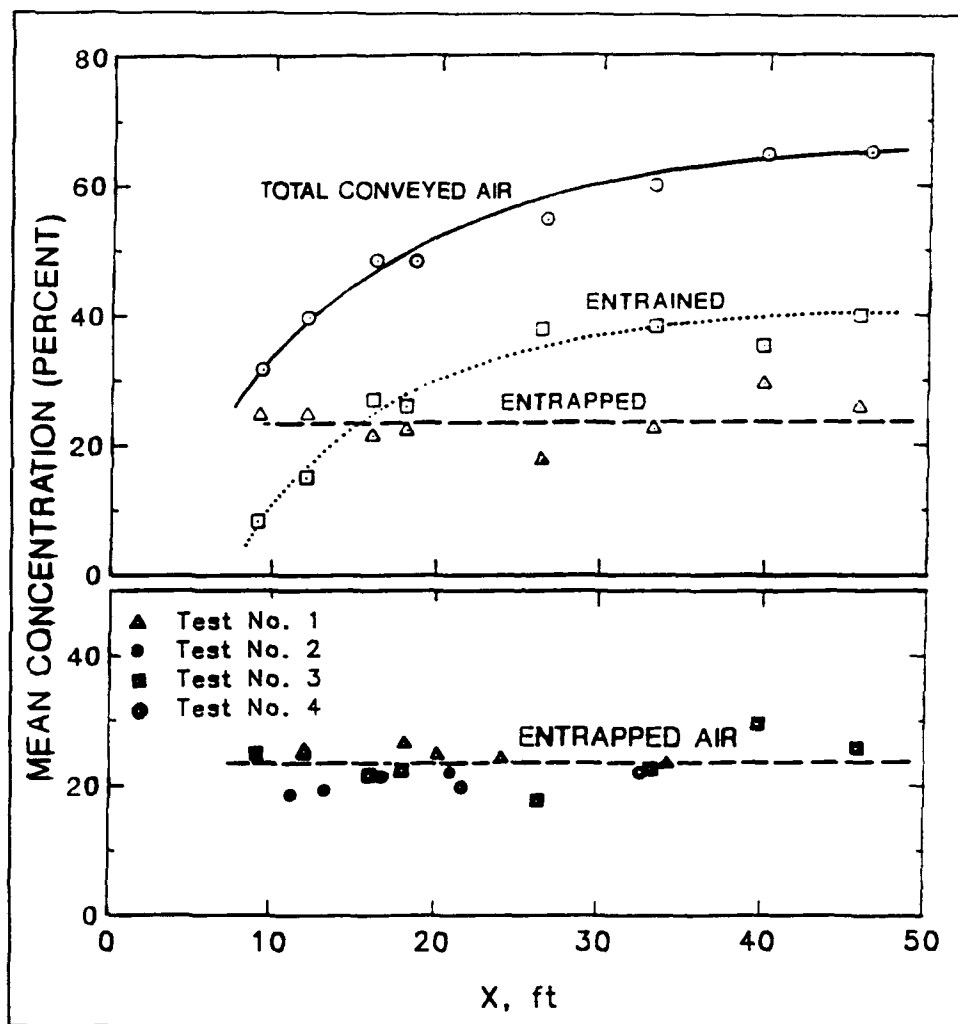
Figure 8.   Results of reanalysis of Killen's (1968) data. Mean concentrations
of profiles from Test No. 3 (above). Mean concentration of
entrapped air for all of Killen's data versus distance along the
channel (below)

For the entrapped air concentration to be constant, the ratio of $\sigma_{Entrapped}$ or
(d_{98} - d_{02}) to depth of flow d_{98} must be constant, implying that the surface
roughness is related to the overall depth of flow. This is reasonable when one
considers the cause of the surface roughness: turbulent eddies being generated
by shear at the floor of the channel. In a steep channel, the strength of these
eddies is sufficient to greatly deform and contort the water surface. Further-
more, the size of these eddies determines the magnitude of the surface rough-
ness; the size of the turbulent eddies is a function of depth in a turbulent
open-channel flow.

To illustrate this phenomenon, one can consider the distribution of turbu-
lence at the "surface" of a turbulent boundary layer (Figure 10). The

14
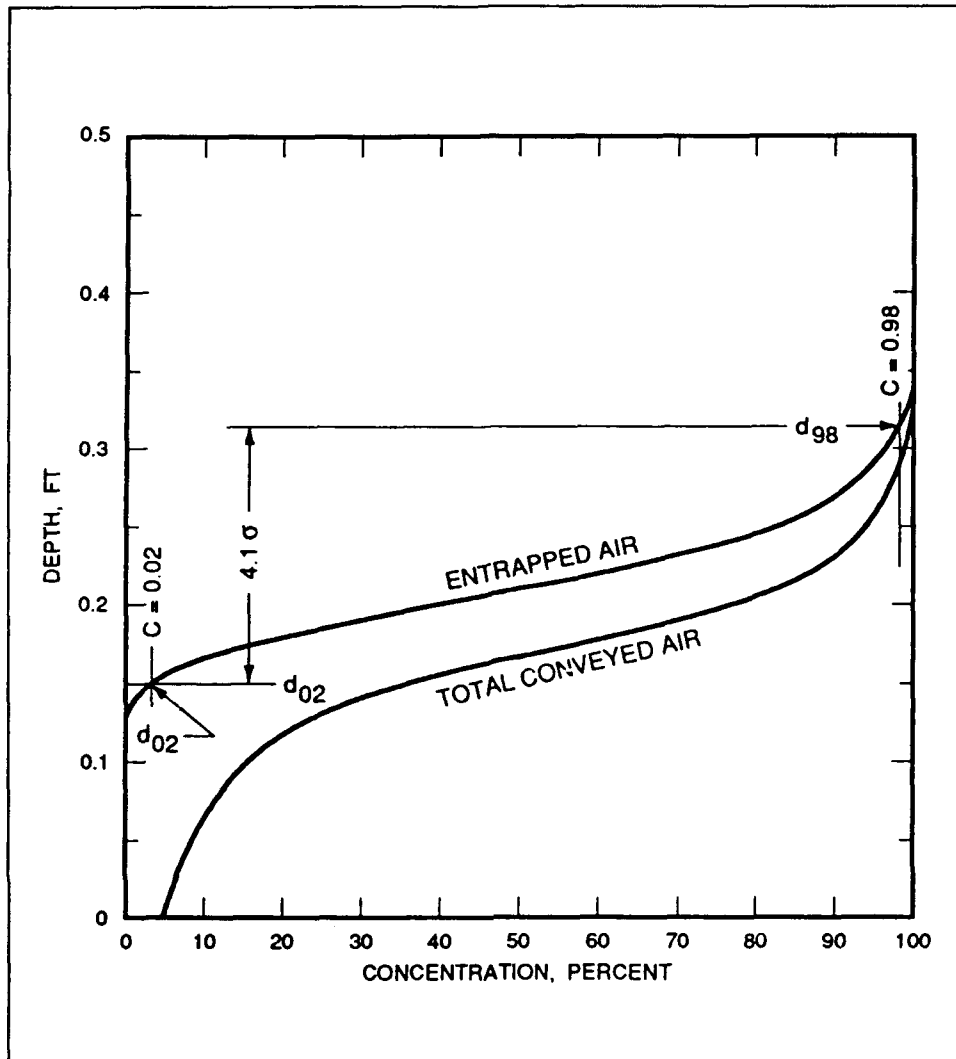
Figure 9.   Entrapped air concentration distribution (percent by volume)

turbulence generated within the boundary layer causes the "surface" of the boundary layer to be "highly contorted" (Tennekes and Lumley 1972). Measurements of turbulence in this region have resulted in the concept of an "intermittency factor," which is the proportion of time at some location in the interfacial region that the fluid is turbulent. Hinze (1959) reported that the distribution of the intermittency factor across this interfacial region was described by a Gaussian error function (a cumulative normal distribution). Further, the extent (thickness) of the intermittent region of turbulent and non-turbulent fluid was proportional to the boundary layer thickness.

With these characteristics of a boundary layer, one can consider the conditions where the boundary layer intersects an interface between two fluids of different densities (Figure 11). Prior to intersecting the interface, the only constraining force on the bursts of turbulence in the intermittent region is

caused by fluid viscosity. Once at the interface, however, the gravitational force caused by the density difference also acts to constrain the extent of the turbulent bursts of fluid. However, the added force of gravity because of the density difference will not change the functional character of the interface, i.e., the Gaussian error function distribution across the interfacial region. Although the width of the distribution may change, it will remain Gaussian in nature.

Close examination of this phenomenon clearly shows that it is analogous to the water surface characteristics measured by Killen (1968). In fact, Killen discussed the similarity of the roughened surface distribution and the intermittency of boundary layer turbulence. Typically, hydraulicians have not considered the aeration process in this light. Most have disregarded the fact that the boundary layer, generated by the spillway, propagates through the depth of flow, manifests itself as the roughened water surface, and actually continues into the air mass above the flowing water. Thus, the characteristics of the water surface are a direct reflection of the turbulence generated by the spillway. Through analogy with the roughened surface of a boundary layer, it can be concluded that the surface roughness should be related to the depth of flow. Therefore, a constant entrapped air concentration would be expected.

Developing flow: Location of the point of inception

As shown in Figure 8, Killen's observations illustrate the developing nature of self-aerated flow. At many, if not at most spillways, the flow conditions will still be in a developing stage rather than having achieved uniform equilibrated flow over the length of the spillway. Thus, the developing nature of aerated flow must be examined, and the location where uniform flow is approached must be defined. To accomplish this, the inception point must
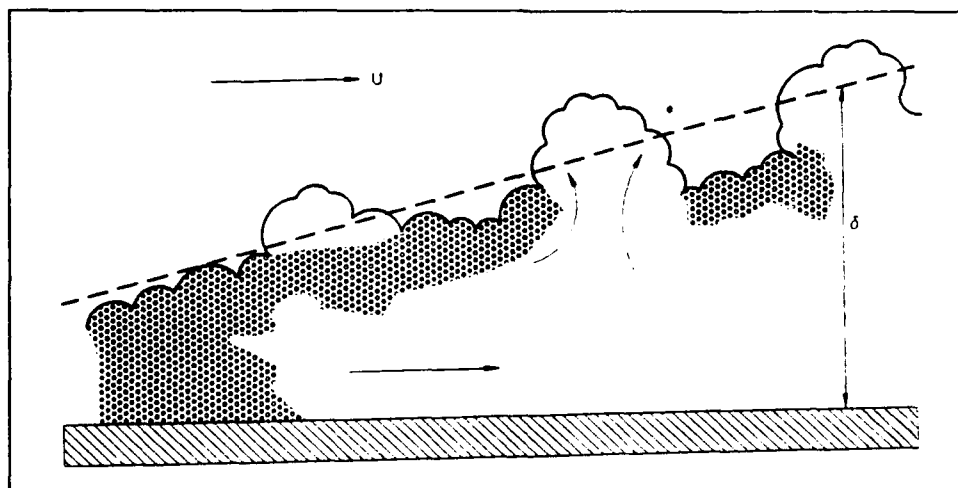
Figure 10. Boundary layer turbulence
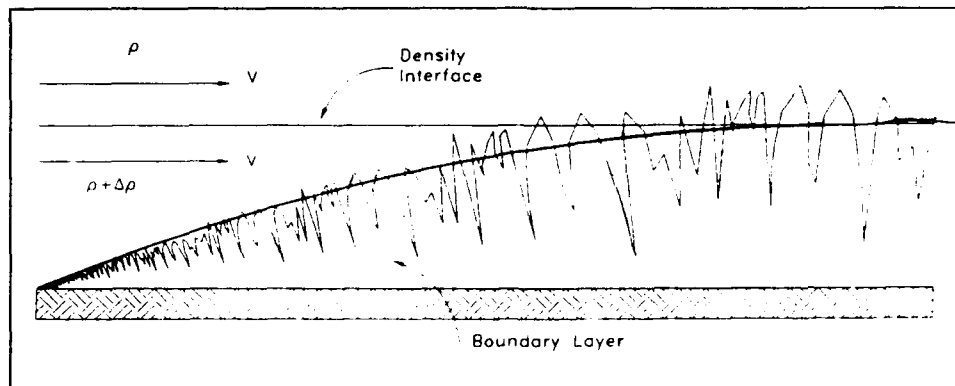
Figure 11. Intersection of a turbulent boundary layer with a density interface

also be determined and the location of downstream flow characteristics defined relative to the point of inception. For three of Killen's tests, the point of inception can be accurately located from the plots in Figure 8, but the points of inception are not available from the Straub and Anderson (1958) data. A method to estimate the location of the point of inception and the depth of flow at inception must therefore be developed.

Upstream of the point of inception, the local depth of flow gradually increases as the boundary layer develops. Bauer (1954) essentially added 10 percent of the boundary layer thickness to the potential flow depth to determine the local depth of flow, i.e., for high Reynolds numbers, 10 percent of the boundary layer thickness is approximately the displacement thickness. The point of inception was the location where the boundary layer intersected the gradually varying water surface. For Killen's tests, to determine the depth of flow at the point of inception, methods presented by Blevins (1984) were used to compute its location based on boundary layer growth on a hydraulically rough plate. This analysis is presented in Appendix D. Table 2 gives observed and calculated locations in flume dimensions for Killen's three tests.

Table 2 Location for Point of Inception for Killen's (1968) Tests			
Slope degree	Unit Discharge ft^3-s^{-1}-ft^{-1}	Distance Along Flume to Observed Point of Inception, ft	Distance Along Flume to Calculated[1] Point of Inception, ft
30	4.3	10.0	6.1
30	8.5	16.2	10.7
52.5	4.3	6.0	4.8
[1] Calculated with Blevins' (1984) method.			

Although few tests are available, it appears that Blevins' (1984) method underestimates the distance required for the emergence of the boundary layer to the water surface. The reason for this is not clear, but one can speculate with some justification about the potential causes. In setting the opening of the control gate on the flume, the intent was to set an opening such that flow would not have to accelerate or decelerate to achieve normal depth of flow. If the gate opening was too large and the flow had to accelerate (Figure 12), then boundary layer development would be retarded and the calculated point of inception would be less than the observed. If the gate opening was too small and the flow had to decelerate, then boundary layer development would be accelerated and the calculated point of inception would be greater than observed. Figure 13 shows the relationship between gate opening G_o and normal depth of flow d_o for Killen's tests. Obviously, the gate opening was larger than normal depth, resulting in retardation of boundary layer development. The control gate on the flume should have been set with an opening less than normal depth by an amount equal to the boundary layer displacement thickness. The dashed line represents these ideal conditions.

Clearly, for these tests the gate opening was too large and the flow accelerated when discharged to the flume. Argument can be made that if the gate opening was set for ideal conditions, then the calculated location for the point of inception would be equal to the observed. Further, it would seem to follow that for larger gate openings, relative to the ideal depth, there would be a larger difference between calculated and observed inception points. Thus, as the ratio d_o/G_o approaches 1.0 from the lower side, the ratio $X_{I(calc)}/X_{I(obs)}$ likewise approaches 1.0 from the lower side, where $X_{I(calc)}$ and $X_{I(obs)}$ are the calculated and observed locations of the point of inception. Because the data are so few, a linear relationship (Equation 6) between these two ratios (Figure 14) is suggested to advance this analysis.

$$\frac{X_{I(calc)}}{X_{I(obs)}} = 1.37 \, \frac{d_o}{G_o} - 0.375 \tag{6}$$

Dimensionless terms

To compare the many observed profiles, several hydraulic variables were considered for dimensionless terms that describe aerated flow characteristics. Past efforts proposed nondimensional terms that have included a "distance Reynolds Number" (Keller, Lai, and Wood 1974), where the critical dimension was distance along the direction of flow. Cain (1978) used the depth of flow at the point of inception Y_I to introduce a dimensionless distance parameter X^*/Y_I, where X^* is the distance from the point of inception (Figure 12). This particular variable has the convenient characteristic of implicitly including the unit discharge. At the point of inception, regardless of discharge, the hydraulic character of the flow is completely developed, and hence the discharge can be described in terms of the depth of flow. It follows that the dimensionless
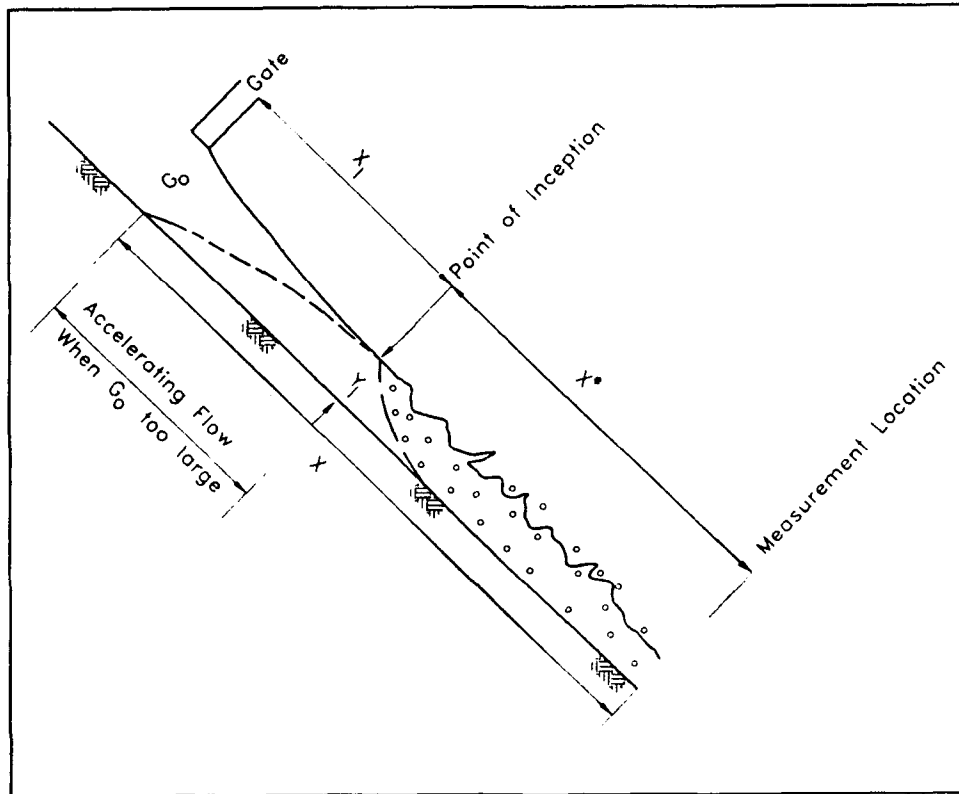
Figure 12. Schematic of flume with gate opening and measurement location and variables used in dimensionless analysis

distance parameter X^*/Y_I should be an appropriate term for analysis of developing flow.

Nondimensionalizing Killen's tests

For each of Killen's tests, the depth of flow at the point of inception Y_I is available from Table D1 (Appendix D). The observed location of the point of inception X_I is presented in Table 2. The developing character of aerated flow depicted in Figures 1, 2, and 8 can be nondimensionalized with

$$X^* = X - X_I \qquad (7)$$

where

X^* = distance along the flume from the point of inception

X = actual distance from the flume control gate to location (Figure 12)
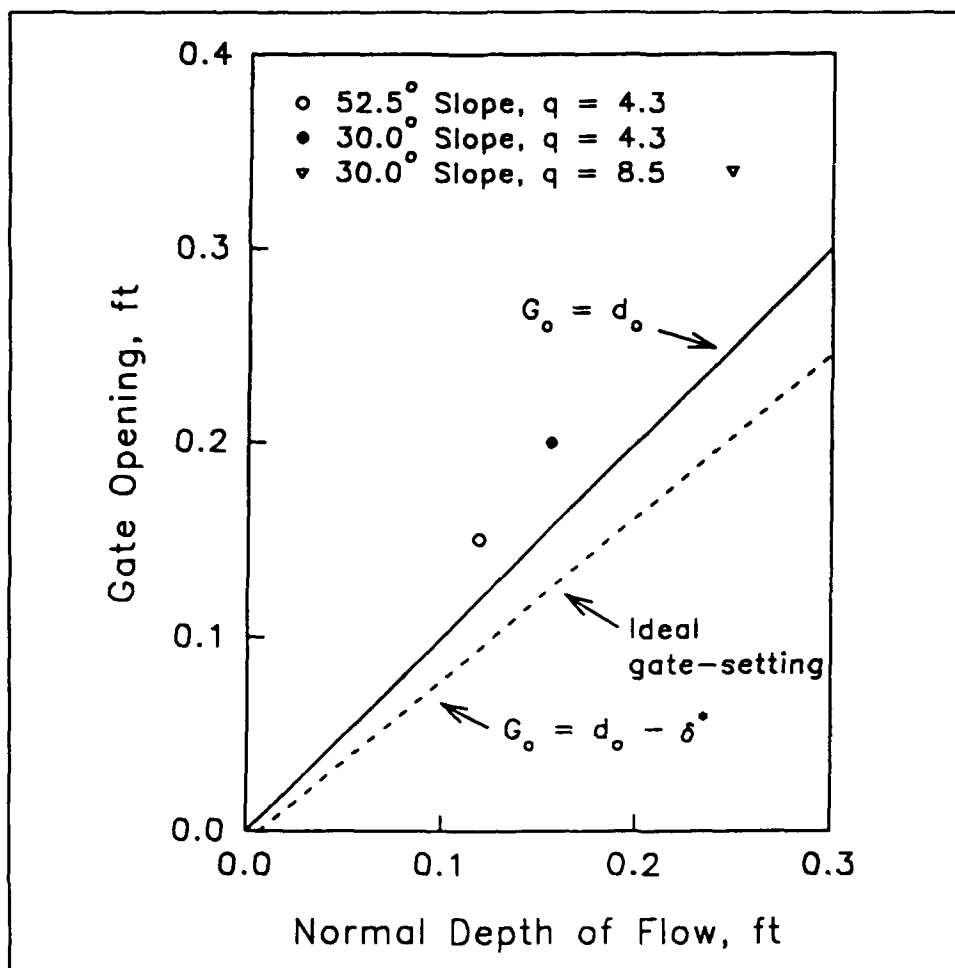
Figure 13. Gate opening versus normal depth of flow for Killen's (1968) tests

At the point of inception, X^* equals zero. Using Equation 7 and the data presented in Appendix B, Figure 8 can be replotted in nondimensional form as shown in Figure 15.

Application of Results for Developing Flow

As mentioned earlier, Straub and Anderson (1958) made extensive measurements of aerated flow for a large variety of slopes and discharges. Their observations, however, consisted only of total conveyed air concentration profiles. Using the analysis presented in previous paragraphs, entrained air concentrations were calculated for Straub and Anderson's profiles by subtracting the constant entrapped air concentration of 23 percent from total conveyed air. By describing the location of Straub and Anderson's profiles relative to the point of inception, their data provide a basis for describing the character of
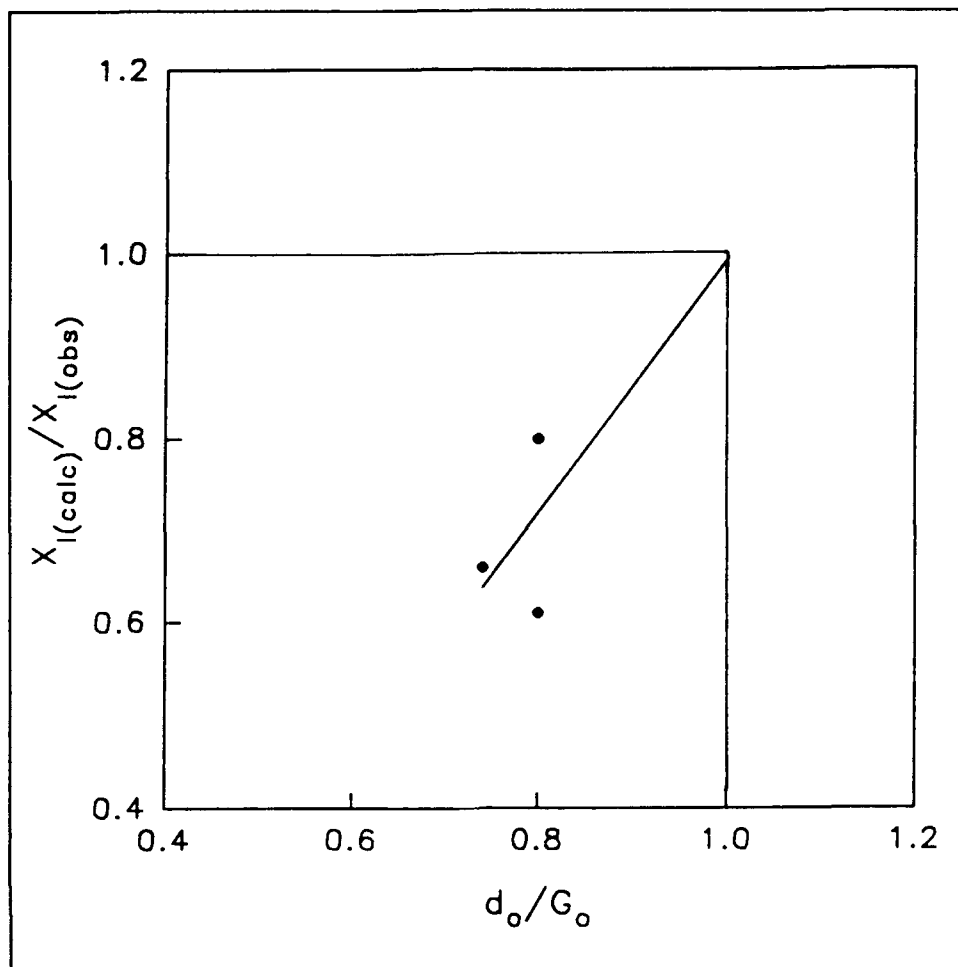
Figure 14. Suggested relationship between d_o/G_o and X_I (calc) / X_I (obs)

developing aerated flow. Although Straub and Anderson tested several slopes, this effort examines their data from a 30-deg slope for direct comparison with Killen's (1968) observations and then concentrates on describing flow conditions for a 45-deg slope, which is most appropriate for application to CE spillways.

Location of points of inception

Table 3 and Figure 16 show the relationship between the gate opening and the normal depth of flow for the Straub and Anderson tests. For many of their tests, as with Killen's (1968) tests, the gate opening was greater than required for the ideal setting. Thus, to estimate the location of the point of inception for their tests, the analysis of Killen's observations is reversed:

   a. Using the normal depth of flow from Table 3, determine the location of the point of inception for the ideal gate setting from Table D1.
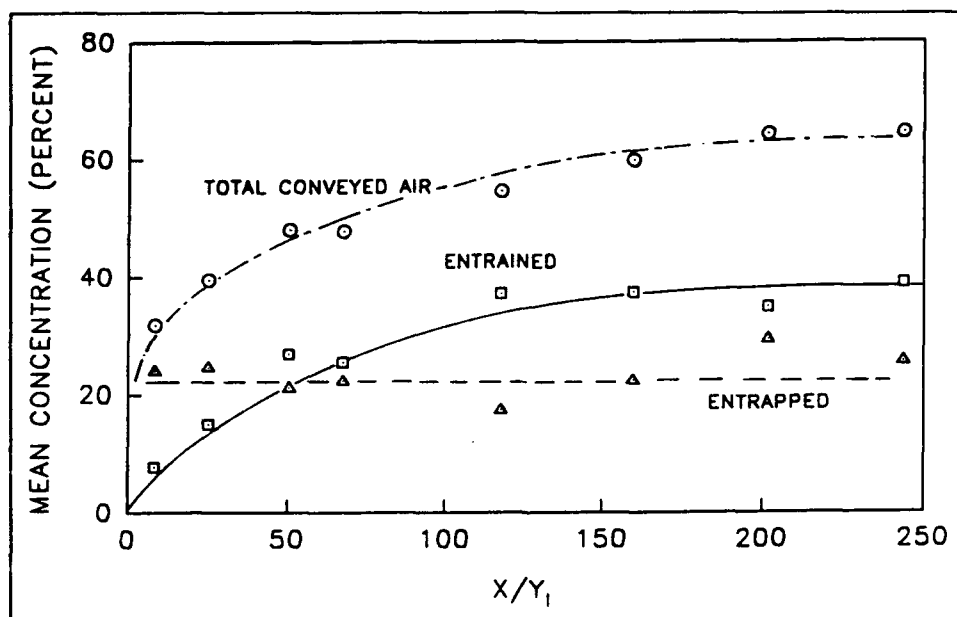
Figure 15. Replot of Figure 8 in dimensionless terms: Mean concentrations of profiles from Test No. 3 of Killen's (1968) data versus dimensionless distance along the flume

b. With Equation 6 and the ratio of d_o/G_o, estimate the ratio $X_{I(calc)}/X_{I(obs)}$, from which the "observed" or actual location of the point of inception can be determined.

Table 4 gives these values for $X_{I(obs)}$ for Straub and Anderson's 30- and 45-deg tests.

Developing aerated flow from Straub and Anderson's tests

Straub and Anderson (1958) intended to measure the entrained air characteristics for uniform equilibrated flow conditions. Wood (1983, 1985), however, showed that only some of their measurements were made in equilibrated uniform flow (Figure 17). In general, for low discharges, their observations were in equilibrated uniform flow. But for higher discharges, aeration was not fully developed. Wood also argued that similarity exists between concentration profiles for different discharges on the same slope.

Ordinarily, if interest was in developing flow (as was Killen's (1968)), then observations would be made at several locations along the developing portion of the flow. Although the intent of Straub and Anderson's tests was to determine the fully developed air concentration profile, a closer examination shows that as discharge increased, the location where the profile was taken was closer to the point of inception in terms of nondimensional distance (relative to the depth of flow). This observation and the arguments presented in the previous

22

Table 3
Gate Openings and Normal Depths of Flow for Straub and Anderson's Test on 30- and 45-Deg Slopes

Test No.	30-Deg Slope		45-Deg Slope	
	Gate Opening, ft	Normal Depth, ft	Gate Opening, ft	Normal Depth, ft
1	0.065	0.077	0.045	0.064
2	0.11	0.098	0.057	0.082
3	0.13	0.118	0.075	0.098
4	0.15	0.136	0.09	0.113
5	0.2	0.156	0.105	0.13
6	0.2	0.169	0.125	0.141
7	0.225	0.184	0.15	0.153
8	0.26	0.204	0.18	0.17
9	N/A	0.213	N/A	0.177
10	0.28	0.227	0.22	0.189
11	0.34	0.248	0.27	0.206
12	0.36	0.275	0.39	0.229

paragraph suggest that Straub and Anderson's (1958) observations, if non-dimensionalized appropriately, may be used to describe the characteristics of developing flow. By using the dimensionless distance described in the previous section to locate these profiles, then all of the profiles for one slope can be analyzed as profiles of developing flow at different locations along the flume.

Straub and Anderson (1958) published profiles, which they considered to be under equilibrated conditions, that were taken at a location approximately 45 ft down their flume from the control gate. In addition, they collected profiles at a location 35 ft along the flume that were not published. These data are presented in graphical and tabular form in Appendices E and F, respectively.

Using the methodology outlined in the previous section to estimate the location of the rough-surface inception point X_I and using the normal depth of flow to define $Y_I = d_o$, a dimensionless distance X^*/Y_I along the flume can be calculated for Straub and Anderson's 35- and 45-ft observations. Integrating the total conveyed air profiles with Equation 4 and subtracting the constant concentration of entrapped air ($C_{entrapped} = 0.23$ by volume) gives the entrained air concentration. Figure 18 shows the developing nature of entrained air concentration from observations on a 30-deg slope from Straub and Anderson's and Killen's tests. This analysis of Straub and Anderson's tests, when

**Table 4
Estimated Values for the Inception Point Location for Straub
and Anderson's Test on 30- and 45-Deg Slopes**

Test No.	30-Deg Slope $X_{i(obs)}$, ft	45-Deg Slope $X_{i(obs)}$, ft
1	2.35	1.54
2	4.55	1.97
3	5.45	2.68
4	6.22	3.29
5	9.05	3.91
6	8.78	4.81
7	10.17	6.04
8	12.32	7.52
9	N/A	N/A
10	13.00	9.76
11	16.98	12.85
12	17.49	22.66

compared with Killen's observations of developing flow, clearly shows the validity of the approach. Hence, this approach was used to develop Figure 19, showing results of applying this procedure to Straub and Anderson's tests on a 45-deg slope.

Mathematical description of air entrainment

Most CE dams are designed with a sloping face of 45 deg, thus, a regression analysis was performed for the data shown in Figure 19. This resulted in the following relationship between dimensionless distance from the point of inception and the entrained air concentration:

$$C_{entrained} = 0.48 - 0.48 \, e^{\left(-0.01081 \, \frac{X^*}{Y_i} \right)} \tag{8}$$

where

$C_{entrained}$ = mean entrained air concentration expressed in terms of void ratio

X^*/Y_i = dimensionless distance from the point of inception
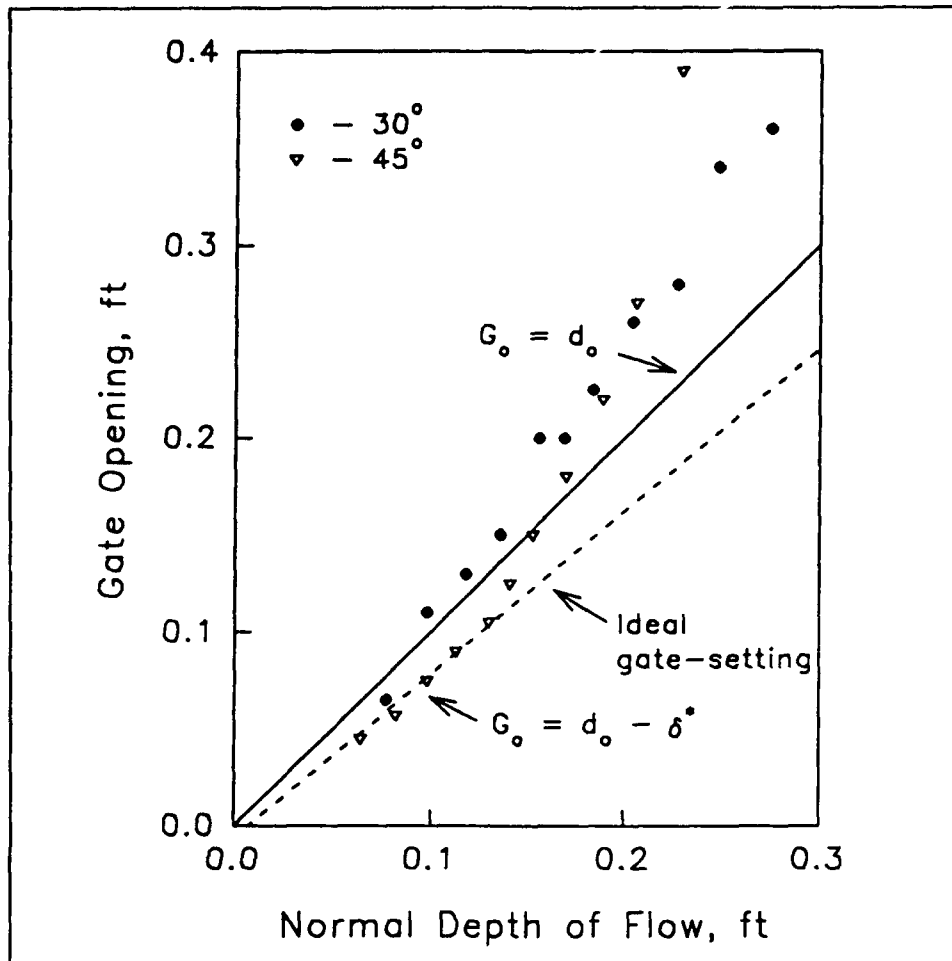
Figure 16. Gate opening versus normal depth of flow for Straub and Anderson's (1958) tests on 30- and 45-deg slopes

This relationship can be used to estimate the entrained air concentration at any location along the flow path on a spillway. The concentration of total conveyed air can be estimated by adding the void fraction of entrapped air, which is constant at 0.23.

Verification and application

To verify the relationships developed in the previous sections, observations in aerated flow from the Aviemore Spillway (Cain 1978) were used. Although the Aviemore Spillway is not a CE project, it has a 45-deg sloping face. Cain measured total conveyed air at several locations along the flow path. Thus, these data represent measurements of developing flow. Cain's observed profiles of total conveyed air concentration were integrated to determine mean concentrations of total conveyed air. From these total conveyed air concentrations, 23 percent was subtracted for mean entrapped air leaving mean concentrations of entrained air. Figure 20 shows the mean along the spillway face for
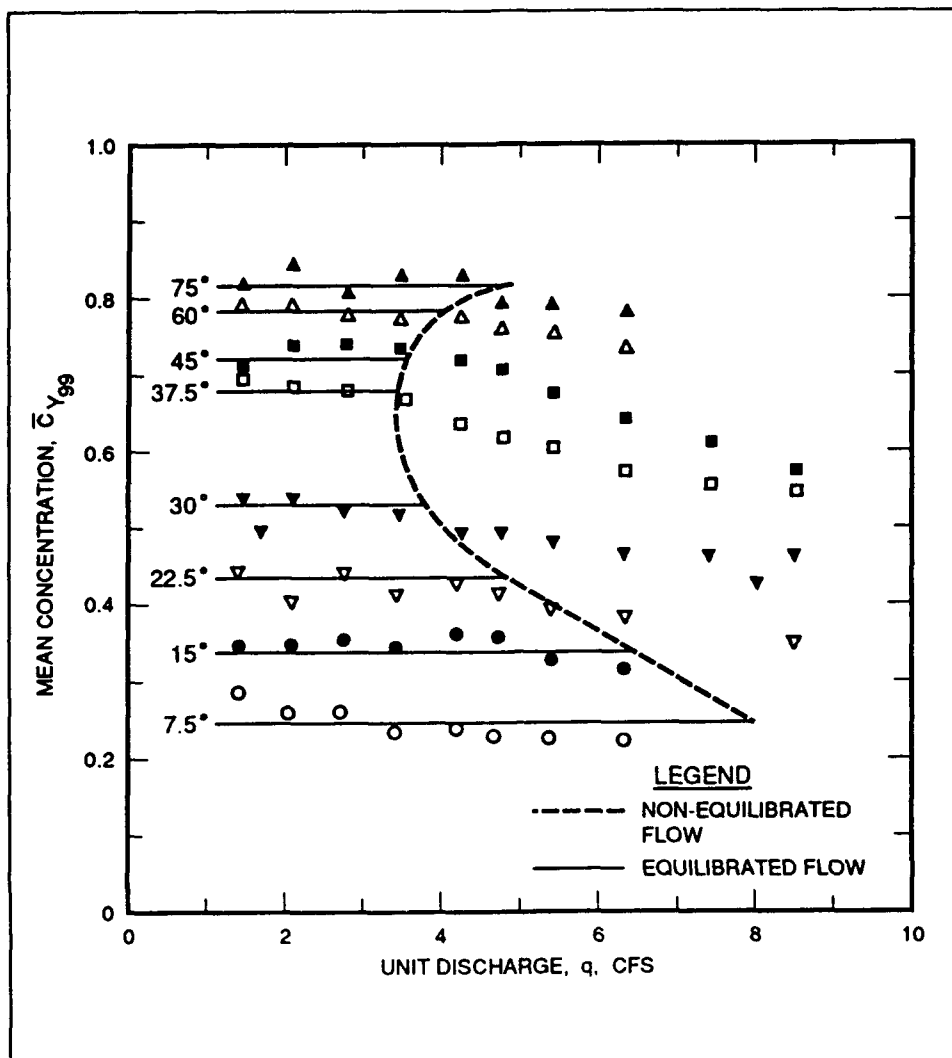
Figure 17. Mean concentration of total conveyed air versus unit discharge for Straub and Anderson's (1958) tests on 30- and 45-deg slopes (after Wood 1983, 1985)

the two discharges Cain tested. Clearly, this comparison demonstrates the appropriateness of the arguments made in earlier sections regarding the non-dimensional terms. The comparison also indicates that the equilibrium concentration is accurately predicted. In the values for entrained air concentration as a function of dimensionless distance region of developing flow, the comparison shows that the equation overpredicted the entrained air concentration by 5 to 6 percent. The reason for this discrepancy is unclear, other than it being the result of measurement uncertainty. However, this error does not negate the usefulness of the relationship for estimating the entrained air concentration in developing flow. Further, it seems likely that this formulation should be applicable to most spillways: even though the relationships were developed from observations made in a laboratory flume, the results reasonably predicted observations from a full-scale project.

26
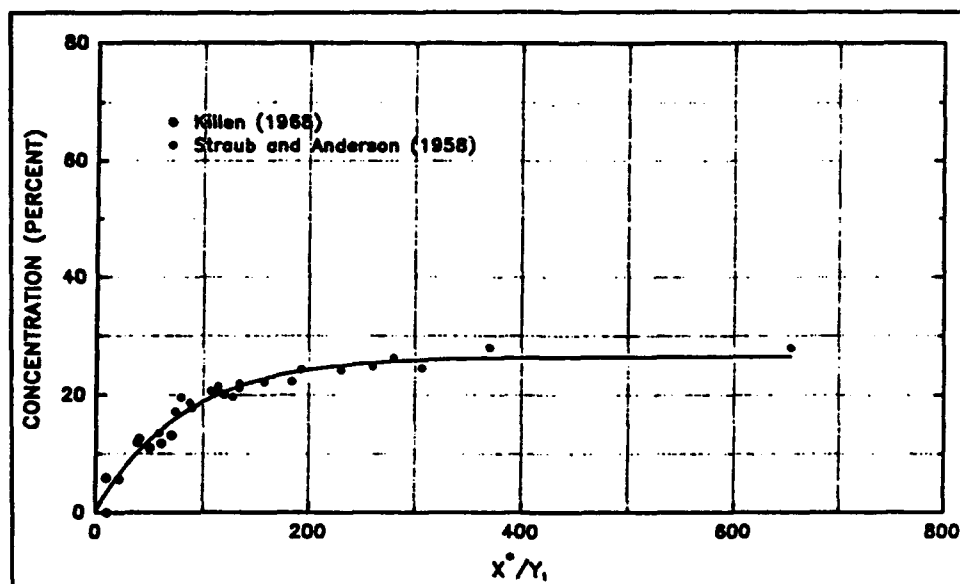
Figure 18. Mean concentration of entrained air (percent by volume) versus dimensionless distance from point of inception for Straub and Anderson's (1958) and Killen's (1968) tests on a 30-deg slope

As described earlier, there are two areas of concern that benefit greatly from the foregoing analysis: (a) prediction of gas transfer rates (oxygen and nitrogen absorption at spillways) and (b) prediction and minimization of cavitation damage. As mentioned in the section where entrained and entrapped air were defined, entrained air on the spillway face contributes to increased surface area for gas transfer that occurs as the water flow passes down the spillway. If the nappe of water and air (entrained and entrapped) plunges into a stilling basin at the foot of the spillway, then total conveyed air contributes to the interfacial area of bubbles in the stilling basin, greatly increasing the gas transfer. Minimizing cavitation damage requires that air concentration in excess of about 8 percent be present near the cavitating surface. At some location along the spillway (in the region of developing flow), air bubbles will reach this concentration near the spillway surface. This can be defined in terms of the dimensionless distance X^*/Y_i.

To estimate the surface area contributed by entrained air bubbles, the volume of entrained air and the size and number of air bubbles under a unit area of surface must be determined. Equation 9 shows the calculation of this entrained air volume:

$$V_{entrained} = \frac{d_o \, C_{entrained}}{1.0 - \left(C_{entrained} + C_{entrapped} \right)} \qquad (9)$$
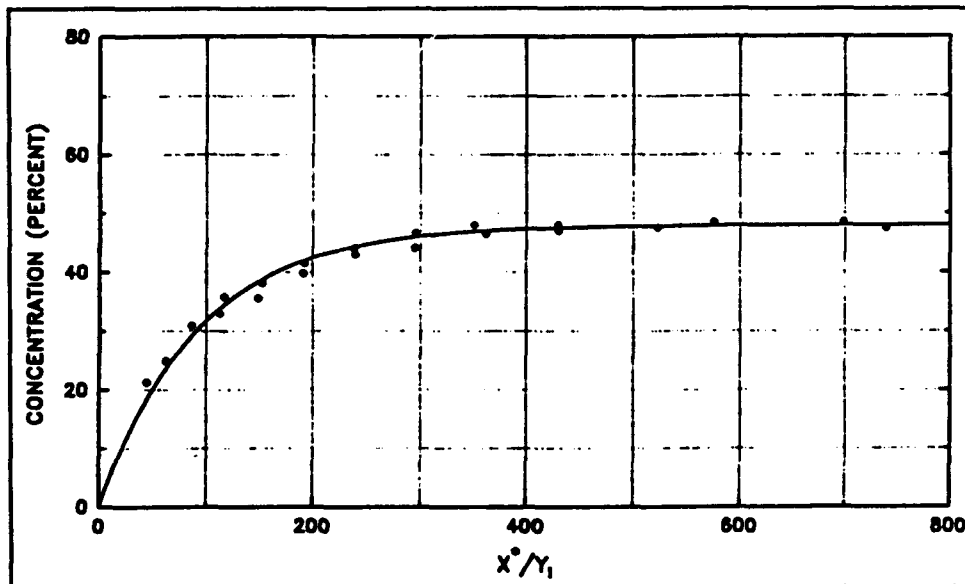
Figure 19. Mean concentration of entrained air (percent by volume) versus dimensionless distance from point of inception for Straub and Anderson's (1958) tests on a 45-deg slope

where

$V_{entrained}$ = volume of entrained air

d_o = normal depth of flow

Gulliver, Thene, and Rindels (1990) developed a method of estimating the maximum bubble diameter in turbulent flow. From photographs of air entrained flow, they developed bubble size distributions from which the mean bubble diameters, weighted by volume and surface area, were determined. With observations from flow on a 12-deg slope ($S = 0.20$), unit discharge of 5.7 ft^3/sec per ft, and a normal depth of flow of 0.20 ft, they determined that the maximum bubble diameter[1] d_m was approximately 2.7 mm. They also determined that the mean bubble diameter, weighted for bubble volume, was 0.62 d_m. The mean bubble diameter, weighted for surface area, was 0.52 d_m.

Gulliver, Thene, and Rindels (1990) used a relationship between surface tension and the shear on the bubble surface proffered by Hinze (1955) to scale the bubble size to other types of flows:

$$d_m = k \left(\frac{\sigma}{\rho}\right)^{3/5} \epsilon^{-2/5} \tag{10}$$

---

[1] Diameter below which lie 95 percent of the air bubbles.

28
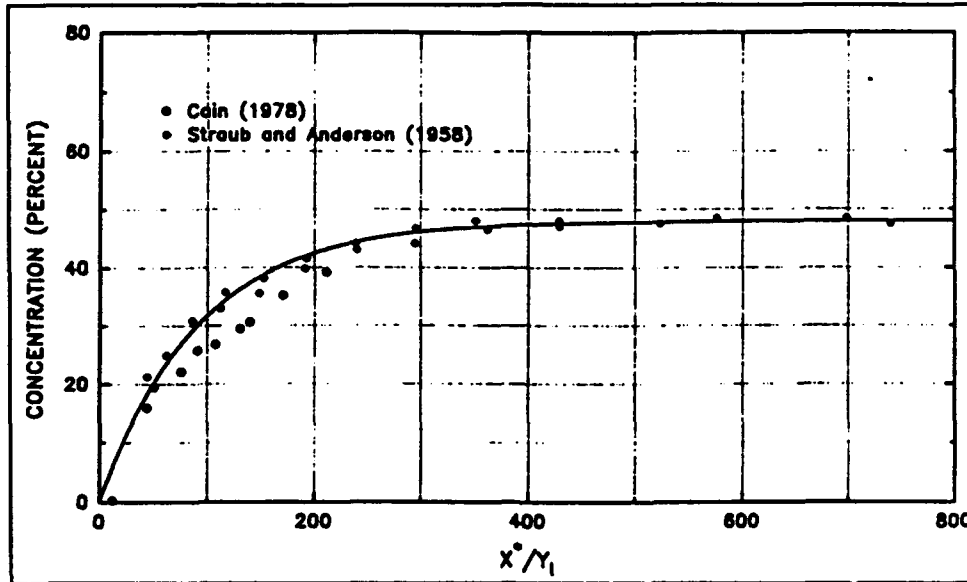
Figure 20. Mean concentration of entrained air (percent by volume) versus
dimensionless distance from point of inception for Straub and
Anderson's (1958) tests on a 45-deg slope and Cain's (1978)
observations on Aviemore Spillway

where

d_m = maximum bubble diameter, mm

k = constant

ρ = density of the liquid

σ = surface tension

ε = rate of turbulent kinetic energy dissipation per unit mass

Hinze found $k = 0.725$ in rotating concentric cylinders; Sevik and Park (1973)
found $k = 1.15$ for water jets entering a plunge pool; and Killen (1982) found
$k = 1.01$ for a boundary layer flow.

If Killen's (1982) boundary layer work is followed and $\varepsilon = U_*^3/d_o$ is used,
where U_* is the shear velocity defined by

$$U_* = \sqrt{g d_o S}$$

and g is the acceleration of gravity, d_o is channel depth, and S is channel slope,
then Equation 10 becomes as follows for spillways:

$$d_m = k \left(\frac{\sigma}{\rho \, g \, S \, d_o^{1/3}} \right)^{0.6} \tag{11}$$

The measurements of Gulliver, Thene, and Rindels (1990) on chute flow with a $d_m = 2.7$ mm gives $k = 0.71$ in Equation 10, which is within the range established by Hinze (1955), Sevik and Park (1973), and Killen (1982).

Given the entrained air volume (Equation 9), the maximum bubble diameter (Equation 11), and the mean bubble diameter based on bubble volume, the number of bubbles making up the entrained air volume can be estimated with the following:

$$N = \frac{V_{entrained}}{V_{average}} = \frac{V_{entrained}}{\frac{\pi}{6} \left(0.62 \, d_m \right)^3} \tag{12}$$

where

N = number of bubbles

$V_{entrained}$ = volume of entrained air

$V_{average}$ = volume of mean bubble (based on volume)

With the number of bubbles in the flow and mean bubble diameter weighted with surface area, the total surface area can be calculated with the following:

$$A_s = N \, \pi \left(0.52 \, d_m \right)^2 \tag{13}$$

where A_s is the total surface area contributed by the bubbles under a unit area of surface.

In the mathematical description of gas transfer (Equation 2), the bubble surface area is one of the key parameters defining the "specific area" A/V . The specific area can be computed using the total surface area A_s and the volume of water under the unit area of surface of surface:

$$\frac{A}{V} = \frac{A_s}{d_o \, a} = \frac{A_s}{d_o} \tag{14}$$

where a is unit area.

To illustrate these calculations, one can consider flow on a 45-deg slope with a unit discharge of 4 ft³/sec per ft, a Manning's n of 0.018, and a normal depth of flow of 0.17 ft (for water only, no consideration of bulking because of entrained air). For equilibrated flow, the entrained air concentration (Figure 19) would be approximately 48 percent by volume. Equation 9 gives 0.28 ft³ or 7.97 (10⁶) mm³ as the entrained air volume under 1.0 ft² of surface. Equation 10, with $k = 0.71$, gives a maximum bubble diameter d_m of 1.0 mm, which can be used in Equation 12 to estimate the total number of bubbles in the entrained air volume:

$$N = \frac{V_{entrained}}{V_{average}} = \frac{7.97\left(10^{6}\right)}{\frac{\pi}{6}\left(0.62\left(1.0\right)\right)^{3}} = 6.39\left(10^{7}\right) \tag{15}$$

The surface area of the bubbles under 1.0 ft² of flow surface can be computed from Equation 13:

$$A_s = \alpha\, N\, \pi\left(0.52\, d_m\right)^2 = \alpha\, 6.39\left(10^{7}\right)\pi\left(0.52\right)^2 = 583\, ft^2 \tag{16}$$

where α equals 1.076 (10⁵) ft²/mm². The specific area A/V from Equation 2 is calculated with Equation 14:

$$\frac{A}{V} = \frac{A_s}{d_o} = \frac{583}{0.17} = 3,433\, ft^{-1} \tag{17}$$

As discussed in Chapter 2, cavitation damage can be minimized or eliminated if near the surface where the cavitation occurs, a minimum air concentration of about 8 percent exists. Figure 21 shows the relationship of entrained air concentration and the concentration of air at the spillway face or flume bottom for all of Killen's (1968) and Straub and Anderson's (1958) observations (measurements made within 0.02 ft of the surface). This figure indicates that for developing flow, a minimum concentration of entrained air of approximately 20 percent is needed to provide an 8-percent entrained air concentration at the surface of the spillway. For a 45-deg slope, this occurs at a dimensionless distance X^*/Y_i along the spillway face of about 75. For the Aviemore Spillway, this translates into distances from the point of inception of approximately 38 and 45 ft for the two flows tested.
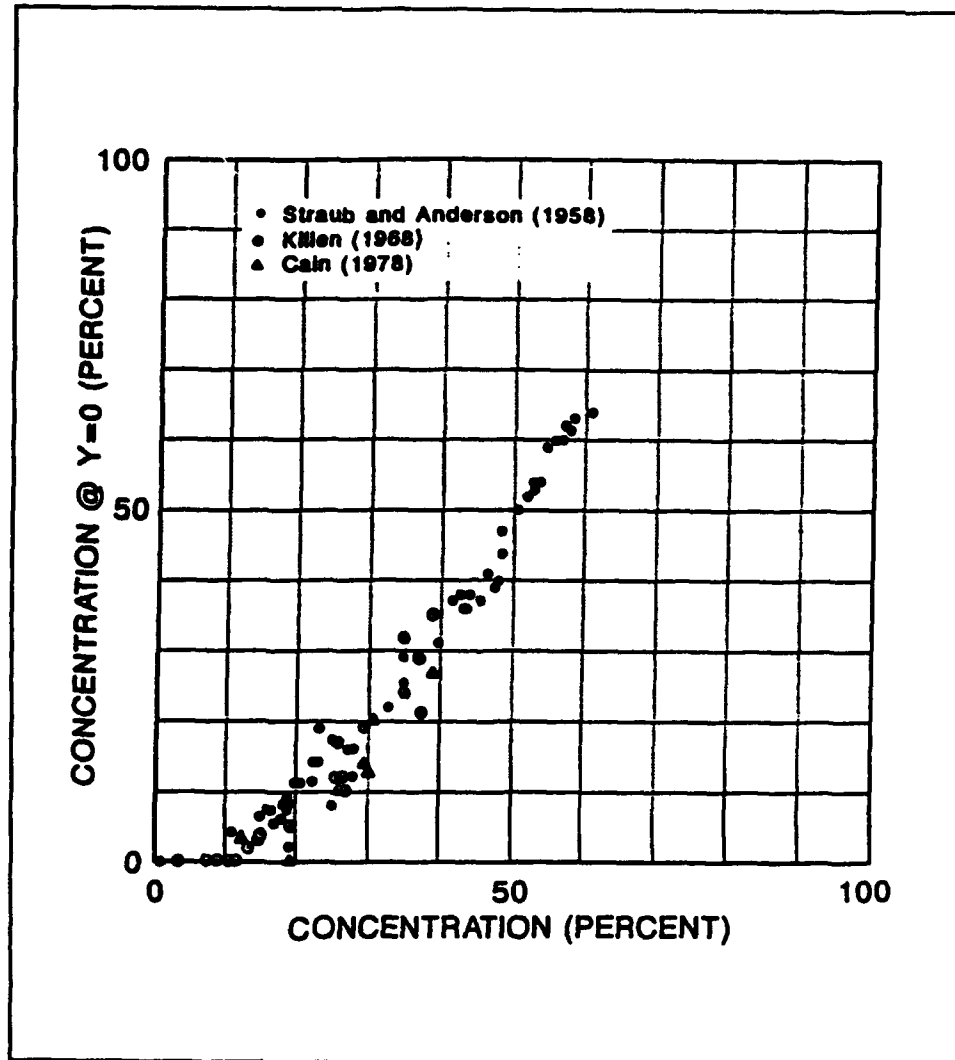
Figure 21. Relationship between entrained air concentration and air concentration at the spillway or flume surface for Straub and Anderson's (1958) data, Killen's (1968) data, and Cain's (1978) data

3 Summary and Conclusions

Hydraulic engineers have historically been interested in self-aerated flow because of bulking and the resulting need for higher sidewalls on spillways and chutes. They have also had interest in this phenomenon because entrained air bubbles can reduce or eliminate cavitation damage if the air bubbles are near the cavitating surface. Further, the air that is transported in self-aerated flows can contribute significantly to oxygen uptake and the transfer of other gases.

The concepts of entrained, entrapped, and total conveyed air were introduced and used to redefine the air concentrations being transported by self-aerated flows. Entrained air is that which is insufflated through the surface of the flow and transported as bubbles. Entrapped air is the air transported within the roughened water surface of the flow. Total conveyed air is the sum of these. For bulking interests, the total conveyed air concentration is the important parameter. For cavitation, the concentration of entrained air at the spillway surface determines the extent of cavitation damage. For gas transfer, entrained air bubbles greatly increase the interfacial area available for gas transfer. If the flow on the spillway plunges into a downstream pool, then some proportion of the entrapped air would become entrained and contribute to the gas transfer.

Killen's (1968) flume measurements of surface characteristics and total conveyed air concentrations provided a basis for separating total conveyed air and entrapped air. The analysis of Killen's measurements of developing aerated flow showed a gradual increase in the concentration of total conveyed air and entrained air, approaching an equilibrium as the flow moved down the experimental channel. However, entrapped air concentration was essentially constant at a concentration of approximately 23 percent. Further, the entrapped air was distributed over the extent of the surface roughness according to a Gaussian error function (cumulative normal distribution). Additional analysis showed, because of this distribution, that if the entrapped air concentration was constant, then the extent of the surface roughness had to be proportional to the depth of flow.

An analogy was drawn between the surface of a turbulent boundary layer and the characteristics of the roughened surface of aerated flow. The surface of the turbulent boundary layer possesses similar characteristics; i.e., the

boundary layer roughness is distributed according to a cumulative normal distribution, and the extent of this distribution is proportional to the thickness (depth) of the layer. Indeed, the surface roughness of self-aerated flow is a manifestation of the turbulence of the boundary layer caused by the spillway or flume surface. This analogy implies that the entrapped air concentration should be a constant and the extent of the surface roughness is proportional to the depth of flow. Entrained air concentration can thereby be computed from observations of total conveyed air by substracting the constant entrapped air concentration of 23 percent.

For Killen's (1968) observations of developing flow, the distance along the flow path between the point of surface roughness inception and the location of the measurements was nondimensionalized by dividing that distance by the depth of flow at the point of inception (POI). This formulation has the unique characteristic of implicitly including discharge: at the POI, the velocity distributions over depth are self-similar, regardless of discharge, when nondimensionalized with the depth of flow. This procedure of nondimensionalization and the concept of self-similarity permit entrained air observations for several discharges to be analyzed together as measurements of developing flow.

Using Killen's (1968) observations, the following procedure was developed to calculate the location of the point of surface roughness inception for other flows in the test flume, specifically Straub and Anderson's (1958) tests.

a. Use Manning's Equation to calculate the normal depth of flow d_o, shown in Table D2.

b. Using the normal depth, solve Equation D9 or use Table D3 for the distance from the flume control gate to the theoretical point of surface roughness inception $X_{I(calc)}$.

c. For most of Killen's (1968) and Straub and Anderson's (1958) tests, the flume control gate was set with openings larger than normal depth causing a retardation of boundary layer development. Thus, adjust the theoretical point of inception with Equation 6 to determine $X_{I(obs)}$.

d. Given $X_{I(obs)}$, compute X^*, the distance along the flow path relative to the POI, with Equation 7.

e. Calculate the dimensionless distance along the flow path with X^*/Y_I, where $Y_I = d_o$.

The results of applying the procedure described above to Straub and Anderson's (1958) observations for a flume slope of 30 deg agreed closely with Killen's (1968) observations of developing flow (Figure 18). Based on this success, the analysis technique was applied to Straub and Anderson's observations for a flume slope of 45 deg (Figure 19), a common slope for CE spillways. Equation 8 was developed through regression analysis and relates entrained air concentration to dimensionless distance along the flow path.

34

Straub and Anderson's observations and the equation were compared with Cain's (1978) observations of developing flow on the Aviemore Spillway in New Zealand (Figure 20). The comparison showed that the equation overpredicted the entrained air concentration by 5 to 6 percent. The reason for this discrepancy is unclear, other than it being the result of measurement uncertainty. However, this error does not negate the usefulness of the relationship for estimating the entrained air concentration in developing flow.

The following steps illustrate a method to apply Equation 8 for estimating the entrained air concentration at any location along the flow path of spillway with a 45-deg slope:

a. Estimate the depth of flow Y_I and the location X_I of surface roughness inception with procedures outlined by Keller, Lai, and Wood (1974).

b. Determine the distance to the POI with Equation 7 and nondimensionalize with X^*/Y_I.

c. Calculate the entrained air concentration with Equation 8 or Figure 19.

For cavitation prevention, a minimum air concentration of 8 percent is required near the cavitating surface to minimize the pitting and surface damage caused by cavitation. An analysis of observed profiles showed that a minimum entrained air concentration of about 20 percent was required to provide that minimum concentration near the spillway or flume surface (Figure 21). The analysis also indicated that this would be achieved on a 45-deg slope at a dimensionless distance of approximately 75 normal depths of flow. For Cain's (1978) tests on the Aviemore Spillway, this translates to distances from the POI of about 38 and 45 ft for the two discharges Cain tested.

The interfacial area contributed by entrained air for inclusion in the mathematical description of gas transfer (Equation 2) can be calculated with the following steps:

a. Use Manning's Equation to calculate the normal depth of flow d_o.

b. With the entrained air concentration from the previous procedure, calculate the volume of entrained air under a unit area of surface with Equation 9.

c. Estimate the maximum bubble diameter d_m with Equation 11.

d. Use Equation 12 to determine the number of bubbles by dividing the volume of entrained air by the volume of the average bubble based on volumetric weighting.

e. Calculate the total bubble surface area under the unit area of surface with Equation 13.

f. Use Equation 14 to calculate the specific surface area *A/V* for use in Equation 2.

The procedures outlined in this report provide a method of estimating the concentration of entrained, entrapped, and total conveyed air for aerated flow on a spillway. The entrapped air concentration is constant at 23 percent by volume. The entrained air concentration gradually varies in the region of developing aerated flow reaching an equilibrated concentration of 48 percent by volume for flow on a 45-deg slope. The concentration of entrained air can be computed for any location along the aerated flow path. Having the concentration of entrained air is useful for two purposes: (a) defining the location where sufficient entrained air is available at the spillway surface to prevent cavitation damage and (b) defining the surface area made available for oxygen absorption by the entrained air bubbles. A procedure is provided that shows calculations of entrained air concentration for these purposes.

References

Bauer, W. J. (1954). "Turbulent boundary layer on steep slopes," *Transactions of the American Society of Civil Engineers* 119(2719), 1212-1242.

Blevins, R. D. (1984). *Applied fluid dynamics handbook.* van Nostrand Reinhold Company, Inc., New York.

Cain, P. (1978). "Measurements within self-aerated flow on a large spillway," Ph.D. thesis, University of Caterbury, Christchurch, New Zealand.

Cain, P., and Wood, I. R. (1981). "Measurements of self-aerated flow on a spillway," *Journal of the Hydraulics Division,* American Society of Civil Engineers, 107 (HY11), 1524-1444.

Danckwerts, P. V. (1951). "Significance of liquid-flim coefficients in gas absorption," *Industrial and Engineering Chemistry* 46(6), 1460-1467.

Ehrenberger, R. (1926). "Flow of water in steep chutes with special reference to self-aeration," Translated by E. F. Wilsey from "Wasserbewegung in Steilen Rinnen (Schusstennen) mit besonder Berucksichtigung der Selbstbeluftung," Osterreichischer Ingenieur - und Architektverein, No. 15/16 and 17/18.

Falvey H. T., and Irvine, D. A. (1988). "Aeration in jets and high velocity flows." *Proceedings of the international symposium on model-prototype correlation of hydraulic structures.* P. H. Burgi, ed., American Society of Civil Engineers, 25-55.

Gulliver, J. S., Thene, J. R., and Rindels, A. J. (1990). "Indexing gas transfer in self-aerated flows," *Journal of the Environmental Engineering Division,* American Society of Civil Engineers, 116(EE3), 1107-1124.

Hinze, J. O. (1955). "Fundamental of the hydrodynamic mechanism of splitting in dispersion processes," *Journal of the American Institute of Chemical Engineering* 1(3), 289-295.

_____. (1959). *Turbulence*. 2nd ed., McGraw-Hill Book Co., New York.

Keller, R. J., Lai, K. K., and Wood, I. R. (1974). "Developing region in self-aerated flows," *Journal of the Hydraulics Division*, American Society of Civil Engineers, 100(HY4), 553-568.

Killen, J. M. (1968). "The surface characteristics of self aerated flow in steep channels," Ph.D. thesis, University of Minnesota, Minneapolis, MN.

_____. (1982). "Maximum stable bubble size and associated noise spectra in a turbulent boundary layer," *Cavitation and Polyphase Flow Forum*. American Society of Mechanical Engineers, 1-3, New York.

Lamb, O. P., and Killen, J. M. (1950). "An electrical method for measuring air concentration in flowing air-water mixtures," Technical Paper No. 2, Series B, University of Minnesota, St. Anthony Falls Hydraulic Laboratory, Minneapolis, MN.

Peterka, A. J. (1953). "The effect of entrained air on cavitation pitting." *Proceedings of the Minnesota international hydraulics convention*. University of Minnesota, St. Anthony Falls Hydraulic Laboratory, Minneapolis, MN, 507-518.

Ruze, X. (1988). "Characteristics of self-aerated flow on steep chutes." *Proceedings of the international symposium on hydraulics for high dams*. International Association for Hydraulic Research, Beijing, China, 68-75.

Sevik, M., and Park, S. H. (1973). "The splitting of drops and bubbles by turbulent fluid flow," *Journal of Fluids Engineering* 95(1), 53-60.

Straub, L., and Anderson, A. (1958). "Experiments on self aerated flow in open channels," *Journal of the Hydraulics Division*, American Society of Civil Engineers, 84(HY7), Paper No. 1890, 1-35.

Tennekes, H., and Lumley, J. L. (1972). *A first course in turbulence*. MIT Press, Cambridge, MA.

Wilhelms, S. C., and Gulliver, J. S. (1990). "Physical processes affecting reaeration at low-head weirs." *Proceedings of the eighth CE water quality seminar, Las Vegas, NV, 6-7 February 1990*. 135-141.

Wilhelms, S. C., Schneider, M. L., and Howington, S. E. (1987). "Improvement of hydropower release dissolved oxygen with turbine venting," Technical Report E-87-3, U.S. Army Engineer Waterways Experiment Station, Vicksburg, MS.

38

Wood, I. R. (1983). "Uniform region of self-aerated flow," *Journal of Hydraulic Engineering*, American Society of Civil Engineers 109 (3), 447-461.

Wood, I. R. (1985). "Air water flows," Keynote address. *Proceedings of the 21st Congress*. International Association for Hydraulic Research, Melbourne, Australia, 6, 18-29.

References

Appendix A
Killen's Measurements of
Self-Aerated Flow, Graphical
Form
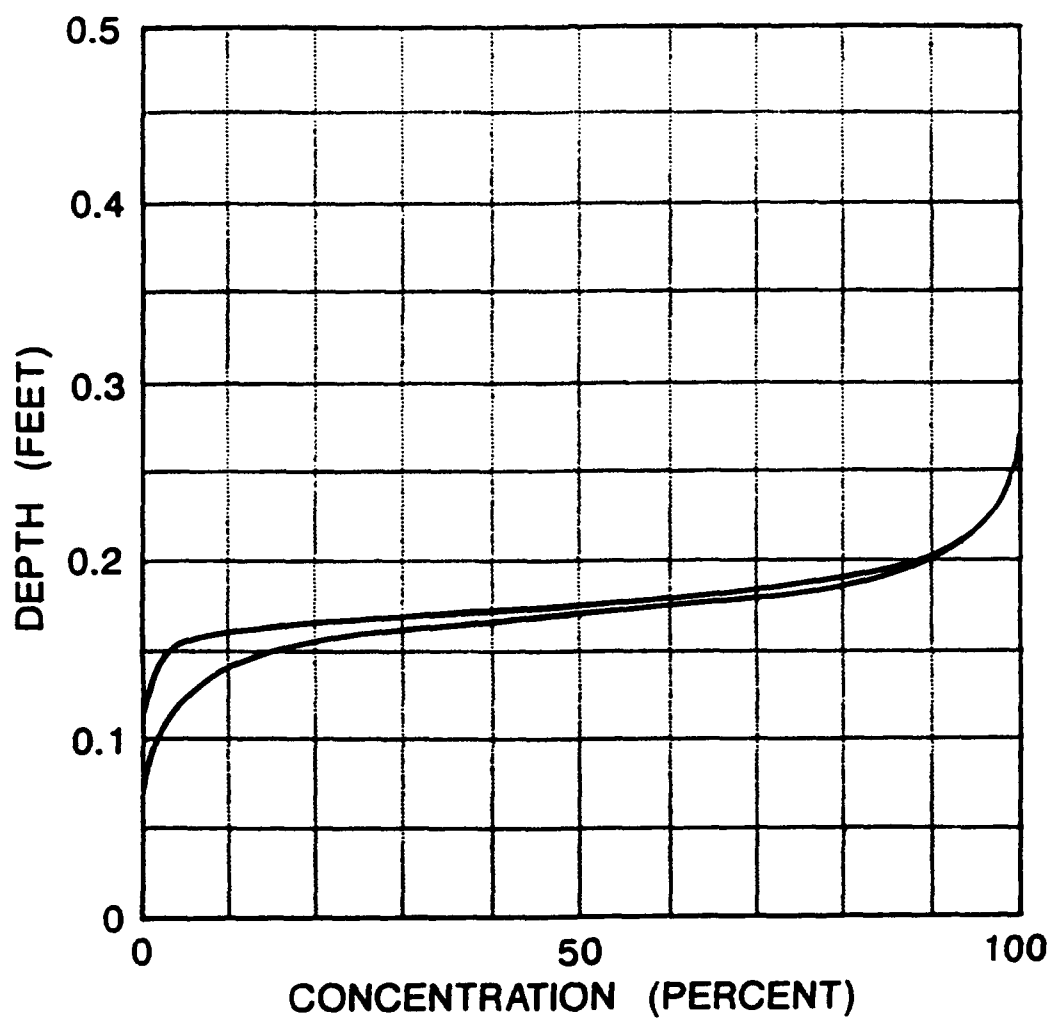
Profile 1.1, Slope = 30 Degrees, Q = 6.4 cfs,
Location in Flume = 12 ft
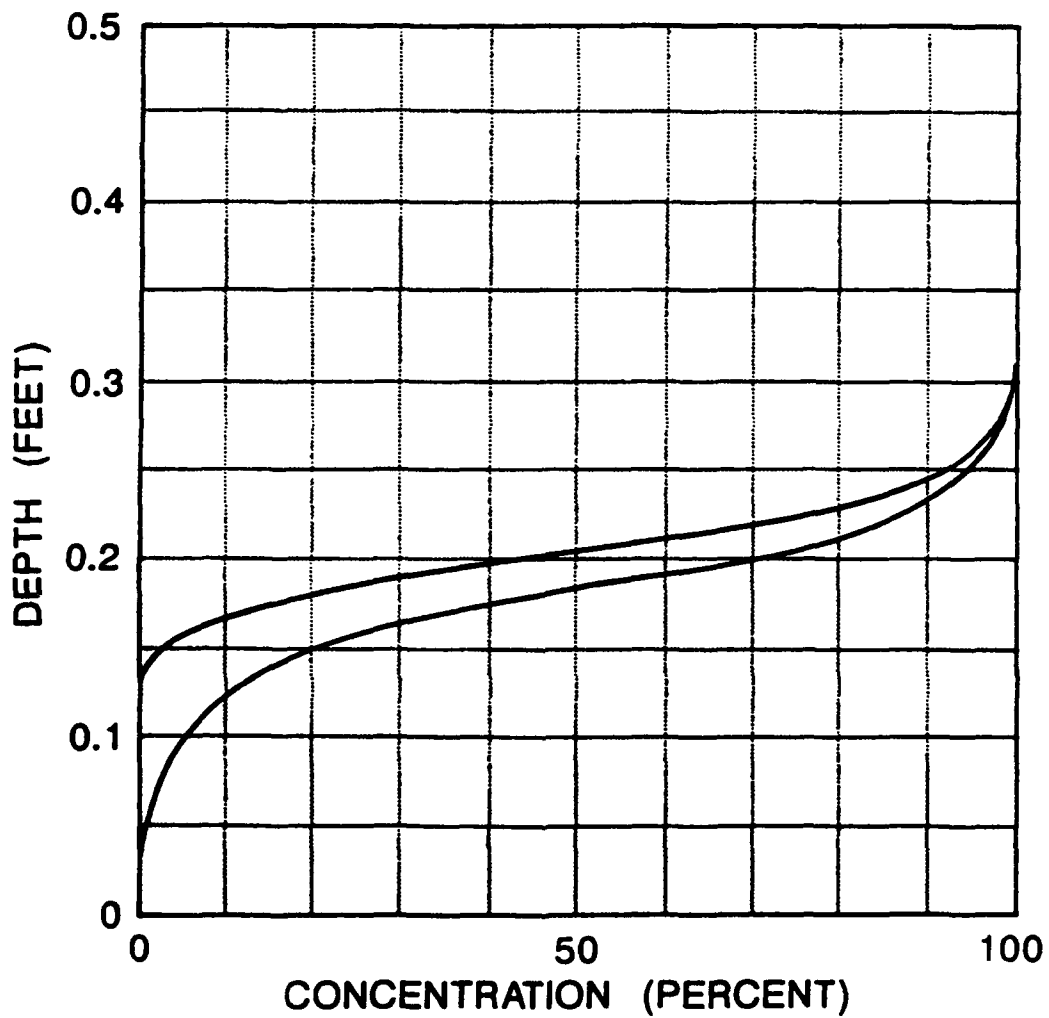
Profile 1.2, Slope = 30 Degrees, Q = 6.4 cfs,
Location in Flume = 18 ft
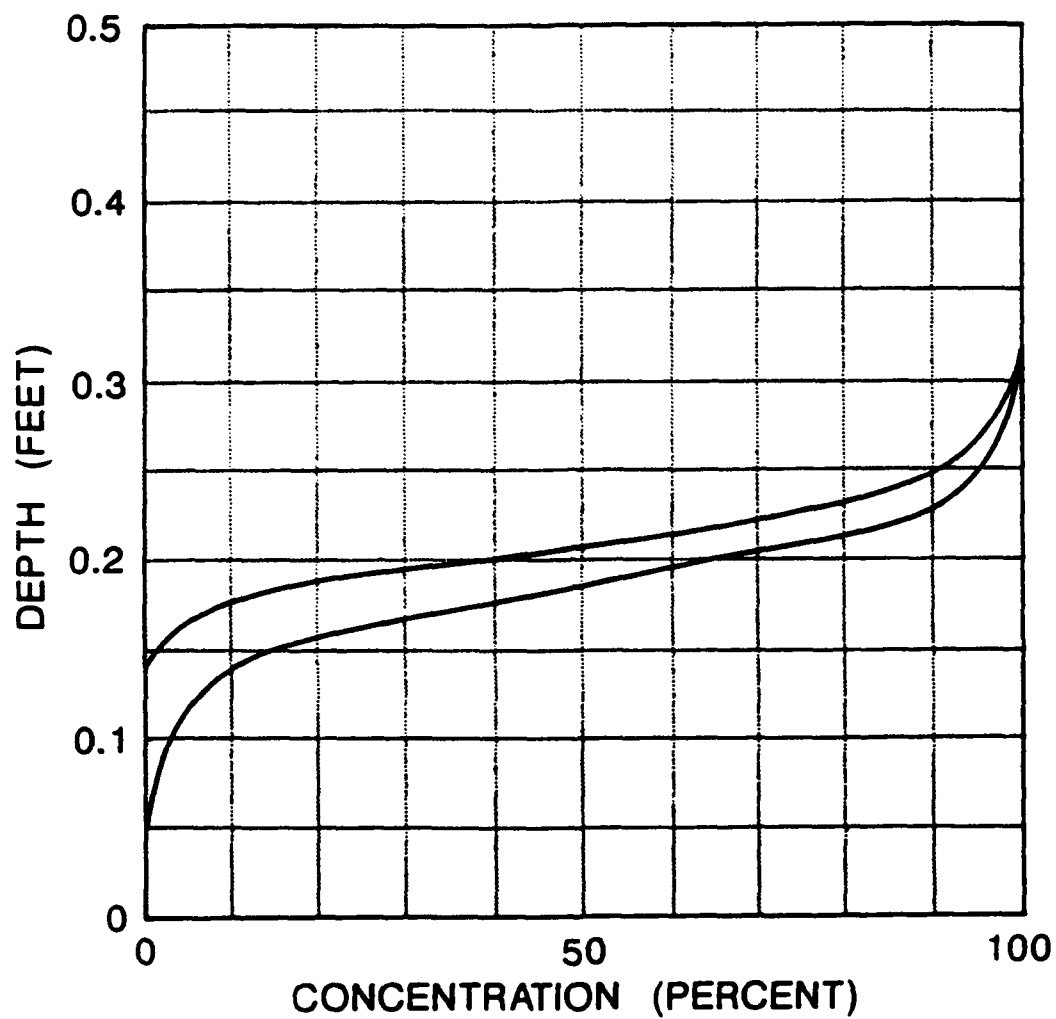
Profile 1.3, Slope = 30 Degrees, Q = 6.4 cfs,
Location in Flume = 30 ft
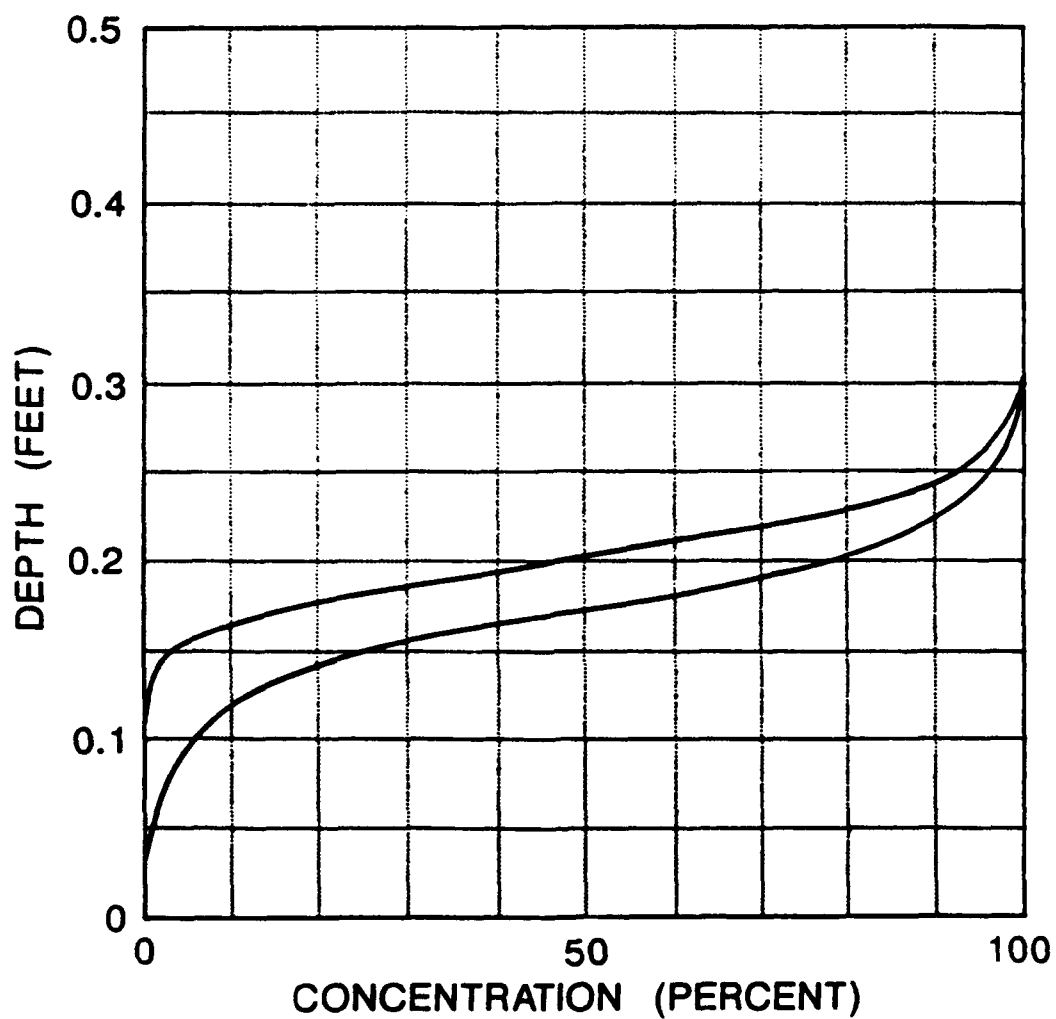
Profile 1.4, Slope = 30 Degrees, Q = 6.4 cfs,
Location in Flume = 24 ft
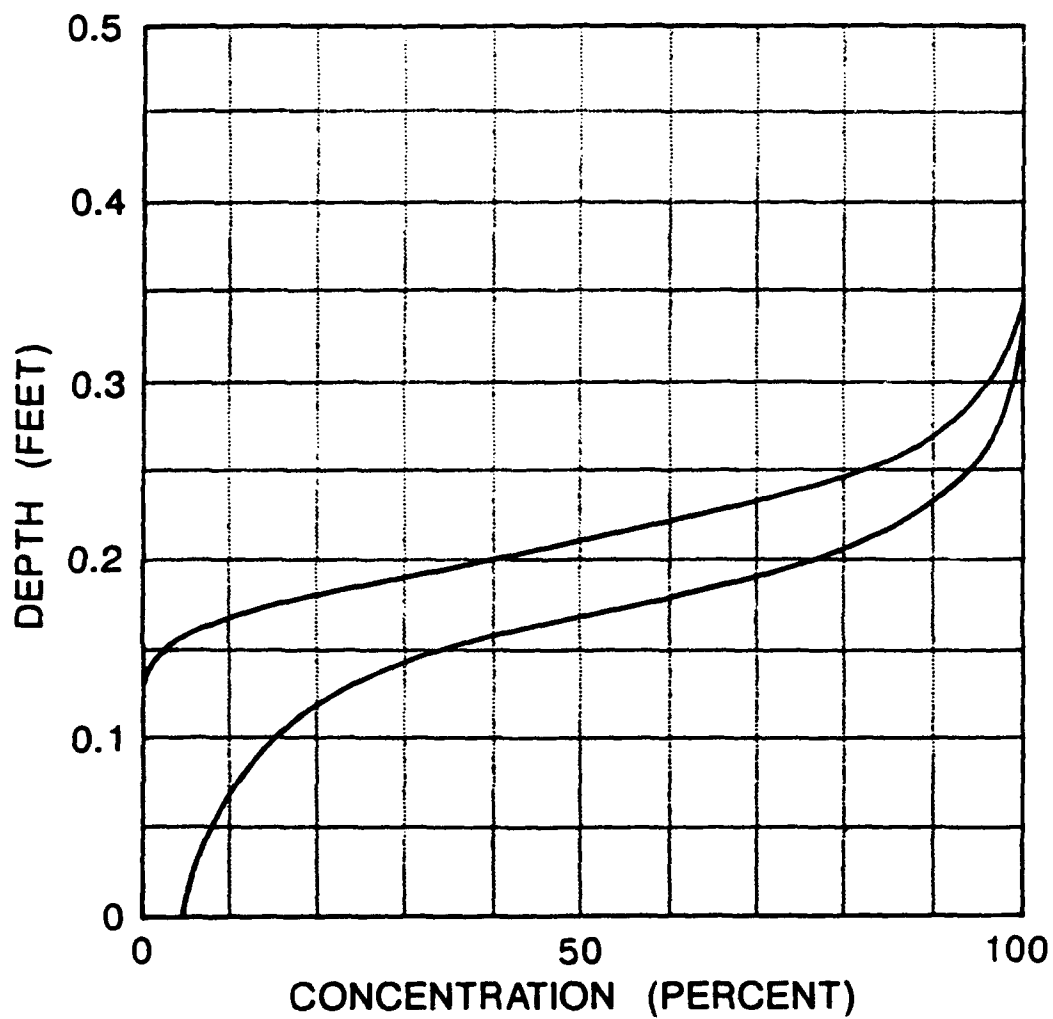
Profile 1.5, Slope = 30 Degrees, Q = 6.4 cfs,
Location in Flume = 34 ft
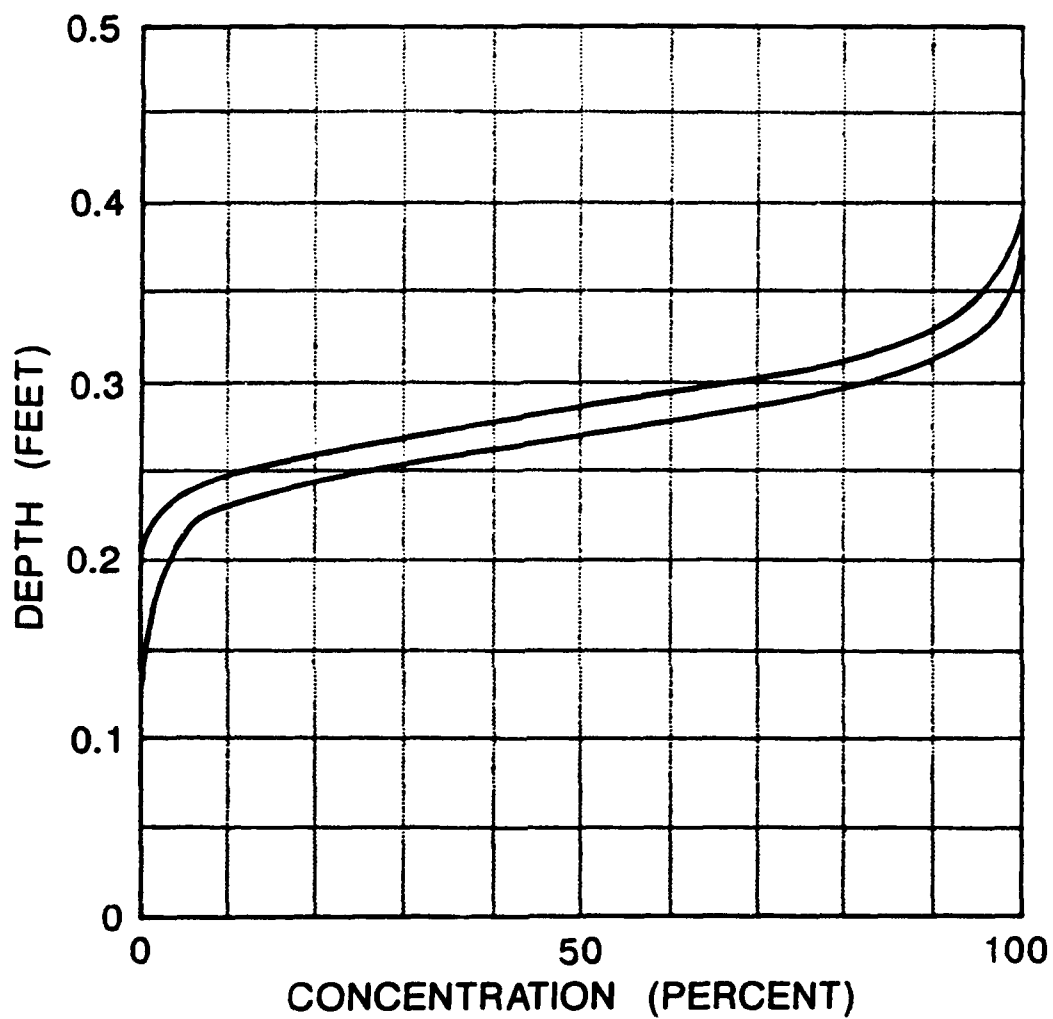
Profile 2.1, Slope = 30 Degrees, Q = 12.8 cfs,
Location in Flume = 20 ft
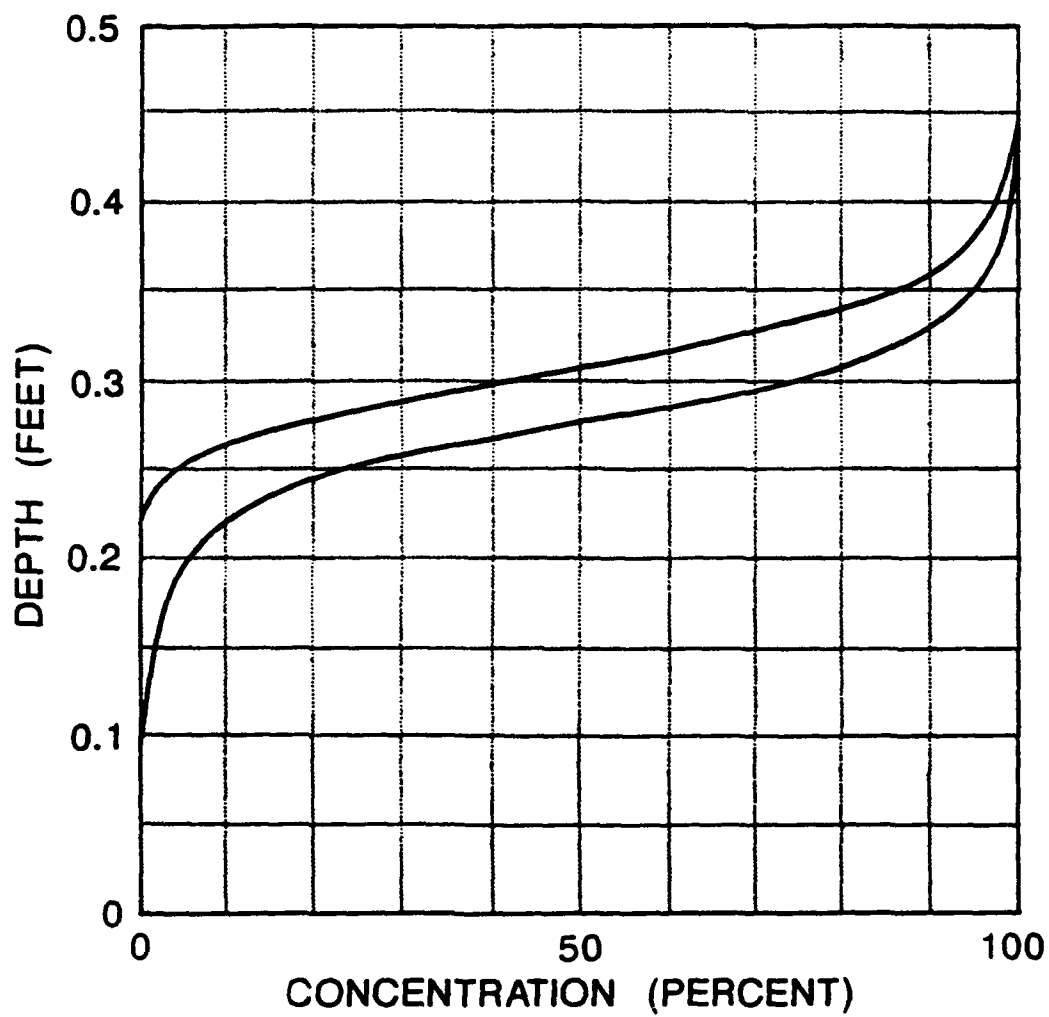
Profile 2.2, Slope = 30 Degrees, Q = 12.8 cfs,
Location in Flume = 24 ft
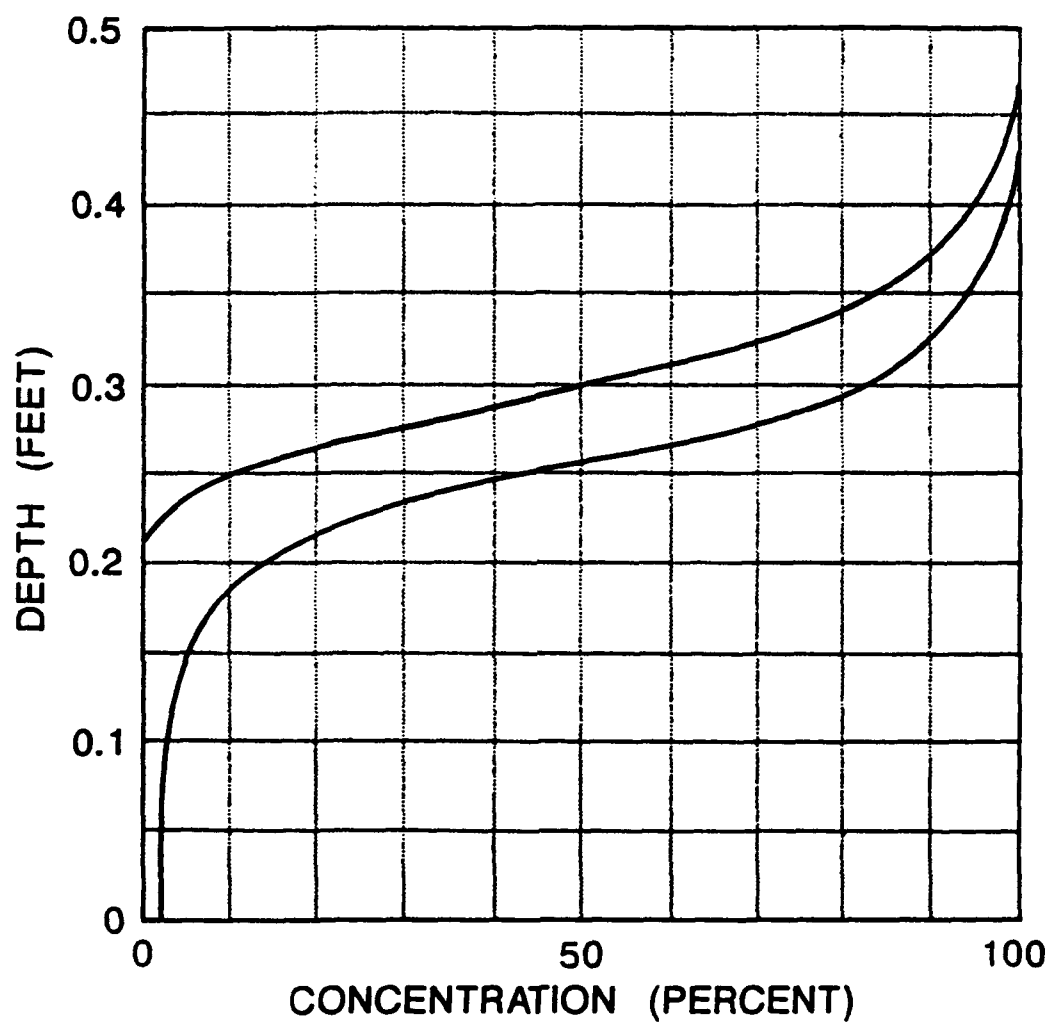
Profile 2.3, Slope = 30 Degrees, Q = 12.8 cfs,
Location in Flume = 30 ft
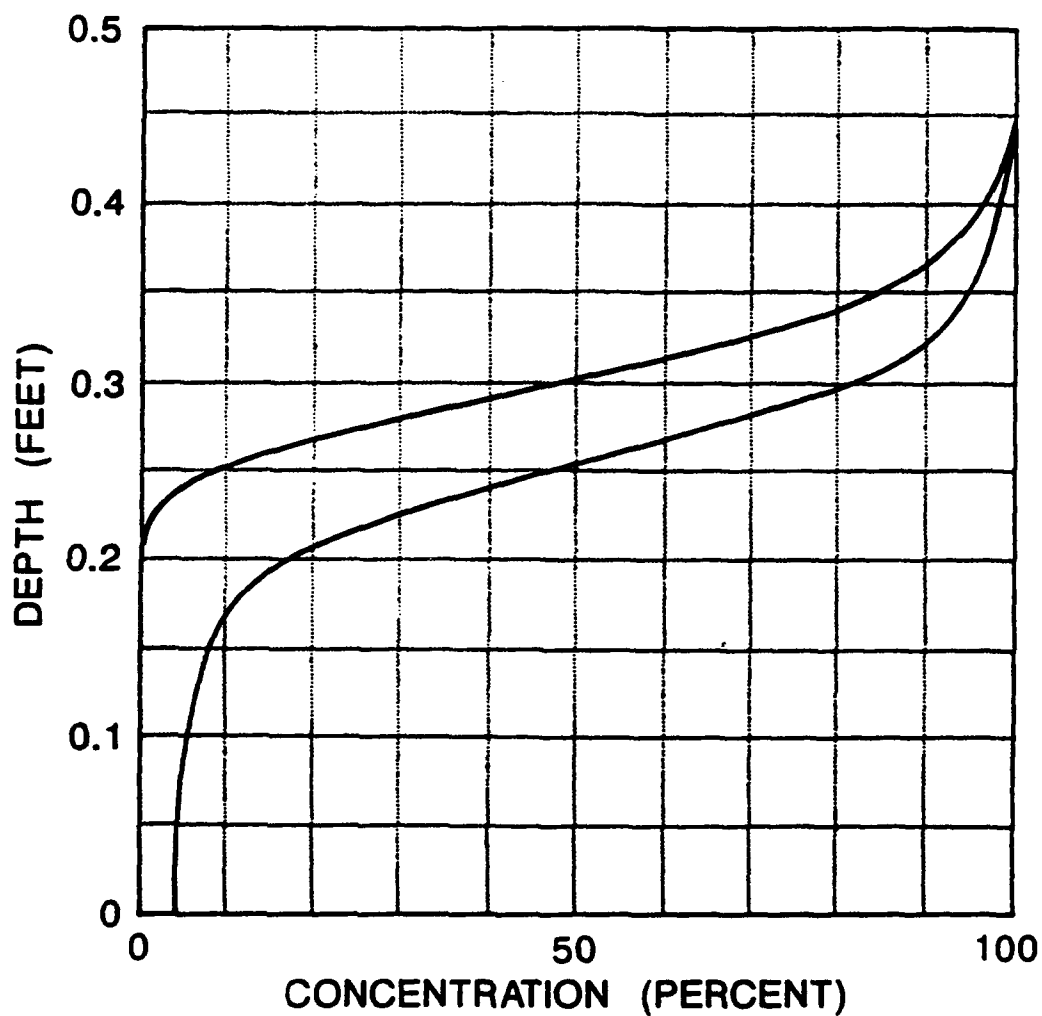
Profile 2.4, Slope = 30 Degrees, Q = 12.8 cfs,
Location in Flume = 38 ft
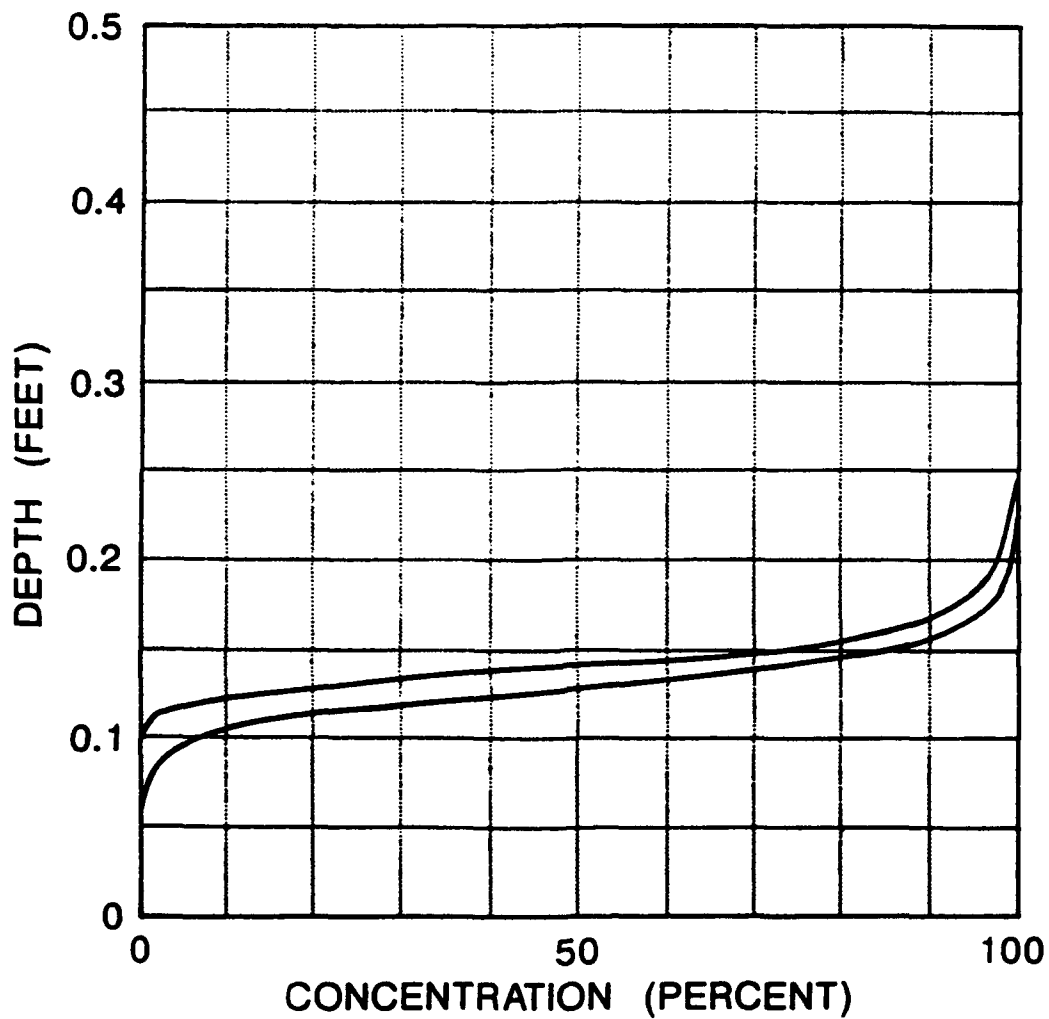
Profile 3.1, Slope = 52.5 Degrees, Q = 6.4 cfs,
Location in Flume = 7 ft
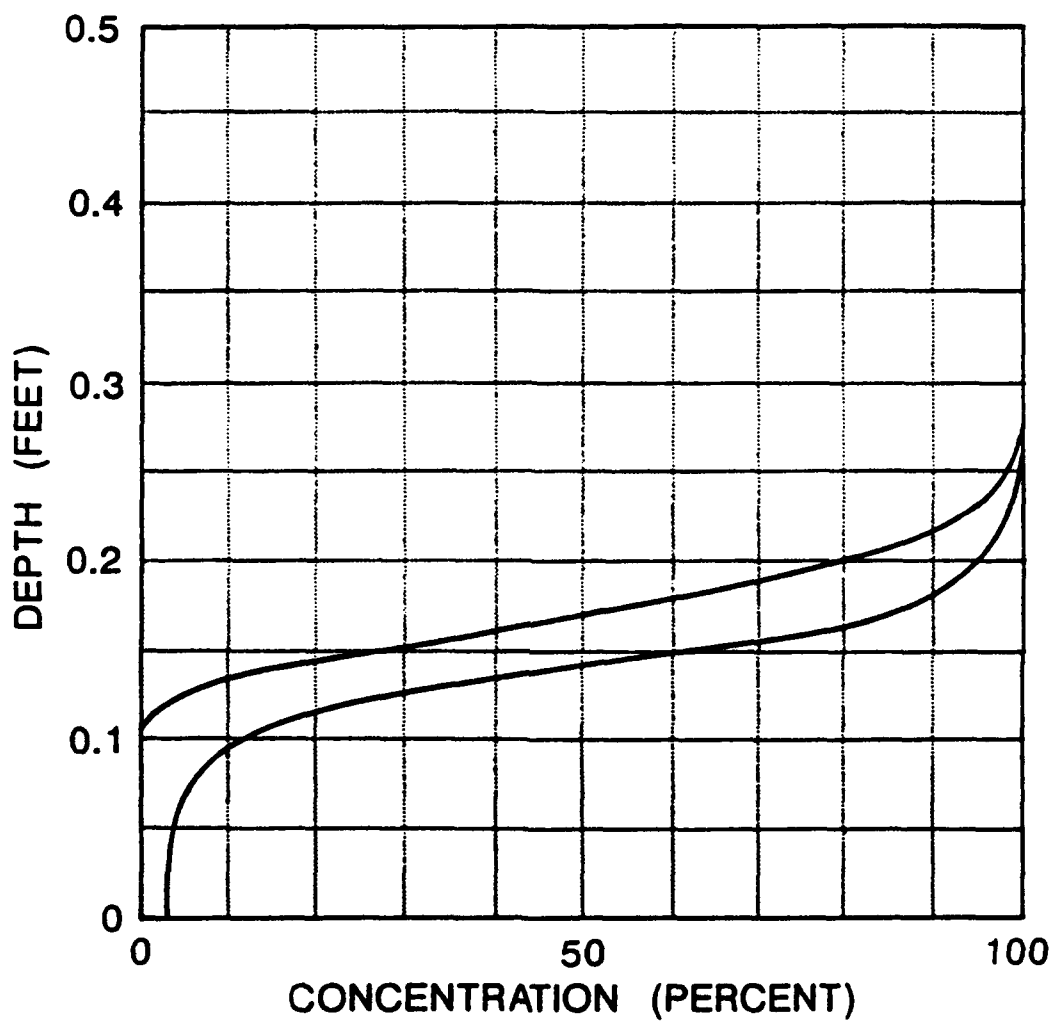
Profile 3.2, Slope = 52.5 Degrees, Q = 6.4 cfs,
Location in Flume = 9 ft
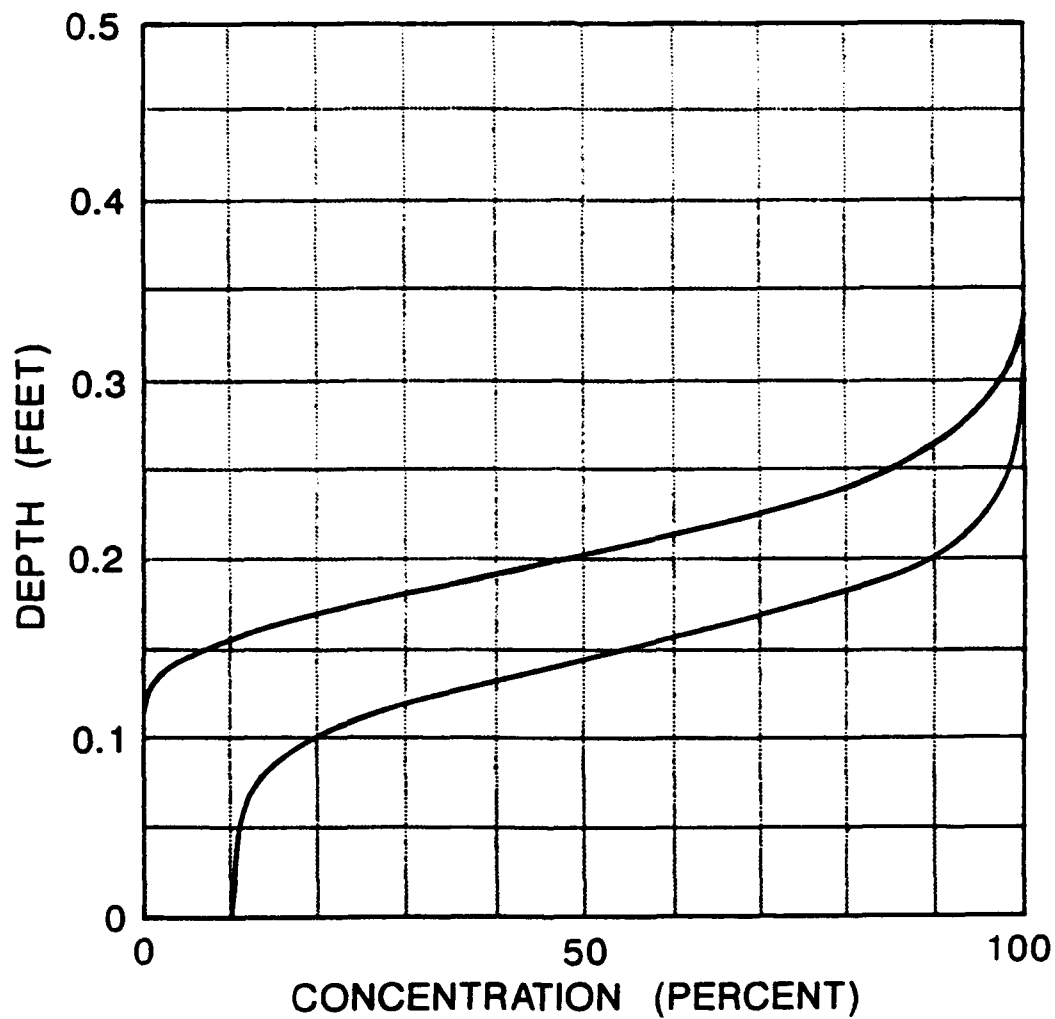
Profile 3.3, Slope = 52.5 Degrees, Q = 6.4 cfs,
Location in Flume = 12 ft
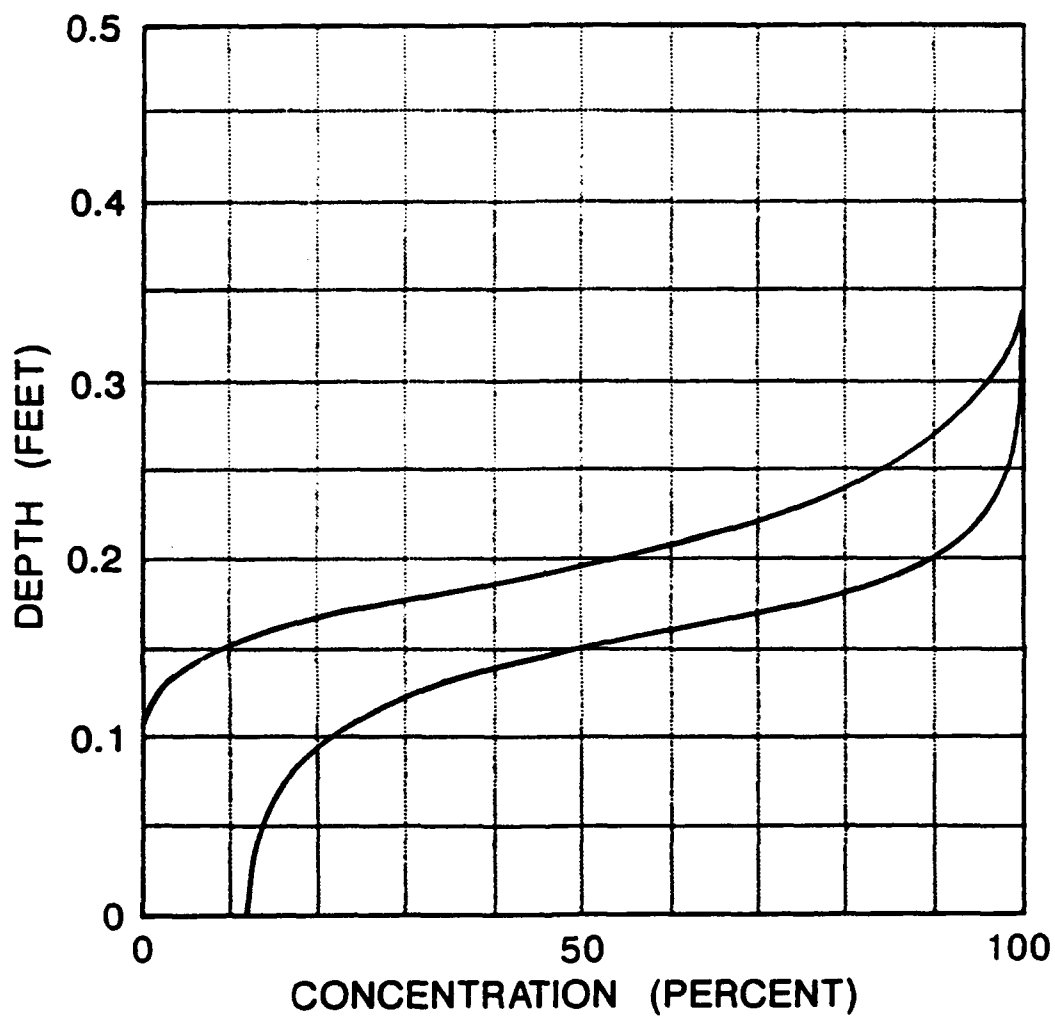
Profile 3.4, Slope = 52.5 Degrees, Q = 6.4 cfs,
Location in Flume = 14 ft
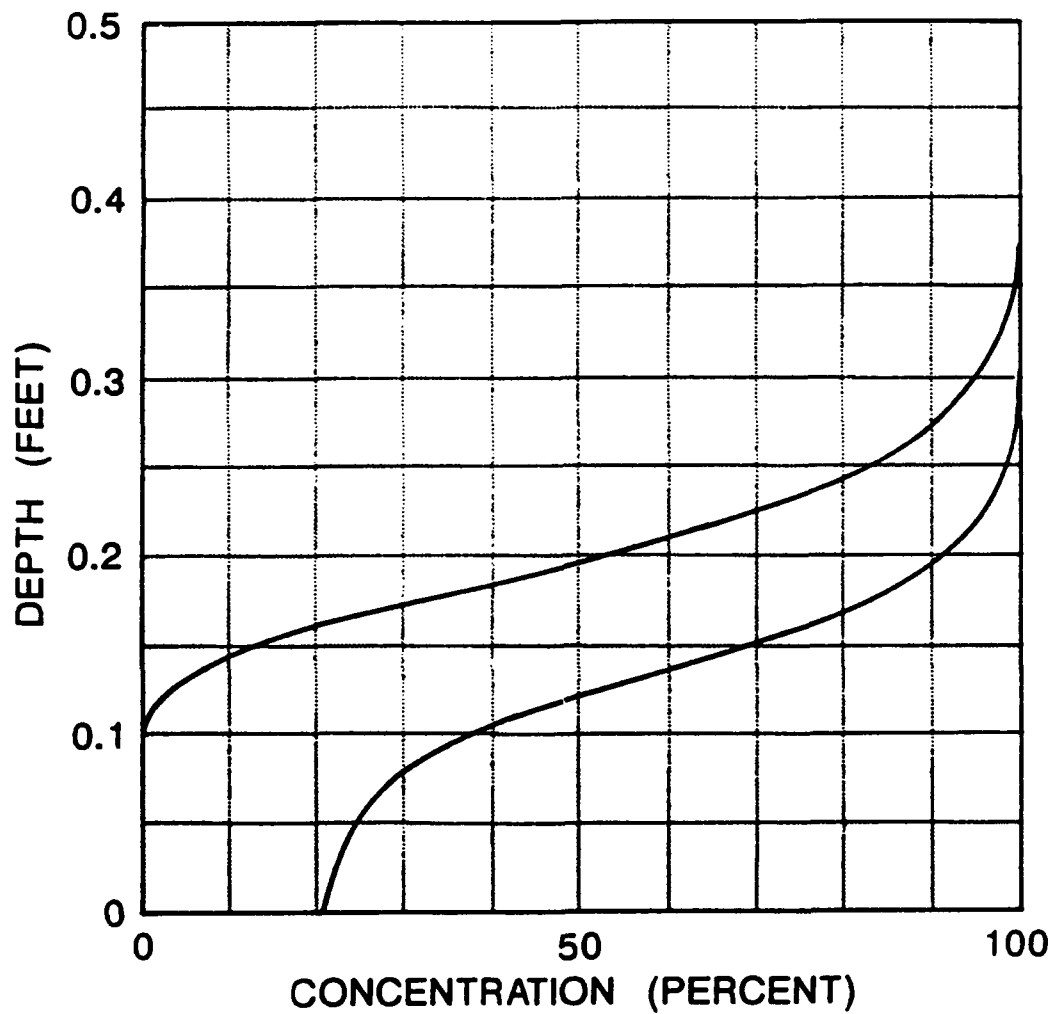
Profile 3.5, Slope = 52.5 Degrees, Q = 6.4 cfs,
Location in Flume = 20 ft
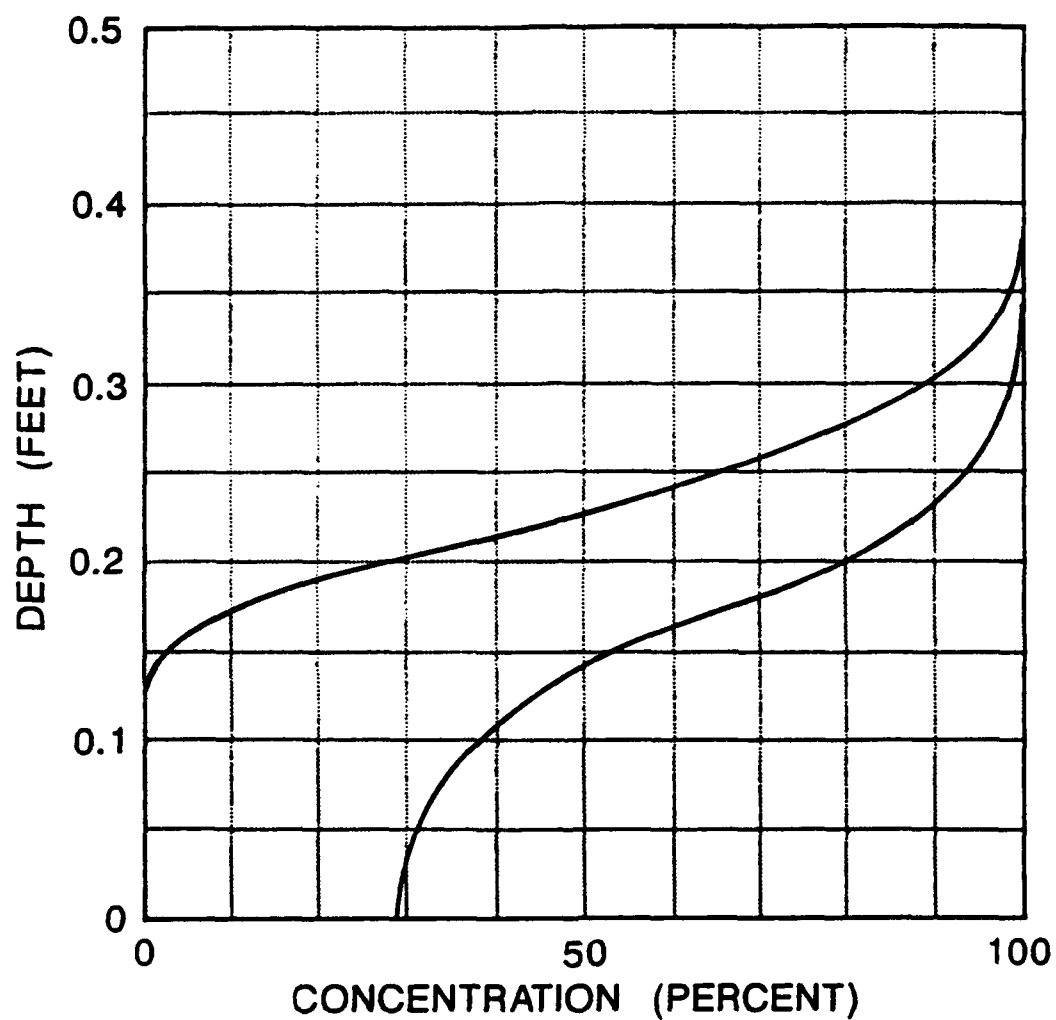
Profile 3.6, Slope = 52.5 Degrees, Q = 6.4 cfs,
Location in Flume = 25 ft
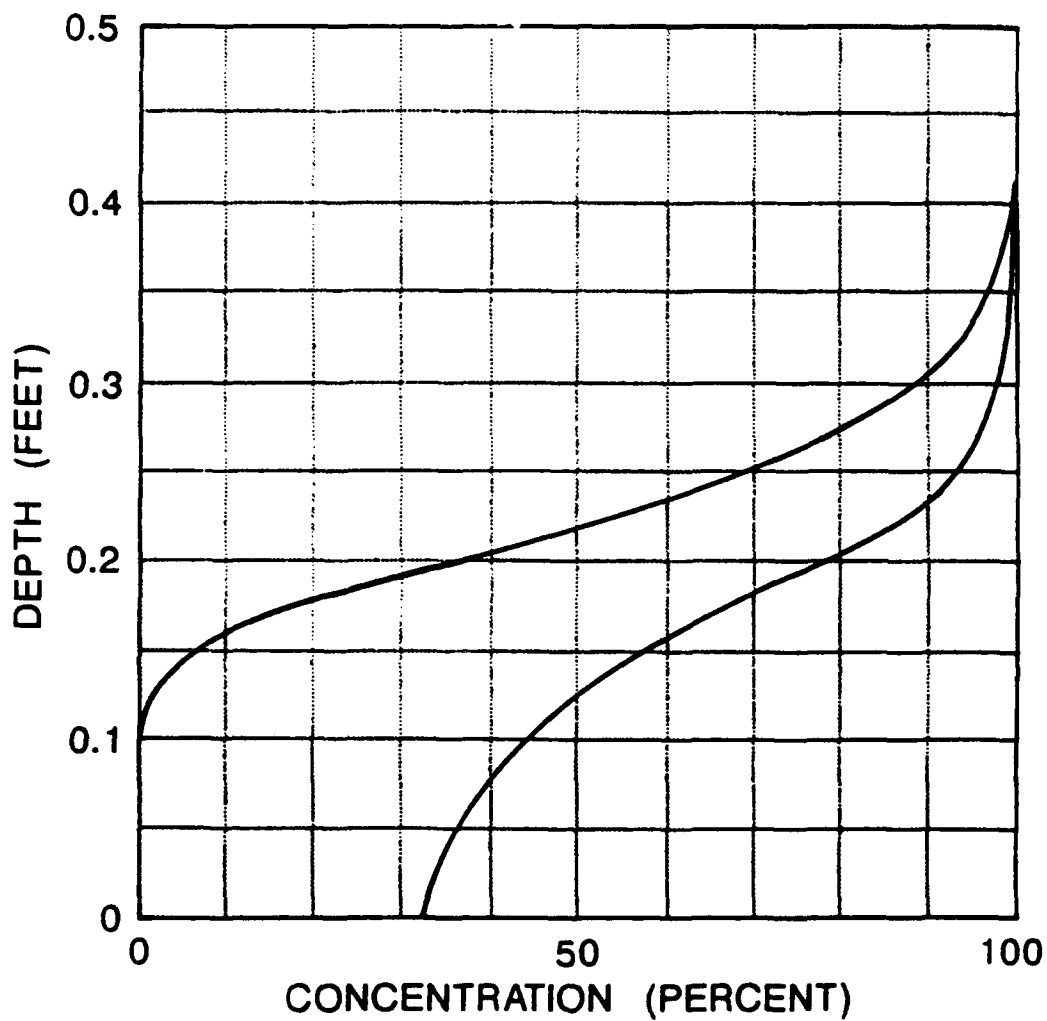
Profile 3.7, Slope = 52.5 Degrees, Q = 6.4 cfs,
Location in Flume = 30 ft
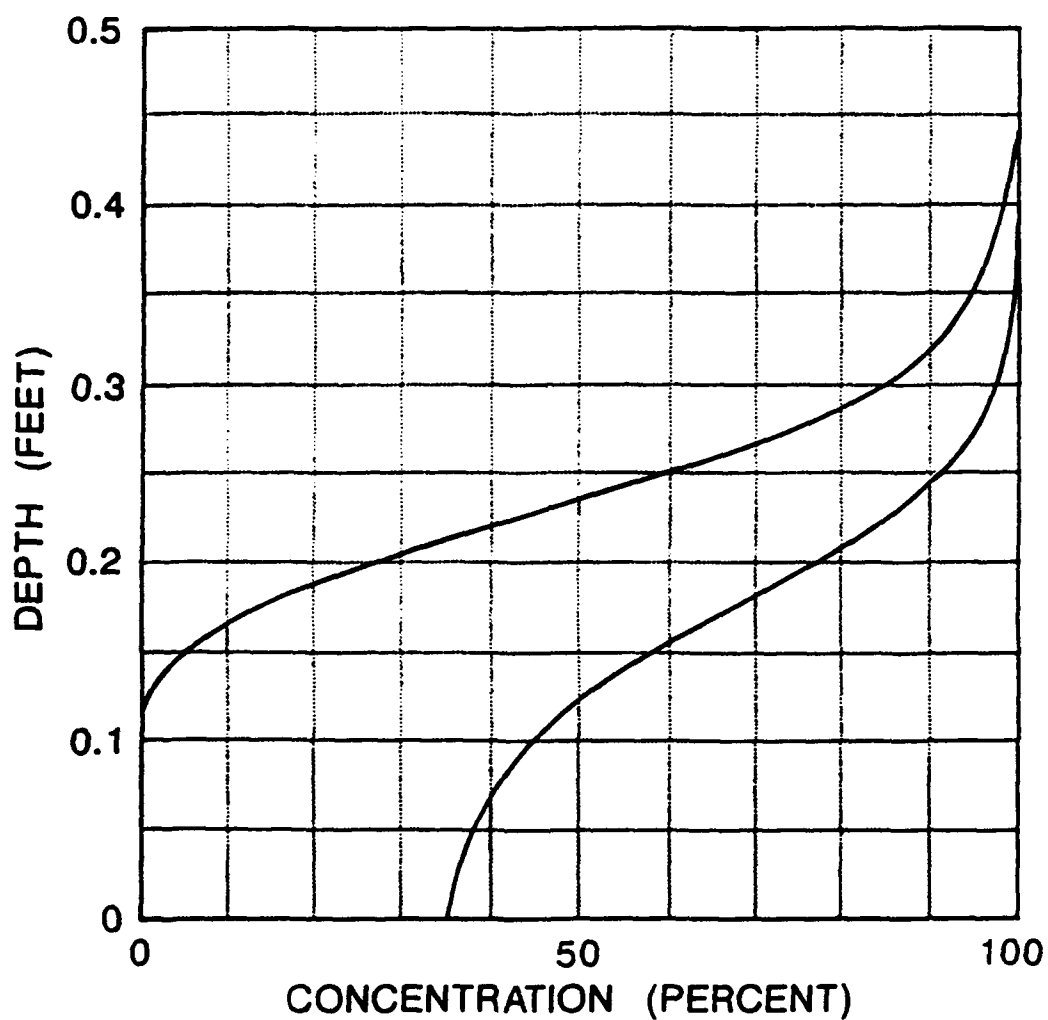
Profile 3.8, Slope = 52.5 Degrees, Q = 6.4 cfs,
Location in Flume = 35 ft
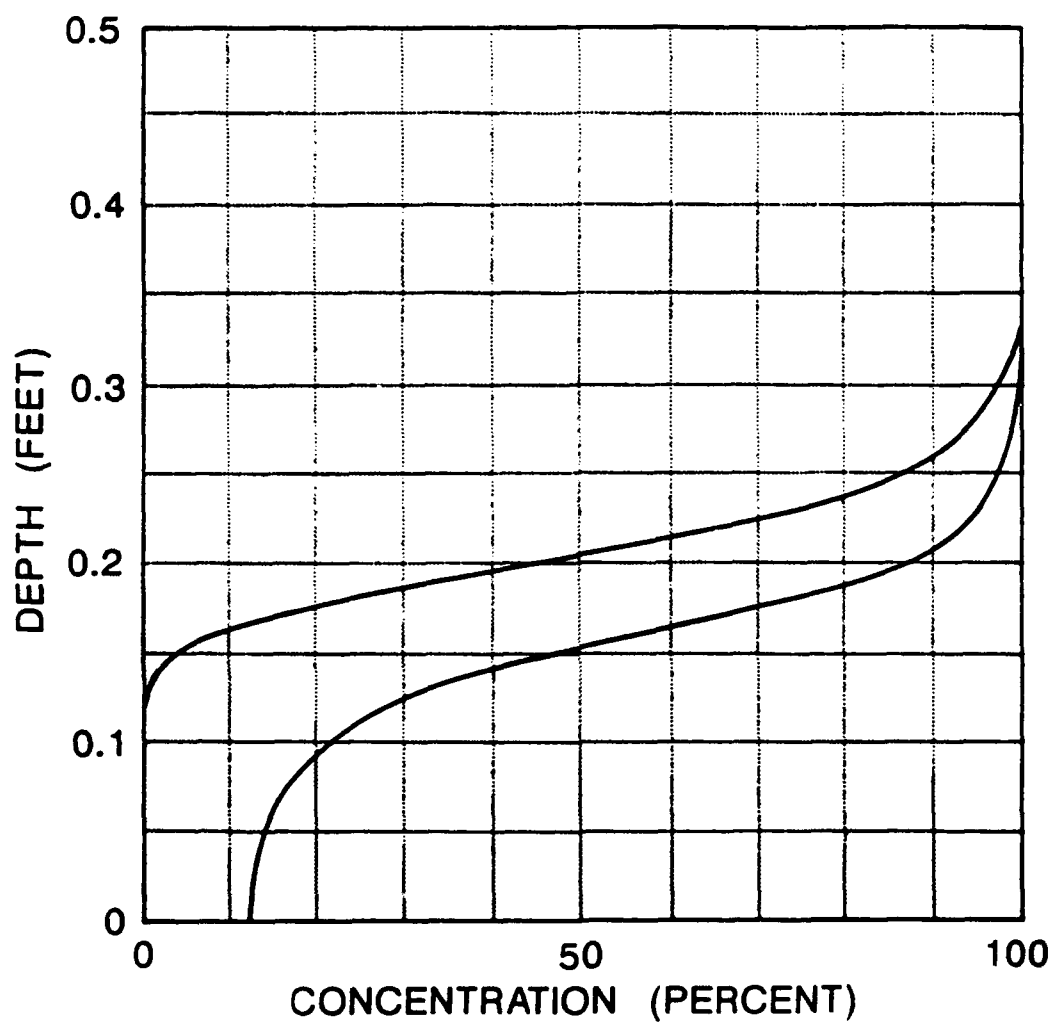
Profile 4.1, Slope = 30 Degrees, Q = 3.2 cfs,
Location in Flume = 12 ft
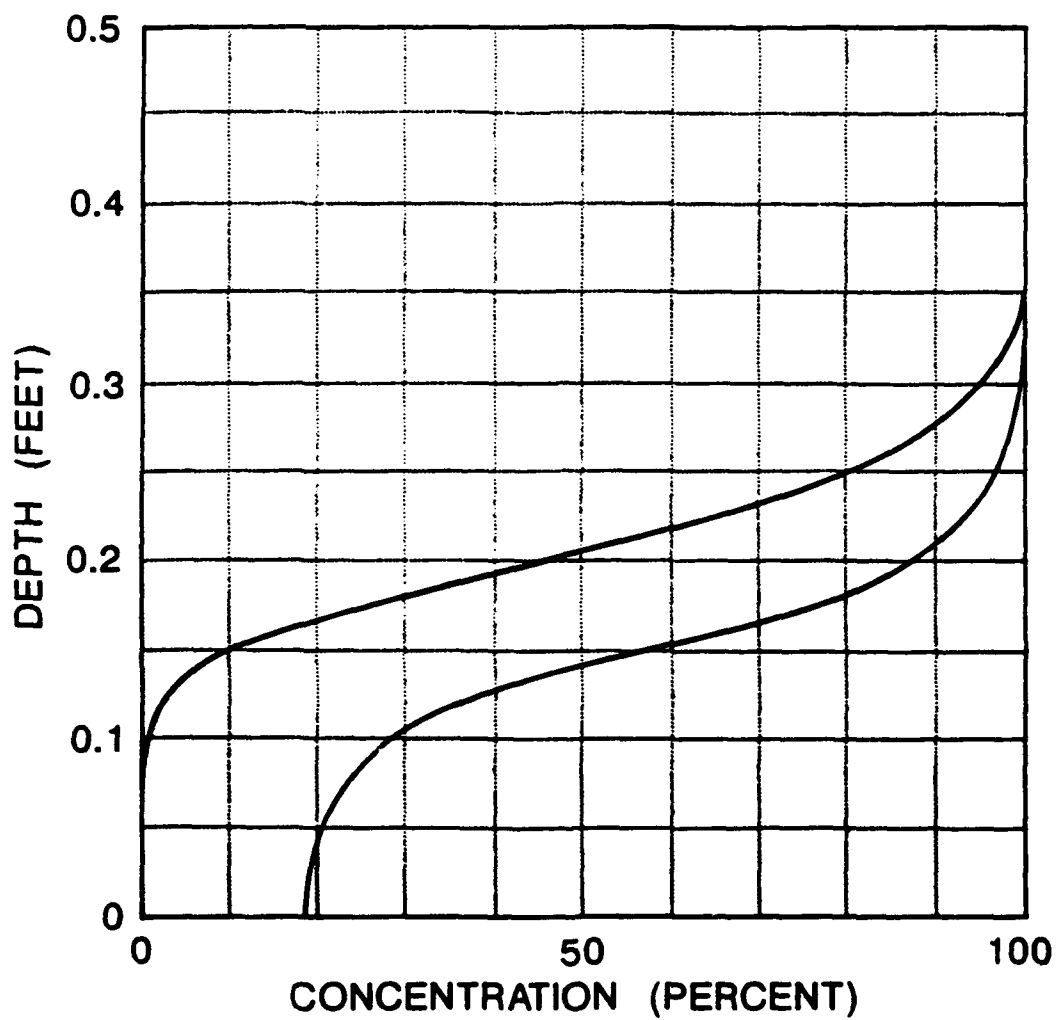
Profile 4.2, Slope = 30 Degrees, Q = 3.2 cfs,
Location in Flume = 18 ft
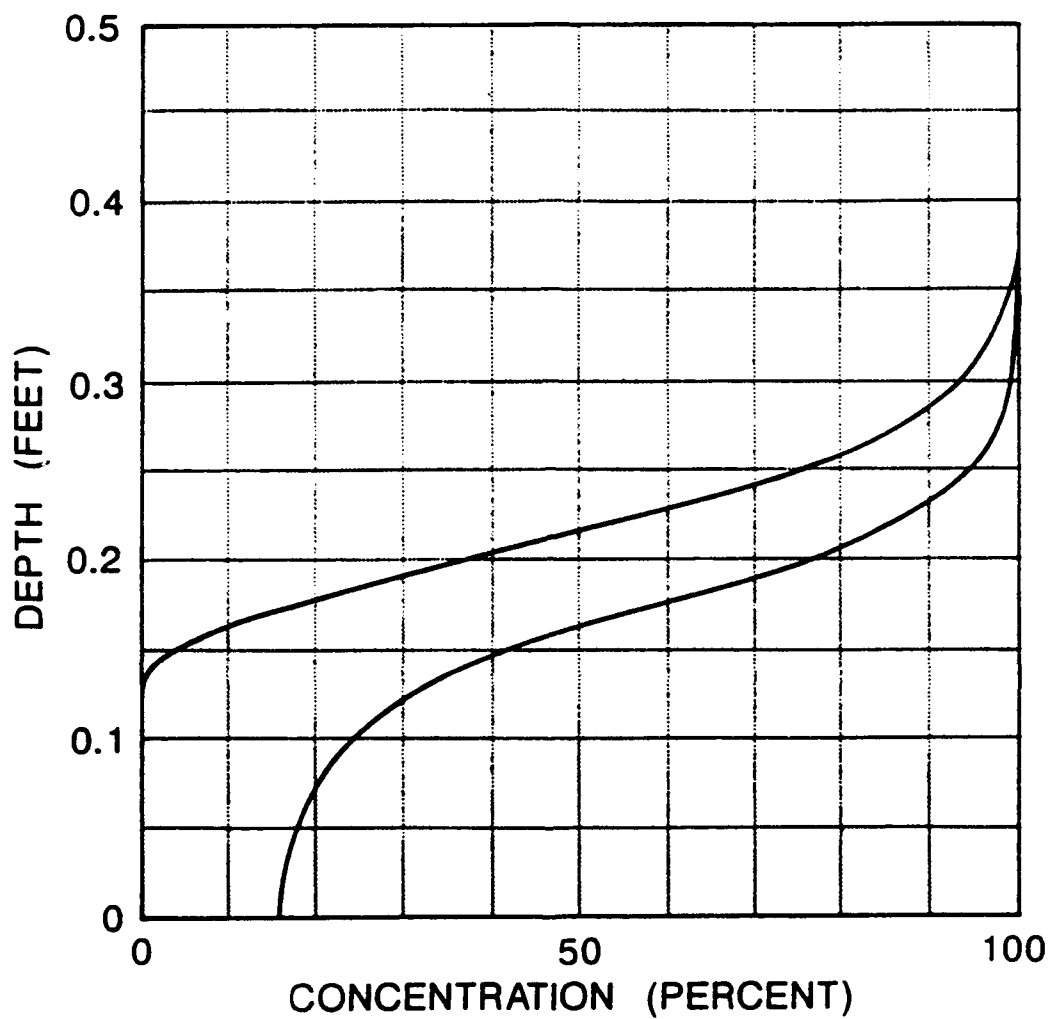
Profile 4.3, Slope = 30 Degrees, Q = 3.2 cfs,
Location in Flume = 35 ft

Appendix B
Killen's Measurements of Self-Aerated Flow, Tabular Form

Table B1
Total Conveyed Air and Entrapped Air Concentrations, Killen Data, Test 1, Slope = 30 deg, Discharge = 6.4 cfs

Profile	1		2		3		4		5	
Distance,[1] ft	12		18		24		30		34	
Depth, ft	Entrapped	Total	Entrapped	Total	Entrapped	Total	Entrapped	Total	Entrapped	Total
0.00	0.00	0.00	0.00	0.00	0.00	0.00	0.00	0.00	0.00	0.05
0.02	0.00	0.00	0.00	0.00	0.00	0.00	0.00	0.00	0.00	0.06
0.04	0.00	0.00	0.00	0.01	0.00	0.01	0.00	0.00	0.00	0.07
0.06	0.00	0.00	0.00	0.02	0.00	0.02	0.00	0.01	0.00	0.09
0.08	0.00	0.01	0.00	0.03	0.00	0.03	0.00	0.02	0.00	0.12
0.10	0.00	0.02	0.00	0.05	0.00	0.06	0.00	0.03	0.00	0.15
0.12	0.01	0.04	0.00	0.09	0.01	0.09	0.00	0.05	0.00	0.21
0.14	0.02	0.10	0.01	0.15	0.02	0.19	0.00	0.11	0.01	0.29
0.16	0.10	0.26	0.06	0.27	0.07	0.34	0.03	0.23	0.06	0.43
0.18	0.59	0.70	0.19	0.44	0.22	0.59	0.13	0.45	0.22	0.62
0.20	0.88	0.90	0.43	0.71	0.47	0.77	0.39	0.65	0.40	0.77

(Continued)

[1] Distance measured along flume from upstream end.

Table B1 (Concluded)

Profile	1		2		3		4		5	
Distance,[1] ft	12		18		24		30		34	
Depth, ft	Entrapped	Total	Entrapped	Total	Entrapped	Total	Entrapped	Total	Entrapped	Total
0.22	0.96	0.96	0.68	0.84	0.69	0.88	0.66	0.85	0.59	0.86
0.24	0.98	0.98	0.87	0.92	0.88	0.94	0.85	0.93	0.76	0.92
0.26	0.99	0.99	0.95	0.96	0.95	0.97	0.94	0.96	0.87	0.96
0.28	1.00	1.00	0.98	0.98	0.98	0.99	0.96	0.98	0.92	0.98
0.30	--	--	0.99	0.99	1.00	1.00	0.98	0.99	0.96	0.99
0.32	--	--	1.00	1.00	--	--	1.00	1.00	0.98	0.99
0.34	--	--	--	--	--	--	--	--	1.00	1.00

Appendix B   Killen's Measurements of Self-Aerated Flow, Tabular Form

Table B2
Total Conveyed Air and Entrapped Air Concentrations, Killen Data, Test 2, Slope = 30 deg, Discharge = 12.8 cfs

Profile	1		2		3		4	
Distance, ft	20		24		30		38	
Depth, ft	Entrapped	Total	Entrapped	Total	Entrapped	Total	Entrapped	Total
0.00	0.00	0.00	0.00	0.00	0.00	0.02	0.00	0.04
0.02	0.00	0.00	0.00	0.00	0.00	0.02	0.00	0.04
0.04	0.00	0.00	0.00	0.00	0.00	0.02	0.00	0.04
0.06	0.00	0.00	0.00	0.00	0.00	0.02	0.00	0.05
0.08	0.00	0.00	0.00	0.00	0.00	0.02	0.00	0.05
0.10	0.00	0.00	0.00	0.00	0.00	0.03	0.00	0.05
0.12	0.00	0.00	0.00	0.01	0.00	0.04	0.00	0.06
0.14	0.00	0.01	0.00	0.02	0.00	0.05	0.00	0.07
0.16	0.00	0.01	0.00	0.02	0.00	0.06	0.00	0.09
0.18	0.00	0.02	0.00	0.03	0.00	0.08	0.00	0.12
0.20	0.00	0.03	0.00	0.05	0.00	0.14	0.00	0.17
0.22	0.02	0.08	0.00	0.10	0.01	0.22	0.01	0.27
0.24	0.06	0.17	0.02	0.18	0.05	0.33	0.04	0.39

(Continued)

Appendix B   Killen's Measurements of Self-Aerated Flow, Tabular Form

Table B2 (Concluded)

Profile	1		2		3		4	
Distance, ft	20		24		30		38	
Depth, ft	Entrapped	Total	Entrapped	Total	Entrapped	Total	Entrapped	Total
0.26	0.21	0.38	0.08	0.32	0.16	0.53	0.15	0.54
0.28	0.44	0.63	0.24	0.55	0.33	0.71	0.31	0.68
0.30	0.66	0.82	0.41	0.74	0.50	0.83	0.47	0.81
0.32	0.85	0.93	0.64	0.86	0.66	0.88	0.64	0.89
0.34	0.93	0.97	0.81	0.93	0.78	0.92	0.78	0.93
0.36	0.97	0.99	0.91	0.96	0.86	0.95	0.88	0.96
0.38	0.99	1.00	0.95	0.98	0.91	0.97	0.92	0.97
0.40	1.00	1.00	0.97	0.99	0.95	0.99	0.96	0.98
0.42	--	--	0.98	1.00	0.97	0.99	0.98	0.99
0.44	--	--	1.00	1.00	0.98	1.00	0.99	0.99
0.46	--	--	--	--	0.99	1.00	1.00	1.00
0.48	--	--	--	--	1.00	1.00	--	--

Table B3
Total Conveyed Air and Entrapped Air Concentrations, Killen Data, Test 3, Slope = 52.5 deg, Discharge = 6.4 cfs

Profile	1		2		3		4		5		6		7		8	
Distance ft	7		9		12		14		20		25		30		35	
Depth ft	Entrapped	Total	Entrapped	Total	Entrapped	Total	Entrapped	Total	Entrapped	Total	Entrapped	Total	Entrapped	Total	Entrapped	Total
0.00	0.00	0.00	0.00	0.03	0.00	0.10	0.00	0.12	0.00	0.21	0.00	0.29	0.00	0.32	0.00	0.35
0.02	0.00	0.00	0.00	0.03	0.00	0.11	0.00	0.12	0.00	0.22	0.00	0.29	0.00	0.34	0.00	0.36
0.04	0.00	0.00	0.00	0.03	0.00	0.11	0.00	0.13	0.00	0.24	0.00	0.30	0.00	0.35	0.00	0.37
0.06	0.00	0.00	0.00	0.04	0.00	0.12	0.00	0.15	0.00	0.26	0.00	0.32	0.00	0.38	0.00	0.39
0.08	0.00	0.01	0.00	0.06	0.00	0.18	0.00	0.17	0.00	0.30	0.00	0.35	0.00	0.40	0.00	0.42
0.10	0.00	0.06	0.00	0.12	0.00	0.19	0.00	0.21	0.00	0.38	0.00	0.38	0.00	0.44	0.00	0.45
0.12	0.07	0.35	0.03	0.23	0.01	0.30	0.01	0.28	0.02	0.48	0.00	0.43	0.01	0.48	0.00	0.49
0.14	0.47	0.74	0.16	0.48	0.03	0.47	0.05	0.41	0.08	0.62	0.01	0.49	0.04	0.55	0.03	0.54
0.16	0.85	0.92	0.39	0.76	0.13	0.65	0.15	0.60	0.20	0.76	0.05	0.58	0.10	0.62	0.07	0.62
0.18	0.94	0.97	0.61	0.89	0.29	0.78	0.35	0.80	0.37	0.85	0.13	0.70	0.21	0.69	0.16	0.69
0.20	0.97	0.99	0.79	0.95	0.47	0.89	0.53	0.89	0.52	0.91	0.27	0.80	0.36	0.77	0.26	0.77
0.22	0.98	1.00	0.91	0.97	0.66	0.95	0.68	0.95	0.67	0.95	0.44	0.87	0.51	0.86	0.40	0.84
0.24	0.99	1.00	0.97	0.99	0.81	0.97	0.80	0.97	0.79	0.98	0.59	0.92	0.63	0.91	0.53	0.89
0.26	1.00	1.00	0.99	1.00	0.88	0.98	0.87	0.98	0.87	0.99	0.71	0.95	0.74	0.94	0.66	0.93
0.28	--	--	1.00	1.00	0.94	0.99	0.92	0.99	0.92	0.99	0.81	0.97	0.82	0.96	0.77	0.96
0.30	--	--	--	--	0.97	1.00	0.96	1.00	0.95	1.00	0.88	0.98	0.88	0.97	0.85	0.97

(Continued)

Appendix B   Killen's Measurements of Self-Aerated Flow, Tabular Form

Table B3 (Concluded)

Profile	1		2		3		4		5		6		7		8	
Distance ft	7		9		12		14		20		25		30		35	
Depth ft	Entrapped	Total	Entrapped	Total	Entrapped	Total	Entrapped	Total	Entrapped	Total	Entrapped	Total	Entrapped	Total	Entrapped	Total
0.32	--	--	--	--	0.99	1.00	0.98	1.00	0.97	1.00	0.94	0.99	0.93	0.98	0.90	0.98
0.34	--	--	--	--	1.00	1.00	1.00	1.00	0.98	1.00	0.97	1.00	0.96	0.99	0.94	0.99
0.36	--	--	--	--	--	--	--	--	0.99	1.00	0.99	1.00	0.97	0.99	0.96	0.99
0.38	--	--	--	--	--	--	--	--	1.00	1.00	1.00	1.00	0.98	0.99	0.97	1.00
0.40	--	--	--	--	--	--	--	--	--	--	--	--	0.99	1.00	0.98	1.00
0.42	--	--	--	--	--	--	--	--	--	--	--	--	1.00	1.00	0.99	1.00
0.44	--	--	--	--	--	--	--	--	--	--	--	--	--	--	1.00	--

Appendix B   Killen's Measurements of Self-Aerated Flow, Tabular Form

B7

Table B4
Total Conveyed Air and Entrapped Air Concentrations, Killen Data,
Test 4, Slope = 30 deg, Discharge = 3.2 cfs

Profile	1		2		3	
Distance, ft	12		18		35	
Depth, ft	Entrapped	Total	Entrapped	Total	Entrapped	Total
0.00	0.00	0.12	0.00	0.19	0.00	0.16
0.02	0.00	0.13	0.00	0.19	0.00	0.16
0.04	0.00	0.14	0.00	0.20	0.00	0.17
0.06	0.00	0.15	0.00	0.22	0.00	0.18
0.08	0.00	0.18	0.00	0.24	0.00	0.21
0.10	0.00	0.22	0.01	0.28	0.00	0.24
0.12	0.00	0.28	0.03	0.36	0.00	0.29
0.14	0.02	0.39	0.07	0.49	0.01	0.37
0.16	0.08	0.56	0.17	0.65	0.07	0.48
0.18	0.23	0.73	0.30	0.78	0.21	0.62
0.20	0.45	0.87	0.45	0.87	0.37	0.76
0.22	0.66	0.94	0.61	0.92	0.53	0.85
0.24	0.82	0.96	0.75	0.96	0.69	0.93
0.26	0.90	0.98	0.84	0.97	0.81	0.96
0.28	0.95	0.99	0.91	0.98	0.88	0.98
0.30	0.97	1.00	0.95	0.99	0.94	0.99
0.32	0.99	1.00	0.98	1.00	0.96	0.99
0.34	1.00	1.00	0.99	1.00	0.98	1.00
0.36	--	--	1.00	1.00	0.99	1.00
0.38	--	--	--	--	1.00	1.00

Appendix C
Investigation of Integration Limit for Entrapped Air Concentration

Because the water surface in aerated flow is highly contorted and extremely rough, it is impossible to clearly define the elevation of the water surface. The depth of flow must therefore be defined in terms of the elevation or depth where a selected air concentration occurs. Since the selection seems relatively arbitrary, several depths were investigated. The effects on calculated entrapped air concentration of arbitrarily setting the water surface (and integration limit in Equation 1, main text) were evaluated. The entrapped air concentrations for Killen's profiles were calculated for depths of Y_{90}, Y_{95}, and Y_{98}, which are the depths where the total conveyed air concentrations are 90, 95, and 98 percent, respectively. Entrapped air concentrations were also computed for a depth of d_{98}, which is the depth where the entrapped air concentration is 98 percent. The results, which are tabulated Table C1, showed, not unexpectedly, that the variability in entrapped air concentration decreased as the integration depth increased. It should be noted that in all cases, d_{98} was less than Y_{98}.

Table C1
Entrapped Air Concentration Integration Limit

Profile	Y_{90}	Y_{95}	Y_{98}	d_{98}
1-1	0.108	0.170	0.253	0.253
1-2	0.116	0.187	0.262	0.262
1-3	0.093	0.167	0.246	0.246
1-4	0.102	0.173	0.243	0.271
1-5	0.094	0.163	0.236	0.234
2-1	0.086	0.130	0.179	0.223
2-2	0.072	0.126	0.187	0.163
2-3	0.088	0.156	0.215	0.303
2-4	0.072	0.135	0.232	0.268
3-1	0.068	0.161	0.241	0.343
3-2	0.075	0.143	0.247	0.307
3-3	0.034	0.090	0.212	0.334
3-4	0.051	0.106	0.223	0.342
3-5	0.030	0.120	0.174	0.402
3-6	0.042	0.123	0.224	0.330
3-7	0.082	0.177	0.294	0.402
3-8	0.075	0.143	0.256	0.399
4-1	0.031	0.104	0.203	0.327
4-2	0.060	0.129	0.258	0.348
4-3	0.077	0.140	0.217	0.350
μ	0.073	0.142	0.230	0.305
σ	0.025	0.027	0.017	0.064
Standardized σ/μ	0.340	0.188	0.074	0.211

Appendix C   Investigation of Integration Limit for Entrapped Air Concentration

Appendix D
Calculation of Inception Point Location

Blevins (1984)[1] provides a method of computing the depth of flow and the location of the point of inception for the flume used by Killen (1968) and Straub and Anderson (1958). At the point of inception, the boundary layer thickness is equal to the depth of flow. Thus, Equation D1 can be used to solve for this location and for the depth of flow.

$$\frac{\delta}{X} = (1 + n)\frac{\delta^*}{X}$$ (D1)

where

δ = boundary layer thickness

X = distance along flume from gate

n = inverse of exponent on power law for velocity distribution

δ^* = displacement thickness

Blevins' (1984) Figure 10-11 shows the relationships between the displacement thickness, the n-value, ratio of distance-to-bottom roughness X / ε, and the "distance" Reynolds Number. With these relationships and Equation D1, the boundary layer thickness can be calculated for any location along the experimental flume.

Over some ranges of the Reynolds Number, the independent variables in Equation D1 are independent of Reynolds Number (See Blevins' Figure 10-11). For Killen's tests and Straub and Anderson's tests, the range of Reynolds Number is

---

[1] References cited in this appendix are located at the end of the main text.

$$7.8 \left(10^6 \right) < \frac{U\,X}{\nu} < 7.7 \left(10^7 \right) \qquad\qquad (D2)$$

where U is the free stream velocity at the gate defined by

$$U = \frac{q}{G_o} \qquad\qquad (D3)$$

where

q = unit discharge

G_o = gate opening

ν = kinematic viscosity of the flow (approximately $1.1\ (10^{-5})$ $\sec^{-1}$)

The range of X/ε for Killen's and Straub and Anderson's tests is

$$1.7 \left(10^3 \right) < \frac{X}{\varepsilon} < 8.6 \left(10^3 \right) \qquad\qquad (D4)$$

where

$\varepsilon = 0.28$ in. $= 0.00233$ ft

Over these ranges of Reynolds Number and roughness ratios, the relationships between the independent variables of Equation D1 are not a function of Reynolds Number in this range.

Hence, if δ^*/X, X/ε, and n are independent of Reynolds Number, then Equation D1 can be rewritten as

$$\frac{\delta}{X} = \left[1 + \xi \left(\frac{X}{\varepsilon} \right) \right] \Phi \left(\frac{X}{\varepsilon} \right) \qquad\qquad (D5)$$

where

$$\frac{\delta^*}{X} = \Phi \left(\frac{X}{\varepsilon} \right) \quad , \quad n = \xi \left(\frac{X}{\varepsilon} \right)$$

Using X/ε as the independent variable, the data presented in Table D1 can be extracted from Blevins' Figure 10-11. A simple curve-fit of these data gives an expression for δ^*/X and n as a function of X/ε:

Table D1 Data Extracted from Blevins' (1984) Figure 10-11		
$\dfrac{X}{\varepsilon}$	$\dfrac{\delta^{*}}{X}$	n
10^4	.0034	5
$4(10^3)$	.0043	4.4
$2(10^3)$	.0V052	3.9

$$\frac{\delta^{*}}{X} = \Phi\left(\frac{X}{\varepsilon}\right) = -0.00258 \, \log_{10}\left(\frac{X}{\varepsilon}\right) + 0.0137 \qquad \text{(D6)}$$

$$n = \xi\left(\frac{X}{\varepsilon}\right) = 1.57 \, \log_{10}\left(\frac{X}{\varepsilon}\right) - 1.29 \qquad \text{(D7)}$$

At the point of inception, the depth of flow Y_I is equal to the boundary layer thickness, which is also the normal depth of flow d_o.

$$Y_I = \delta = d_o \qquad \text{(D8)}$$

Normal depth of flow for Killen's (1968) and Straub and Anderson's (1958) observations can be calculated using Manning's equation. Table D2 shows d_o for their range of flow rates and the 30-, 45-, and 52.5-deg flume slopes. Substituting Equations D6, D7, and D8 into Equation D5, collecting terms, and simplifying, results in

$$\frac{d_o}{X} = \left[1.57 \, \log_{10}\left(\frac{X}{\varepsilon}\right) - 0.29 \right]$$

$$\left[-0.00258 \, \log_{10}\left(\frac{X}{\varepsilon}\right) + 0.0137 \right] \qquad \text{(D9)}$$

Given the normal depth of flow, the location of the point of inception can be calculated by a simple numerical solution for Equation D9. Predictions of inception point for a range of normal depths of flow are presented in Table D3.

Table D2
Normal Depth of Flow for Killen's (1968) and Straub and Anderson's (1958) Flume Tests

	Q cfs	30-Deg Slope d_o	45-Deg Slope d_o	52.5-Deg Slope d_o
1	2.2	.077	.064	--
2	3.2	.098	.082	--
3	4.2	.118	.098	--
4	5.2	.136	.113	--
5	6.4	.156	.130	.119
6	7.2	.169	.141	--
7	8.2	.184	.153	--
8	9.6	.204	.170	--
9	10.2	.213	.177	--
10	11.2	.227	.189	--
11	12.8	.248	.206	--
12	15.0	.275	.229	--

Table D3 Distance Along Straub and Anderson Flume to Point of Inception [1]	
Normal Depth	X-Incipient
.01	.39
.02	.76
.03	1.13
.04	1.50
.05	1.87
.06	2.28
.07	2.66
.08	3.07
.09	3.46
.10	3.87
.11	4.28
.12	4.76
.13	5.17
.14	5.58
.15	6.06
.16	6.47
.17	6.91
.18	7.46
.19	7.87
.20	8.28
.21	8.83
.22	9.24
.23	9.78
.24	10.33
.25	10.74
.26	11.29
.27	11.83
.28	12.24
.29	12.79
.30	13.34

[1] Distance based on intersection of boundary layer and surface at normal depth of flow for ideal conditions, e.g., correct setting of gate opening to prevent acceleration or deceleration of flow when released to flume.

Appendix E
Straub and Anderson's Unpublished Measurements of Self-Aerated Flow on 30- and 45-Deg Slopes, 35-Ft Distance Along Flume, Graphical Form
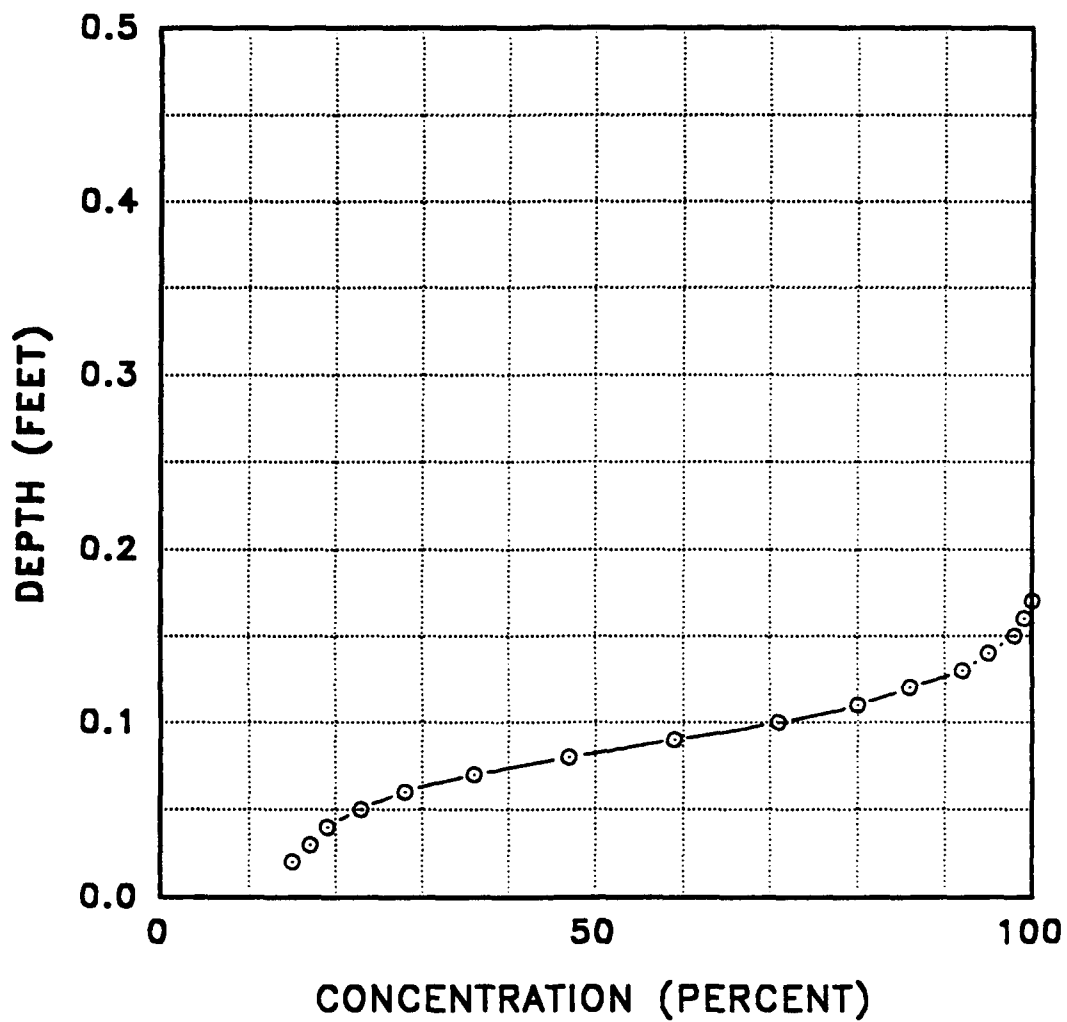
Profile 1, Slope = 30 Degrees, Q = 2.2 cfs,
Location in Flume = 35 ft
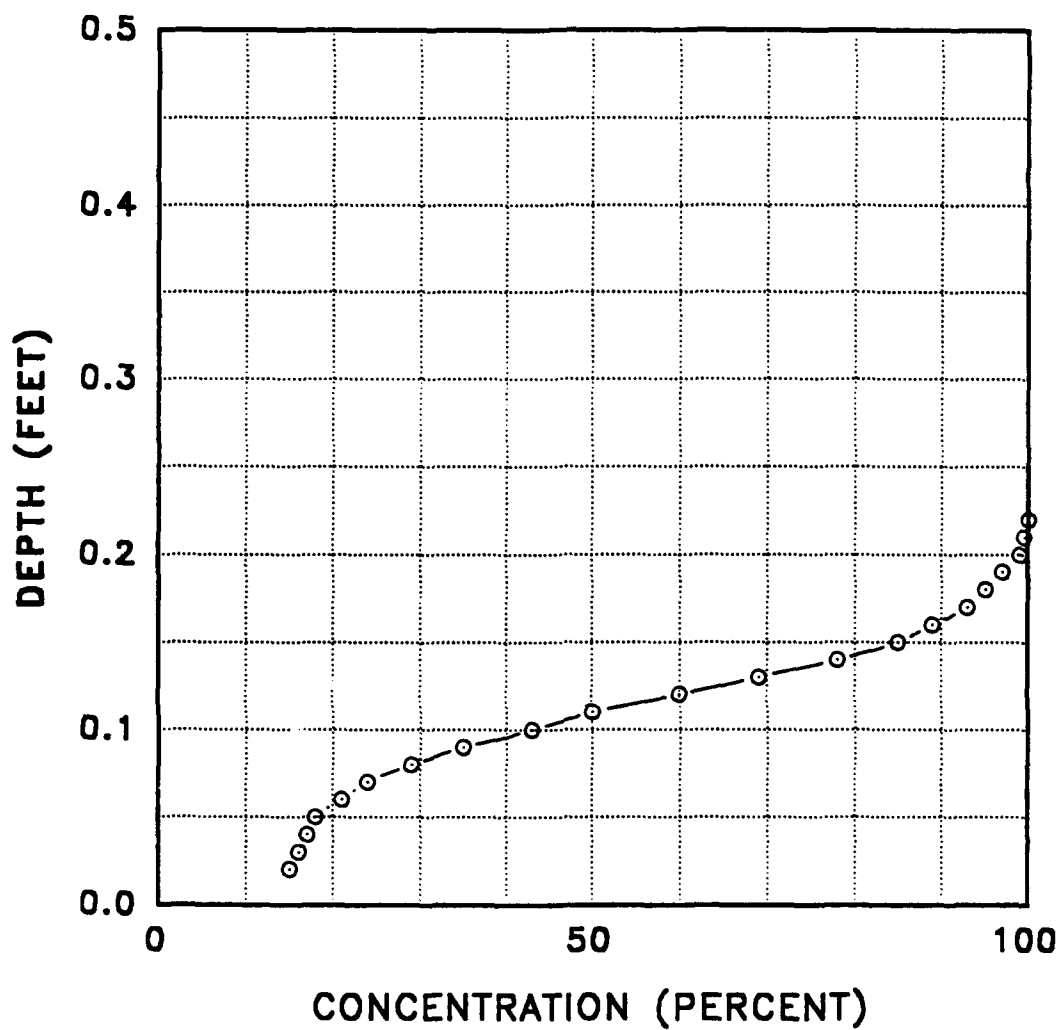
Profile 2, Slope = 30 Degrees, Q = 3.2 cfs,
Location in Flume = 35 ft
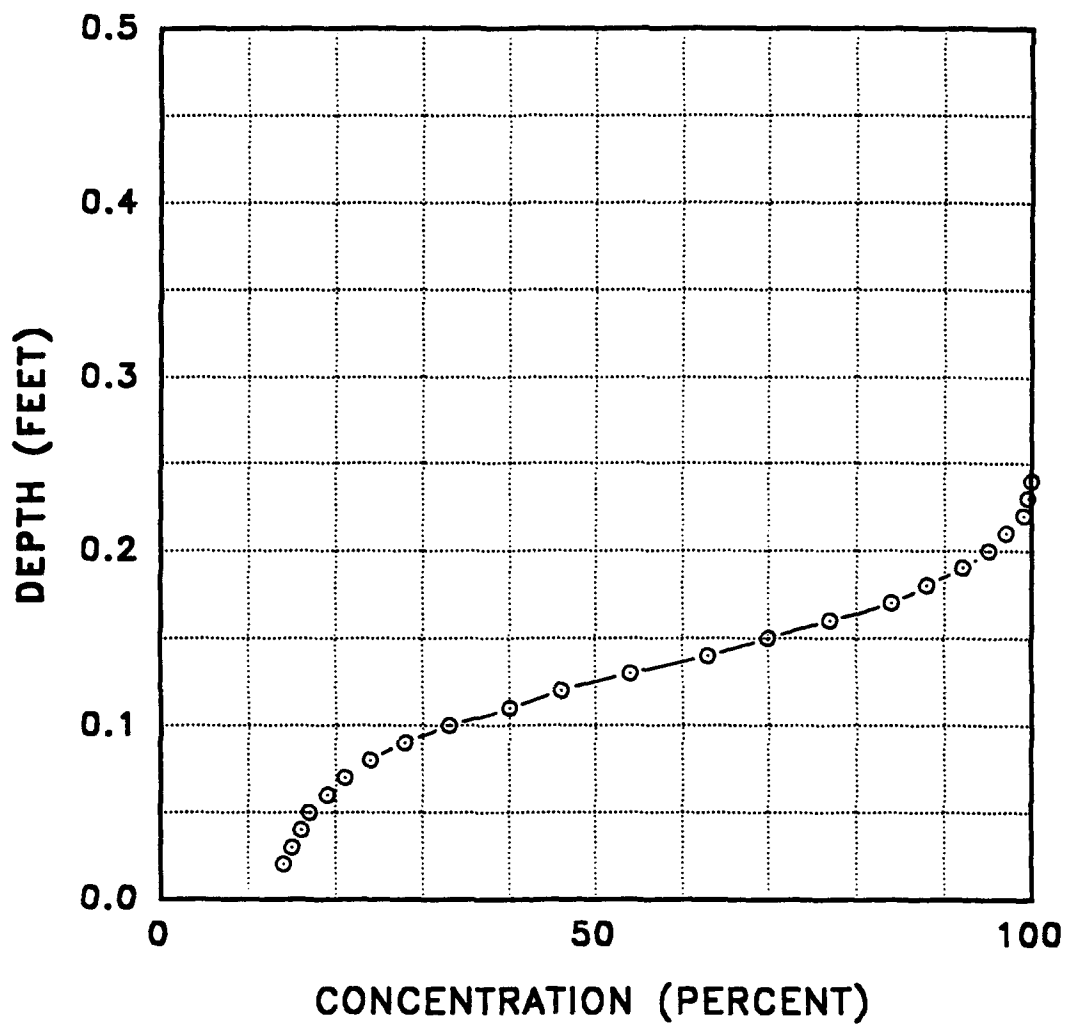
Profile 3, Slope = 30 Degrees, Q = 4.2 cfs,
Location in Flume = 35 ft
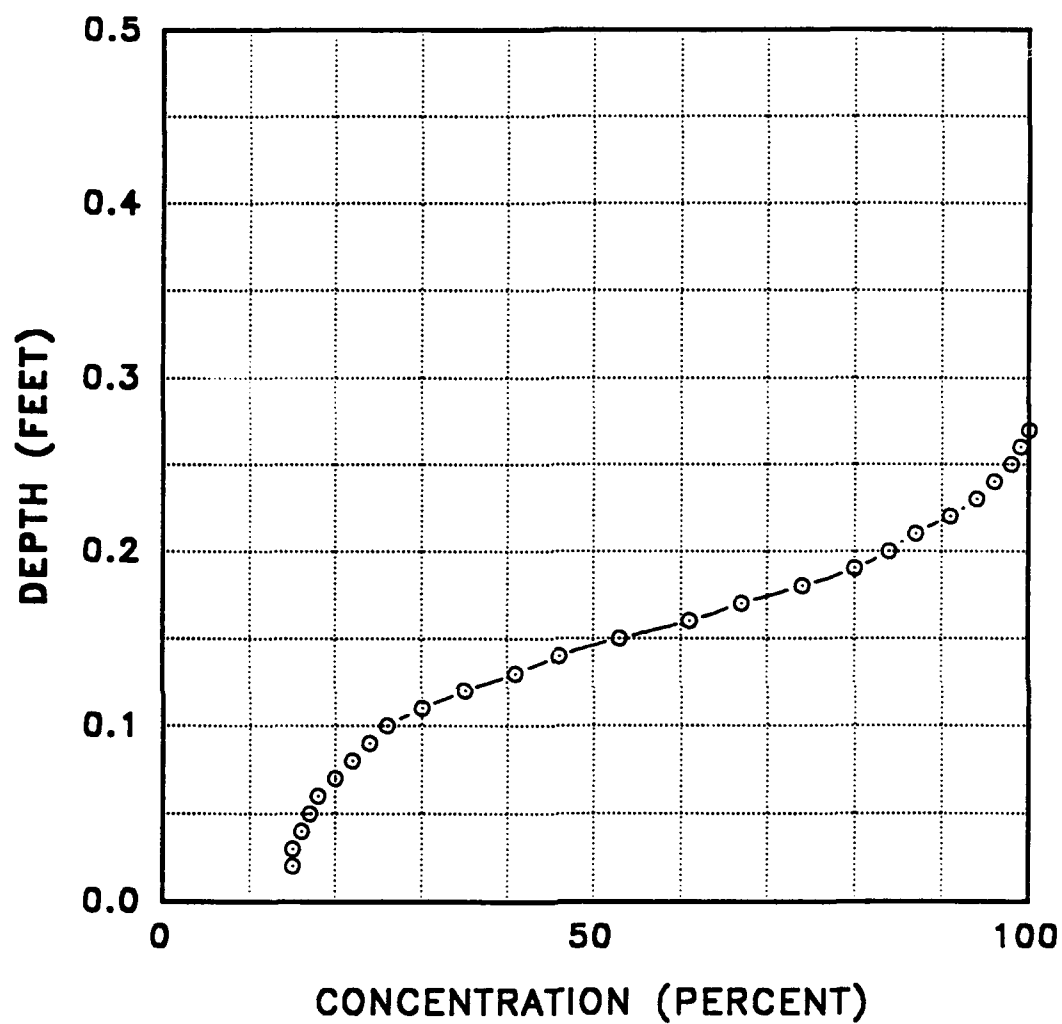
Profile 4, Slope = 30 Degrees, Q = 5.2 cfs,
Location in Flume = 35 ft
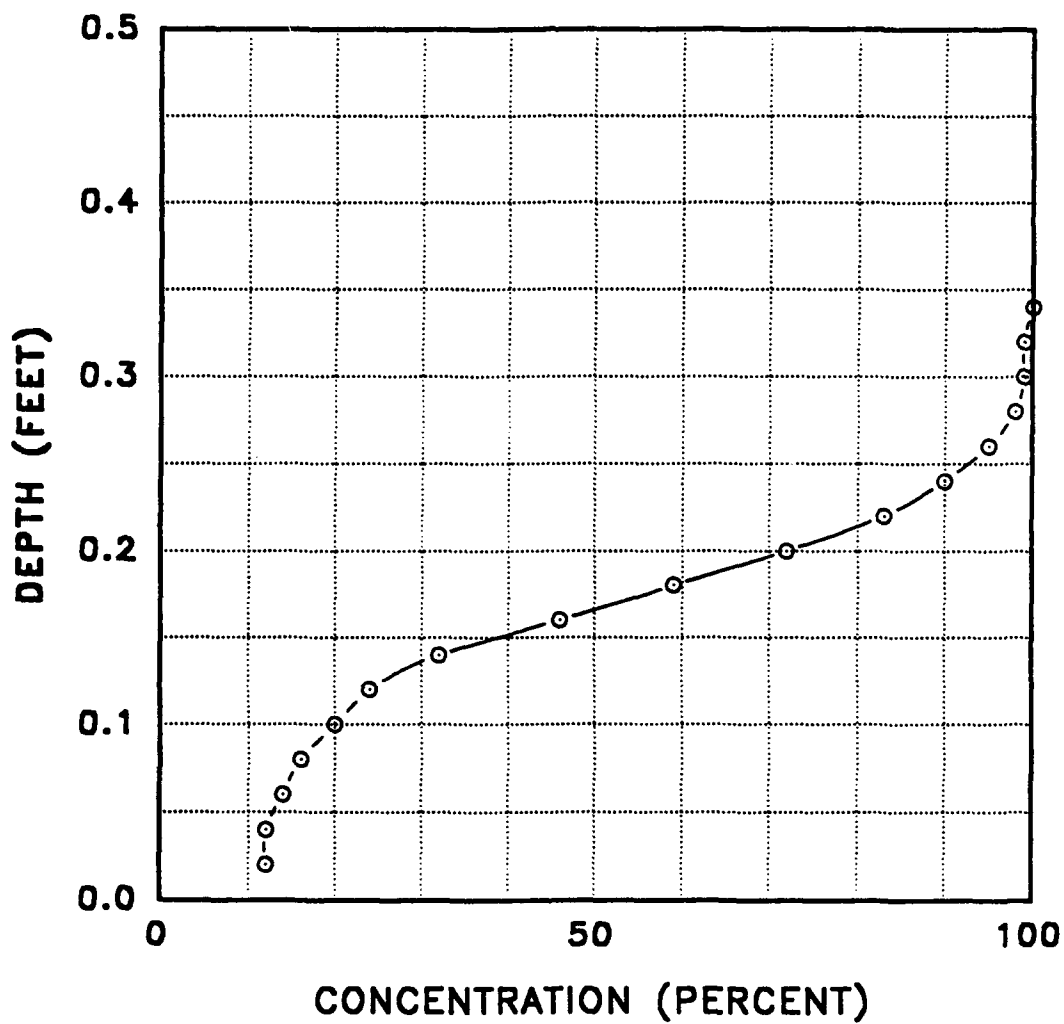
Profile 5, Slope = 30 Degrees, Q = 6.4 cfs,
Location in Flume = 35 ft
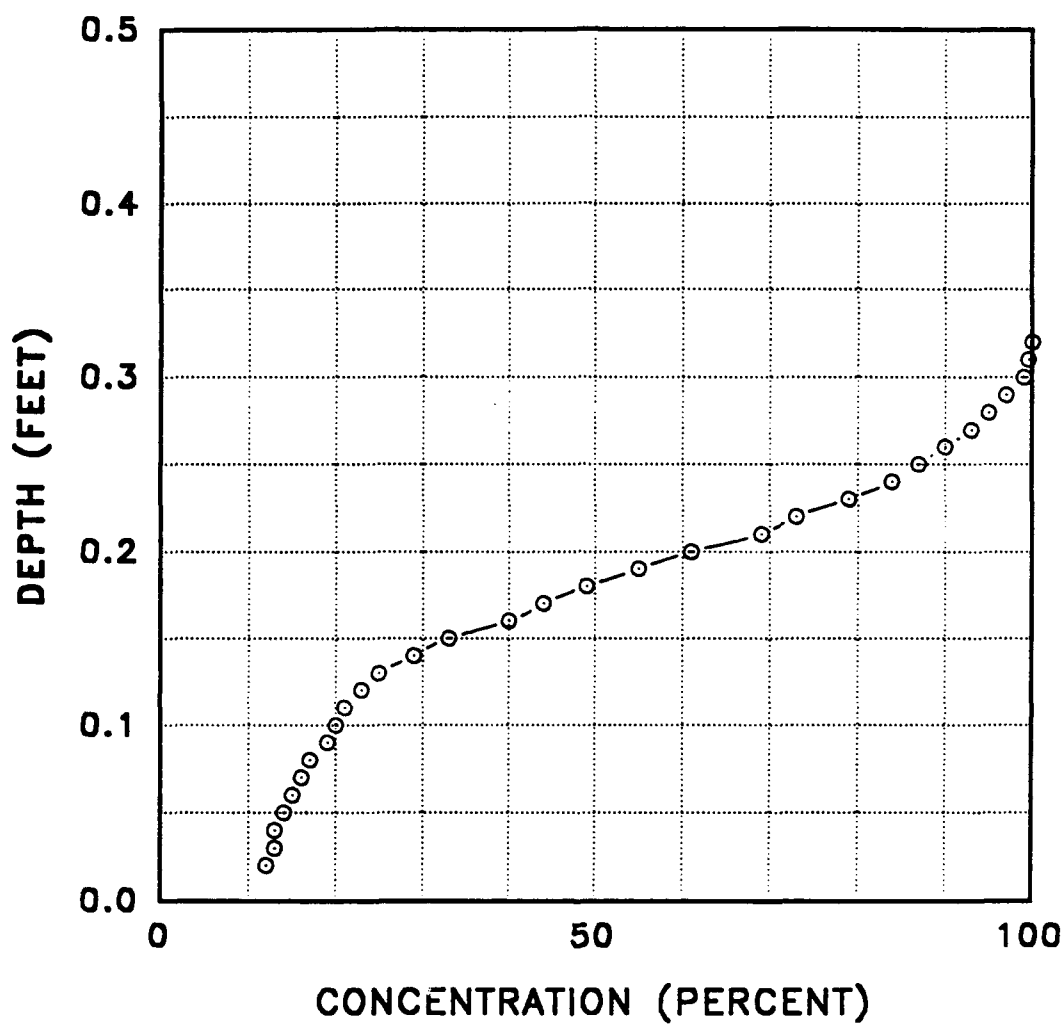
Profile 6, Slope = 30 Degrees, Q = 7.2 cfs,
Location in Flume = 35 ft
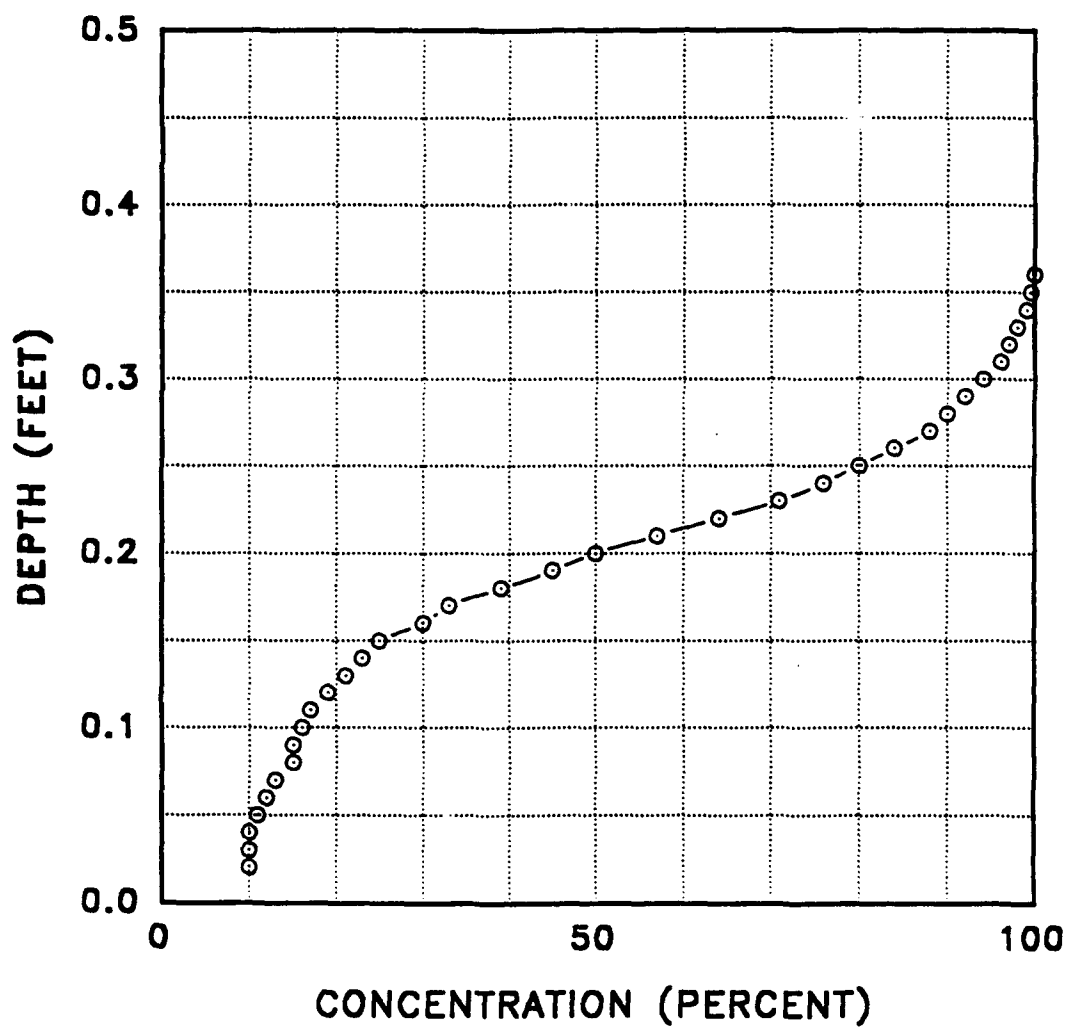
Profile 7, Slope = 30 Degrees, Q = 8.2 cfs,
Location in Flume = 35 ft
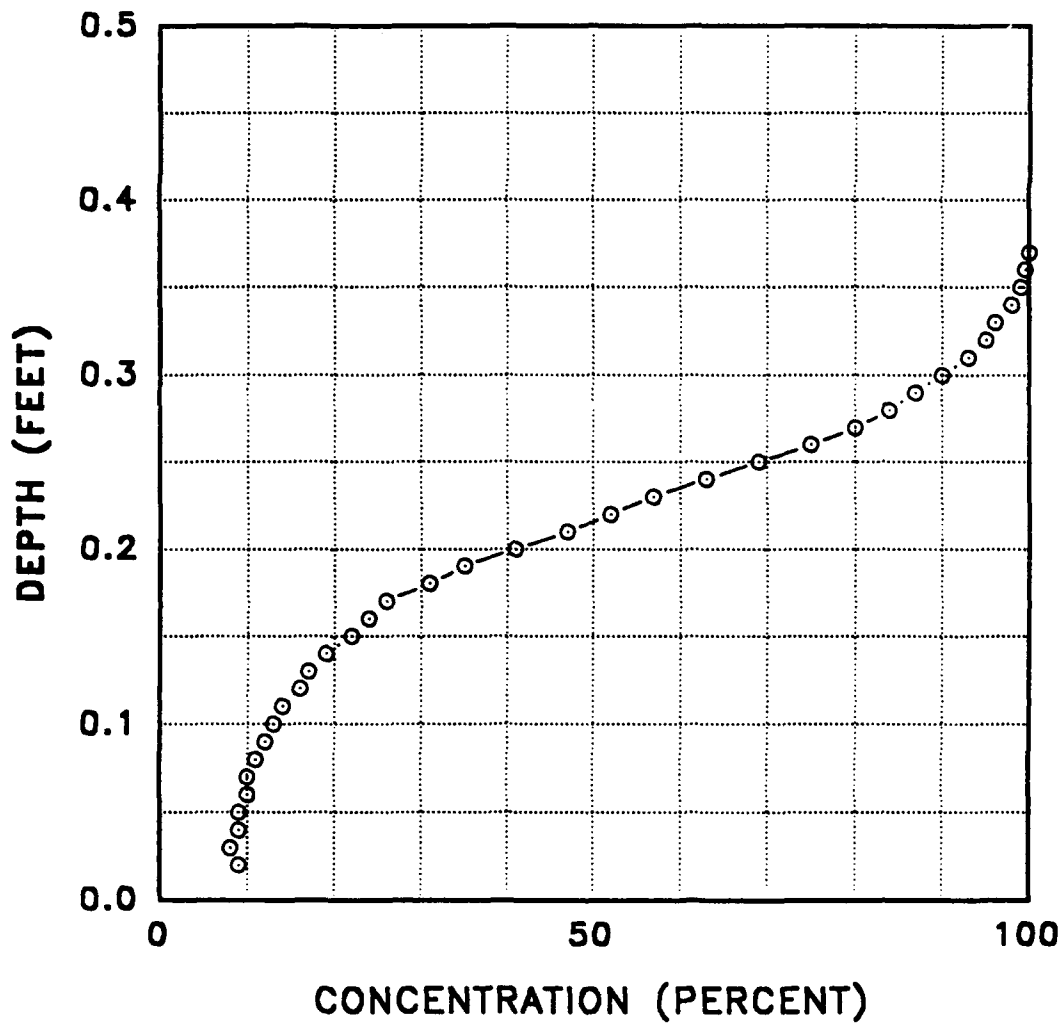
Profile 8, Slope = 30 Degrees, Q = 9.6 cfs,
Location in Flume = 35 ft
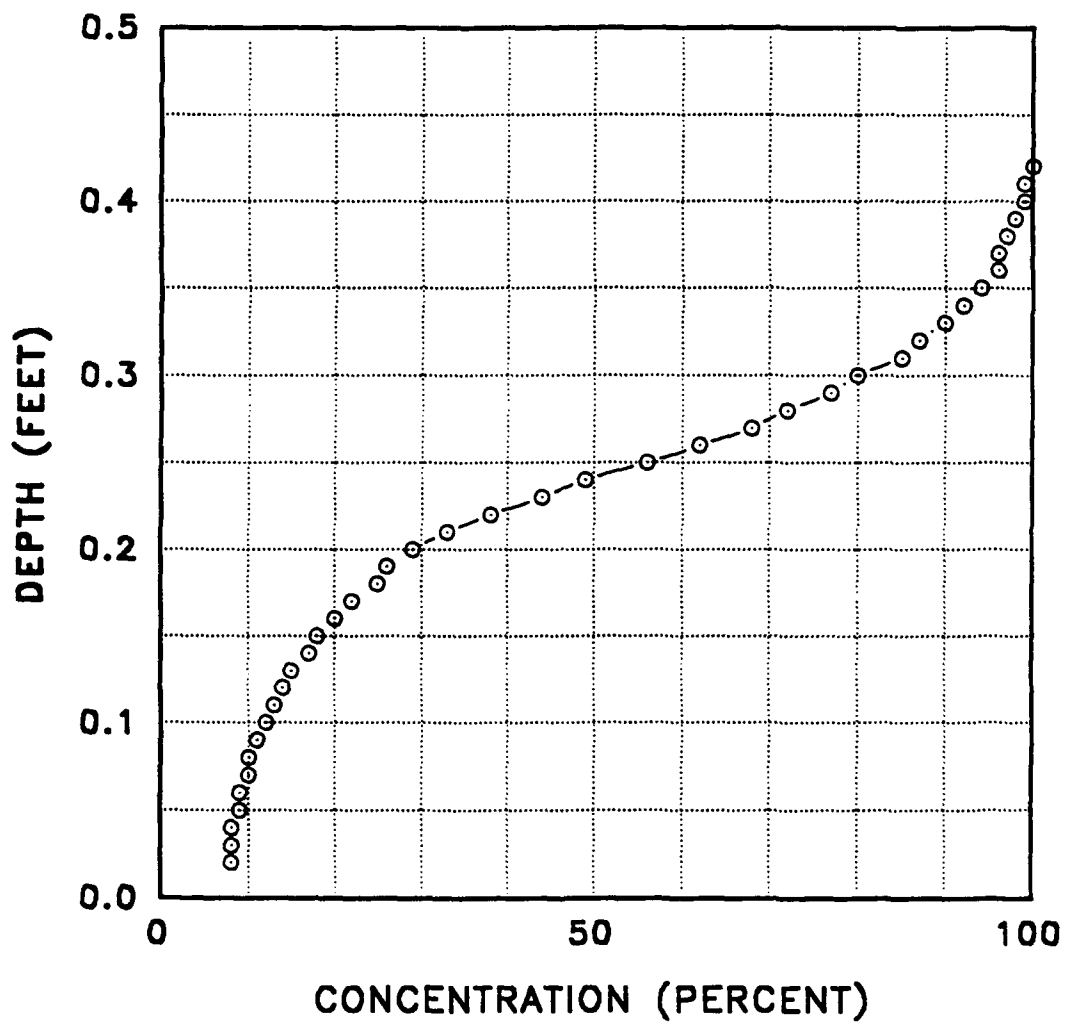
Profile 9, Slope = 30 Degrees, Q = 11.2 cfs,
Location in Flume = 35 ft
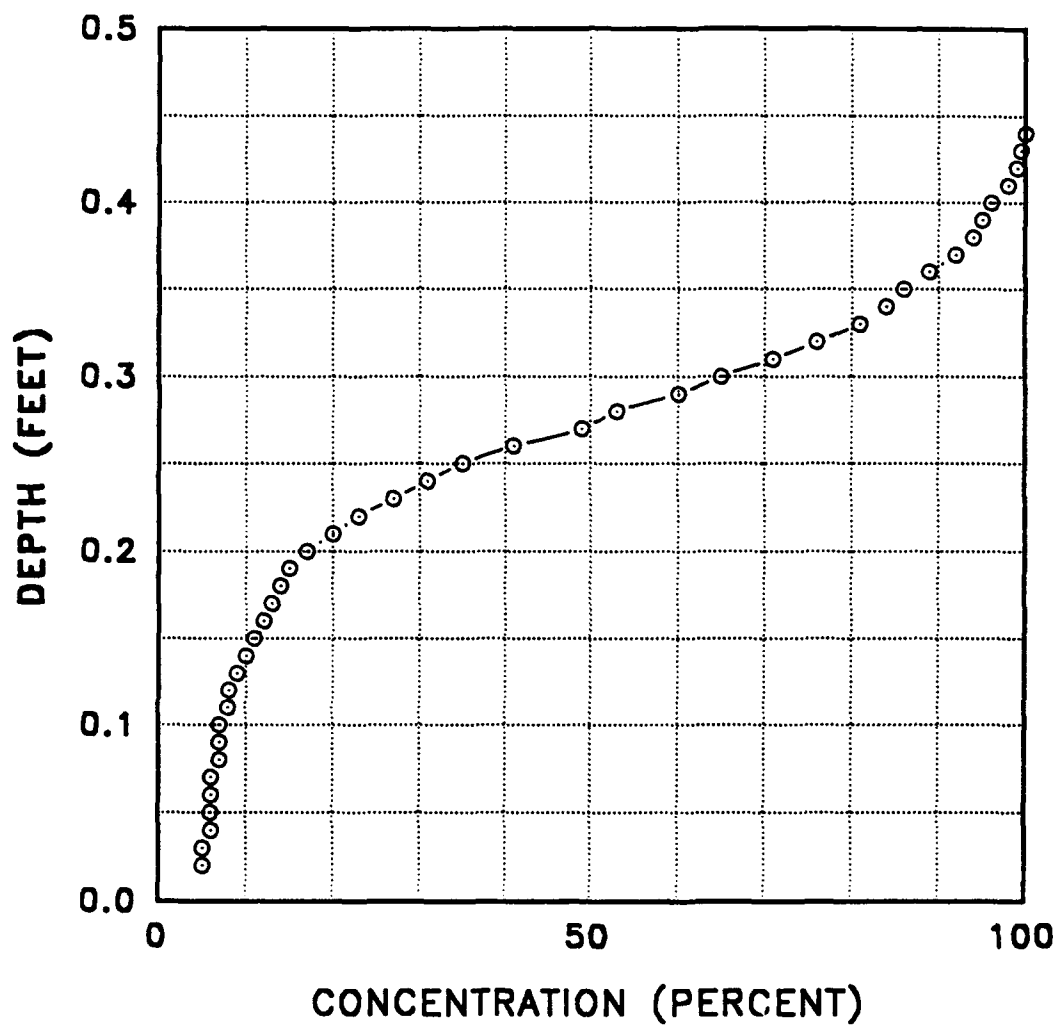
Profile 10, Slope = 30 Degrees, Q = 12.1 cfs,
Location in Flume = 35 ft
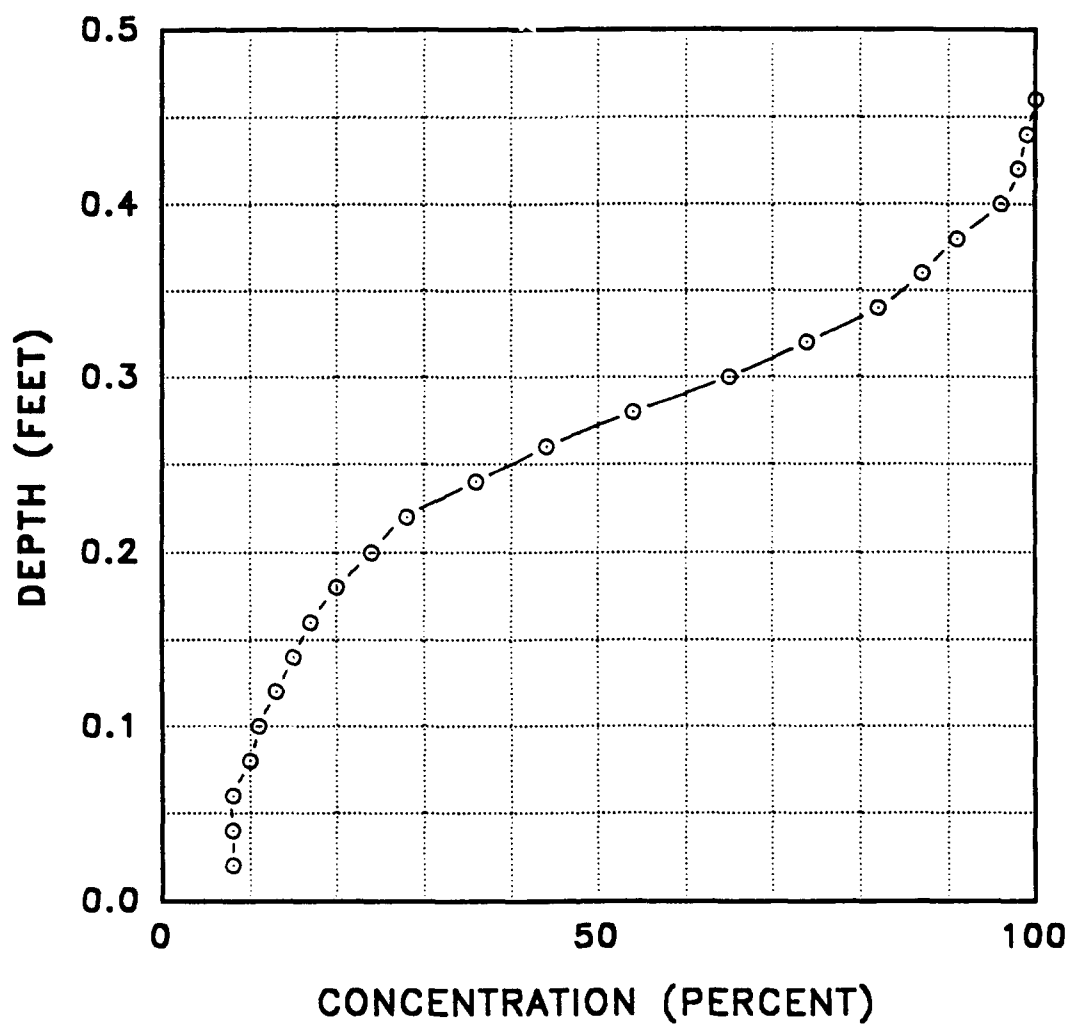
Profile 11, Slope = 30 Degrees, Q = 12.8 cfs,
Location in Flume = 35 ft
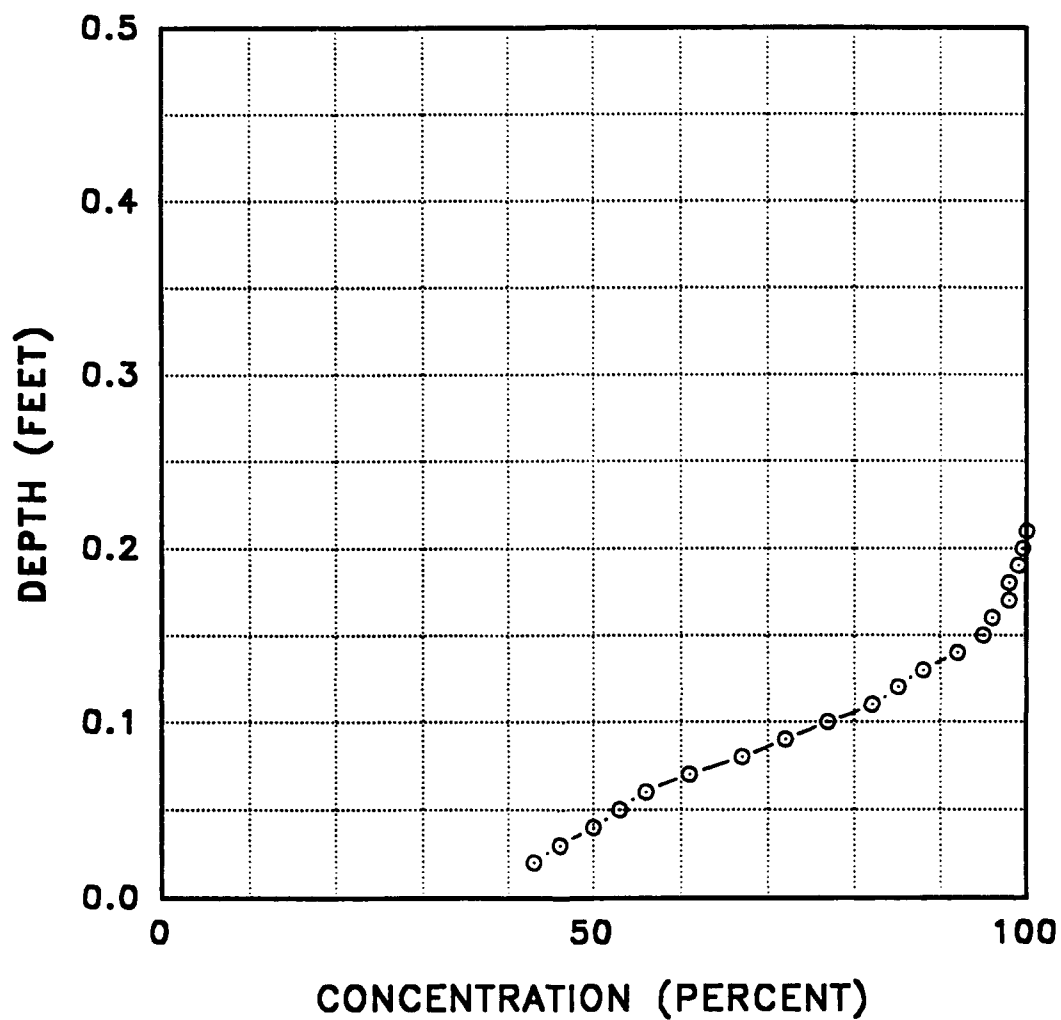
Profile 1, Slope = 45 Degrees, Q = 2.2 cfs,
Location in Flume = 35 ft
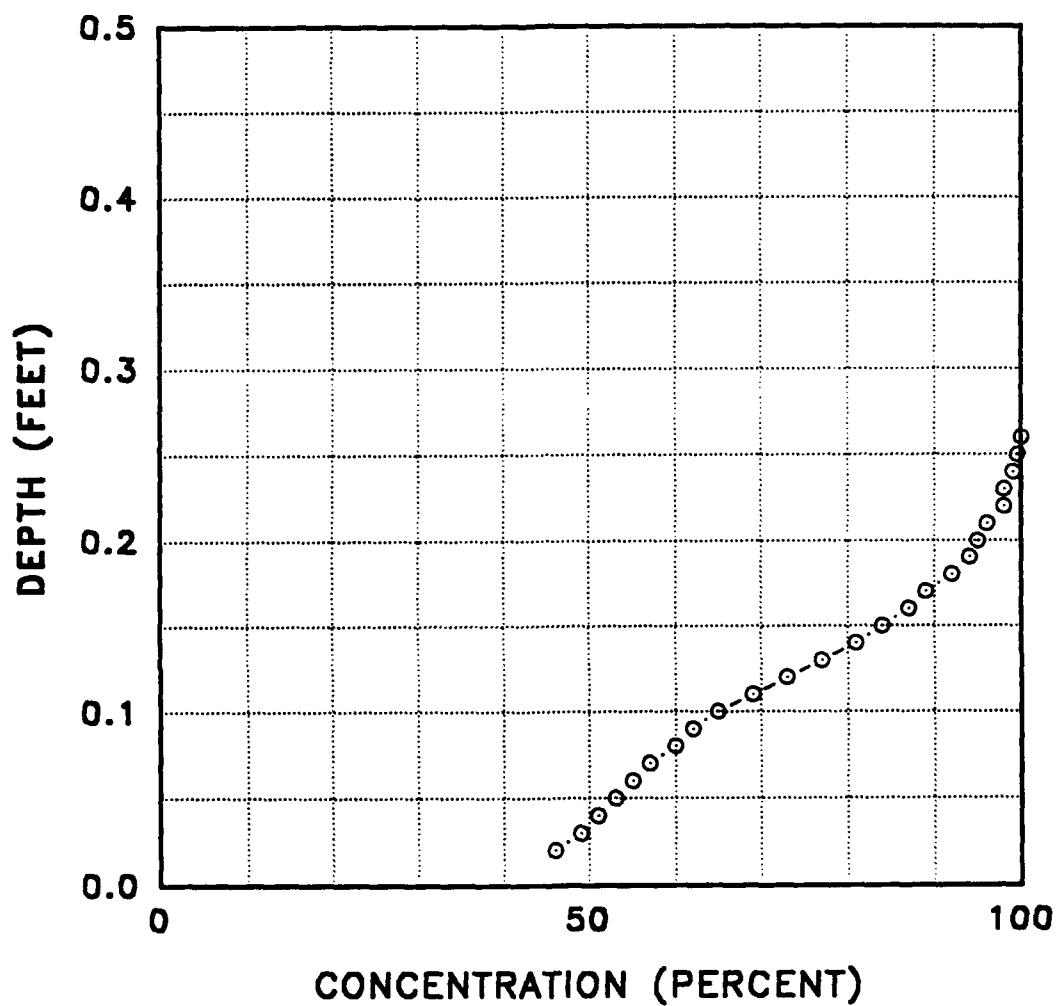
Profile 2, Slope = 45 Degrees, Q = 3.2 cfs,
Location in Flume = 35 ft
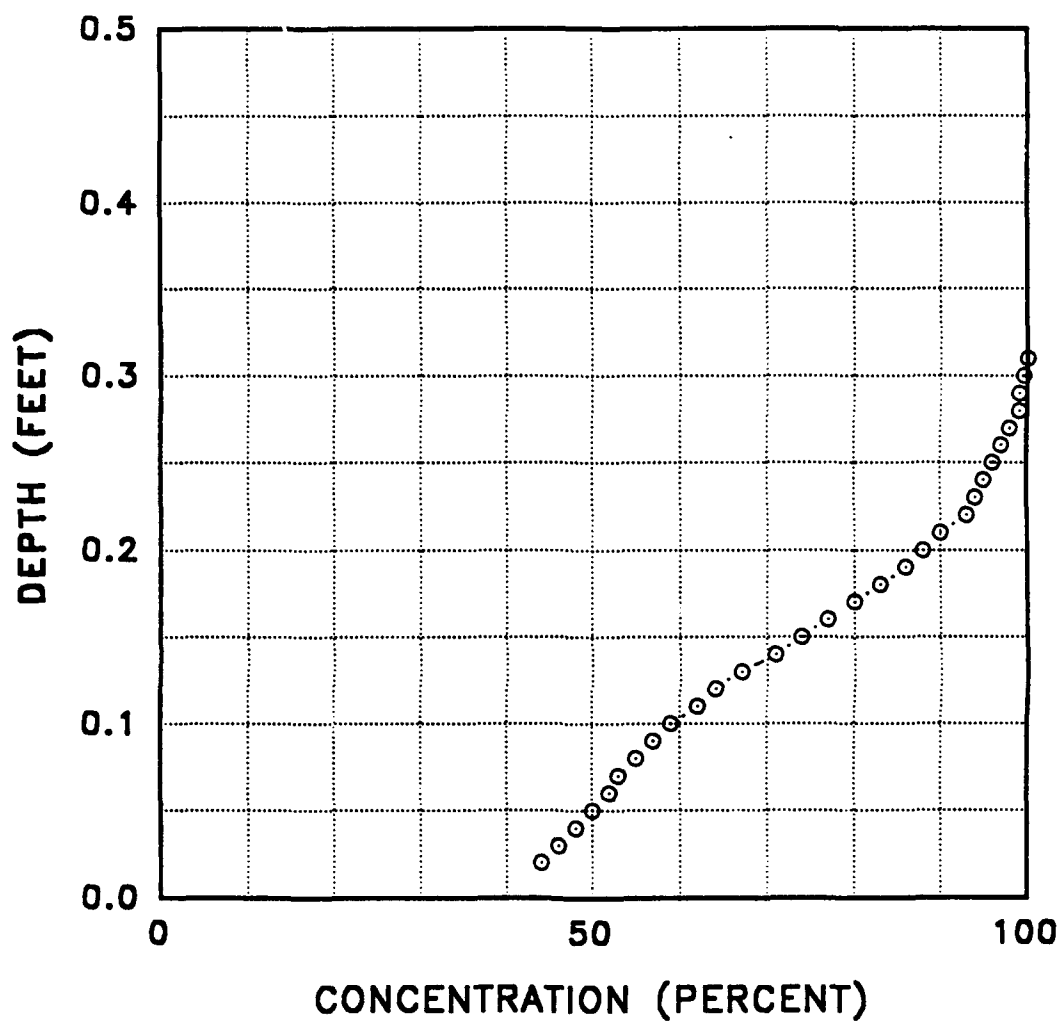
Profile 3, Slope = 45 Degrees, Q = 4.2 cfs,
Location in Flume = 35 ft
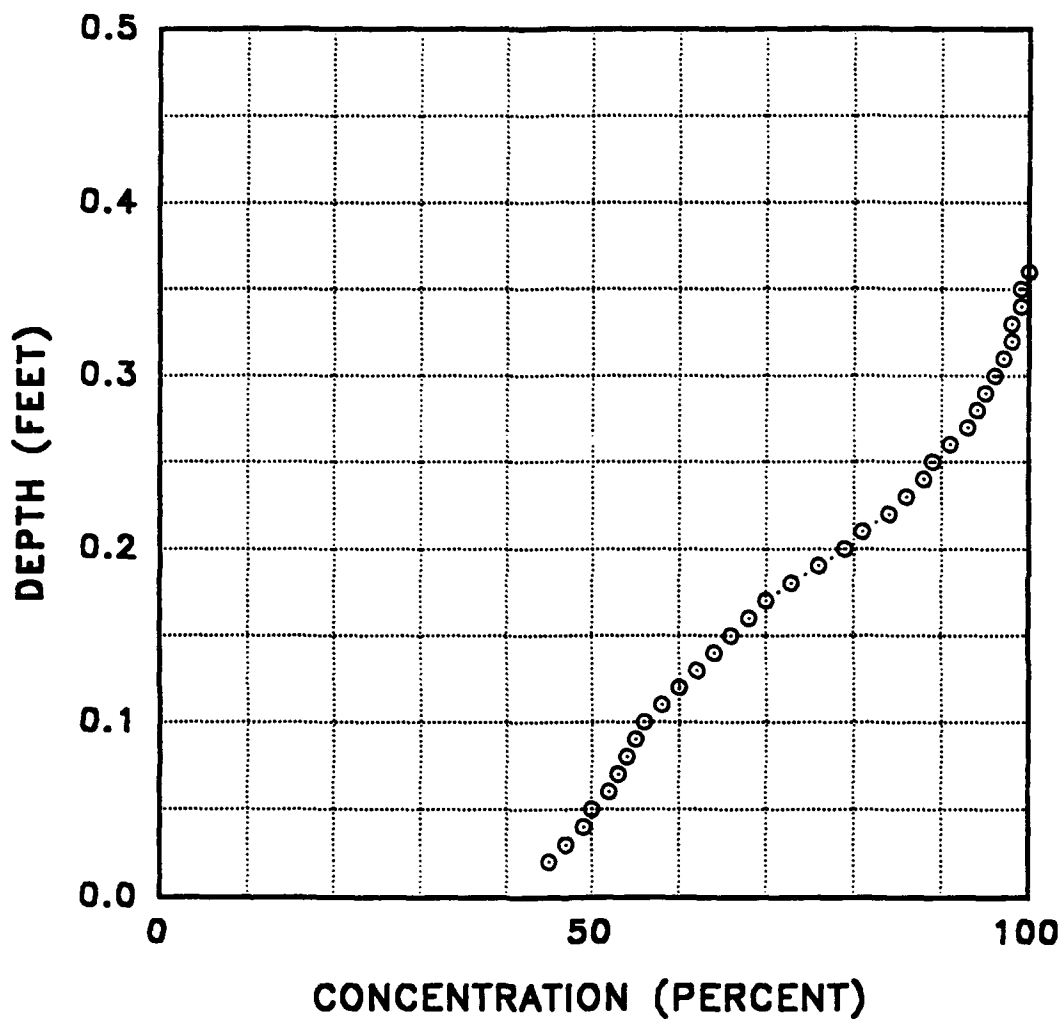
Profile 4, Slope = 45 Degrees, Q = 5.2 cfs,
Location in Flume = 35 ft
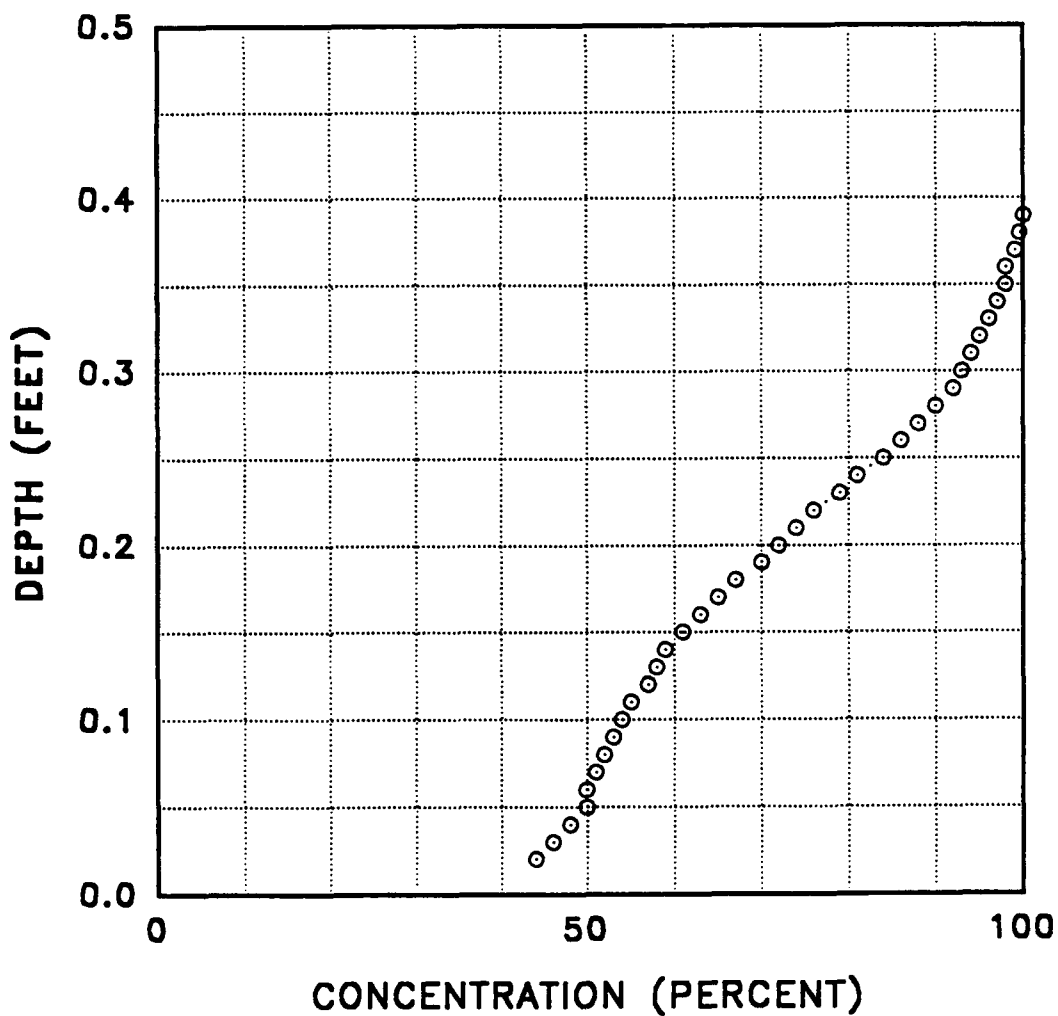
Profile 5, Slope = 45 Degrees, Q = 6.4 cfs,
Location in Flume = 35 ft
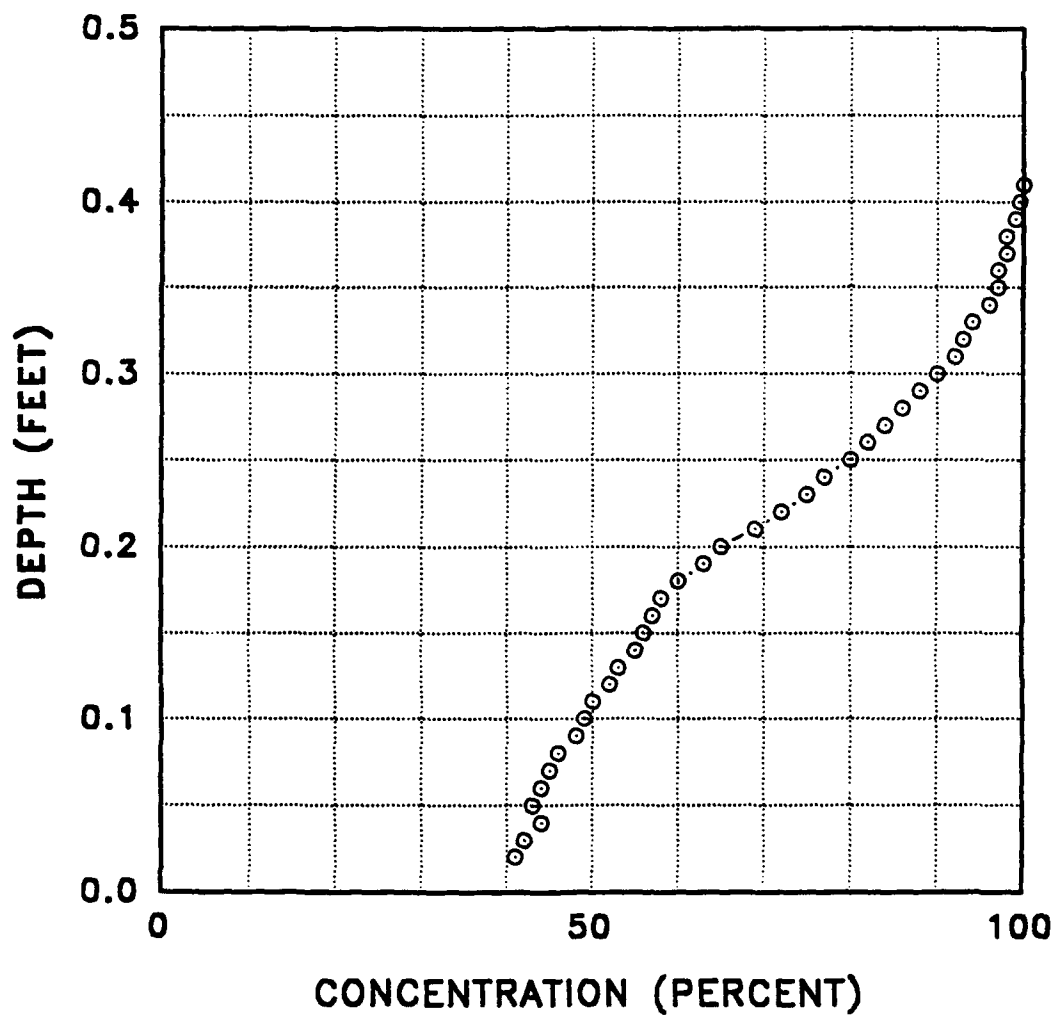
Profile 6, Slope = 45 Degrees, Q = 7.2 cfs,
Location in Flume = 35 ft
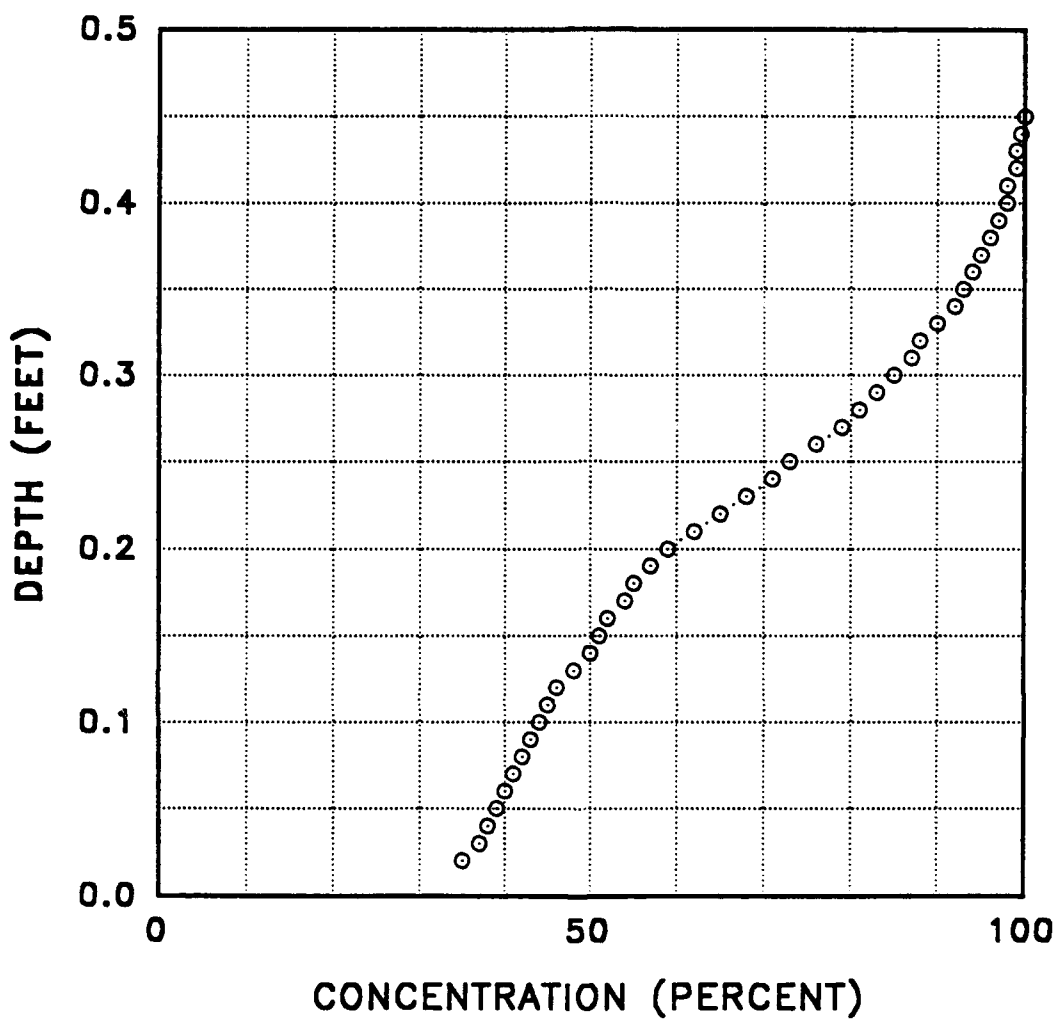
Profile 7, Slope = 45 Degrees, Q = 8.2 cfs,
Location in Flume = 35 ft
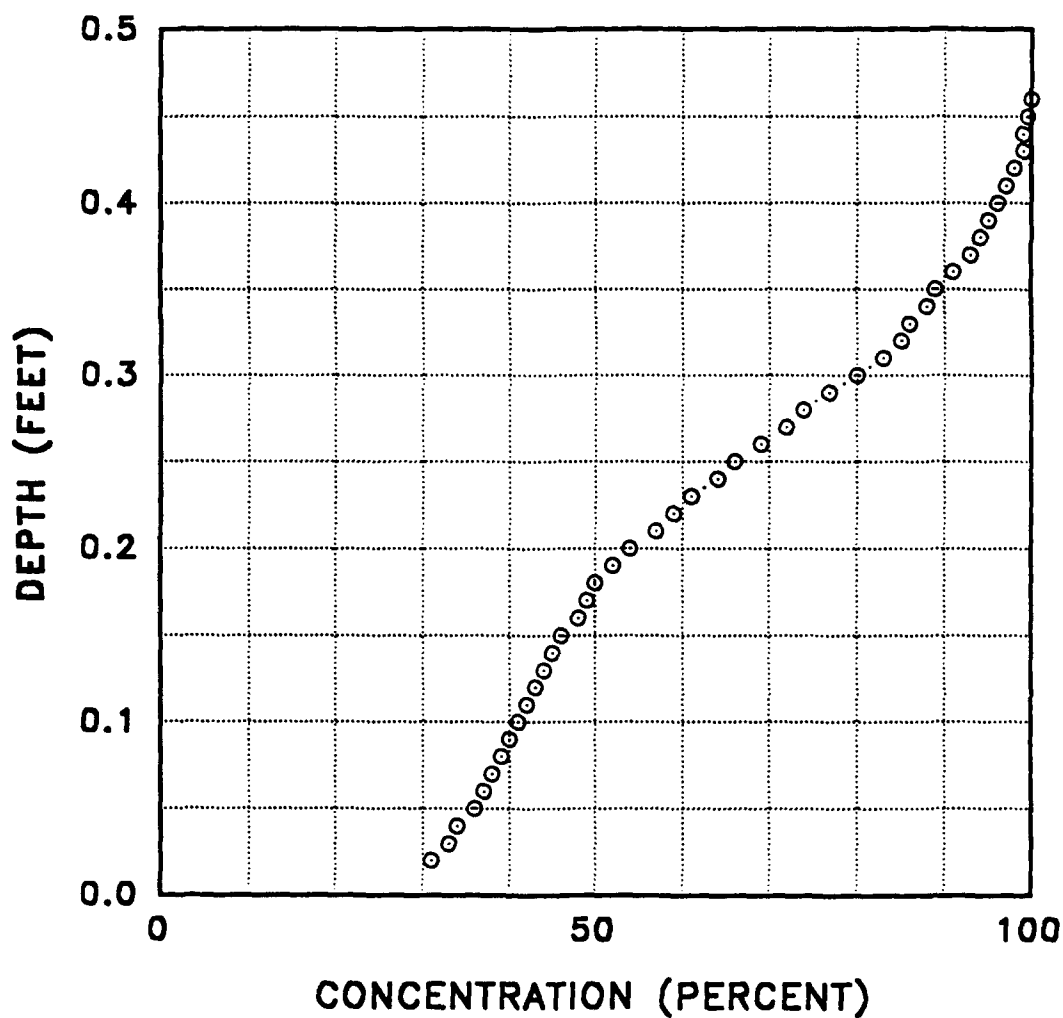
Profile 8, Slope = 45 Degrees, Q = 9.6 cfs,
Location in Flume = 35 ft

Profile 9, Slope = 45 Degrees, Q = 11.2 cfs,
Location in Flume = 35 ft

Profile 10, Slope = 45 Degrees, Q = 12.8 cfs,
Location in Flume = 35 ft

Profile 11, Slope = 45 Degrees, Q = 15.0 cfs,
Location in Flume = 35 ft

Appendix F
Straub and Anderson's Unpublished Measurements of Self-Aerated Flow on 30- and 45-Deg Slopes, 35-Ft Distance Along Flume, Tabular Form
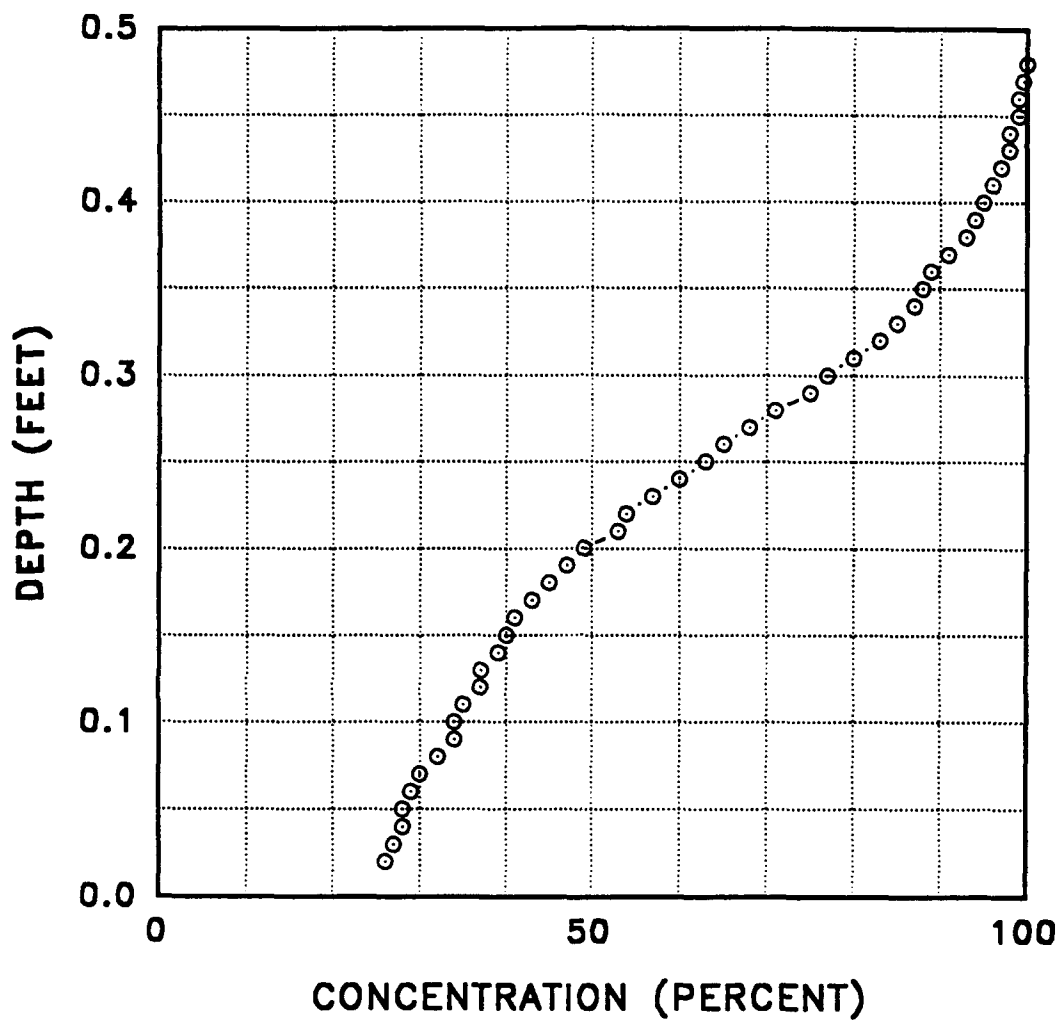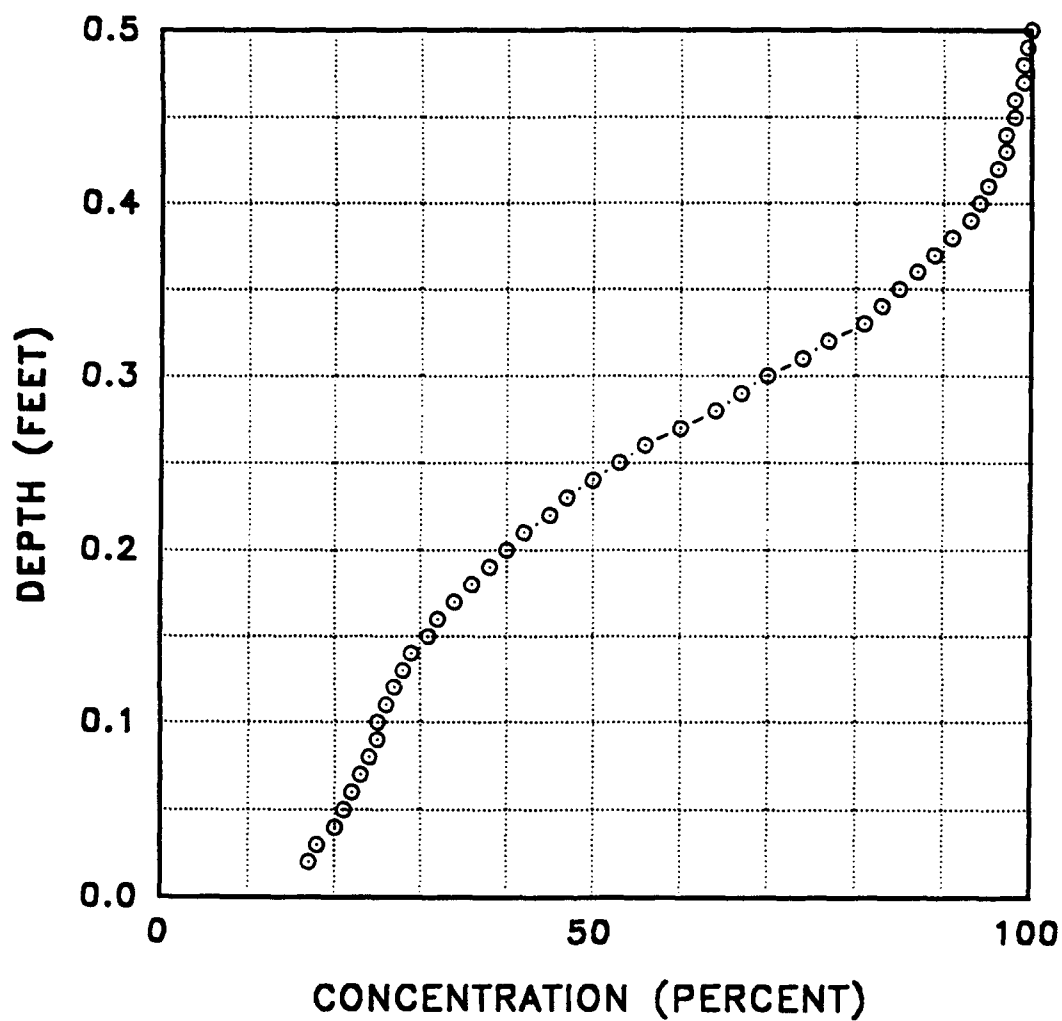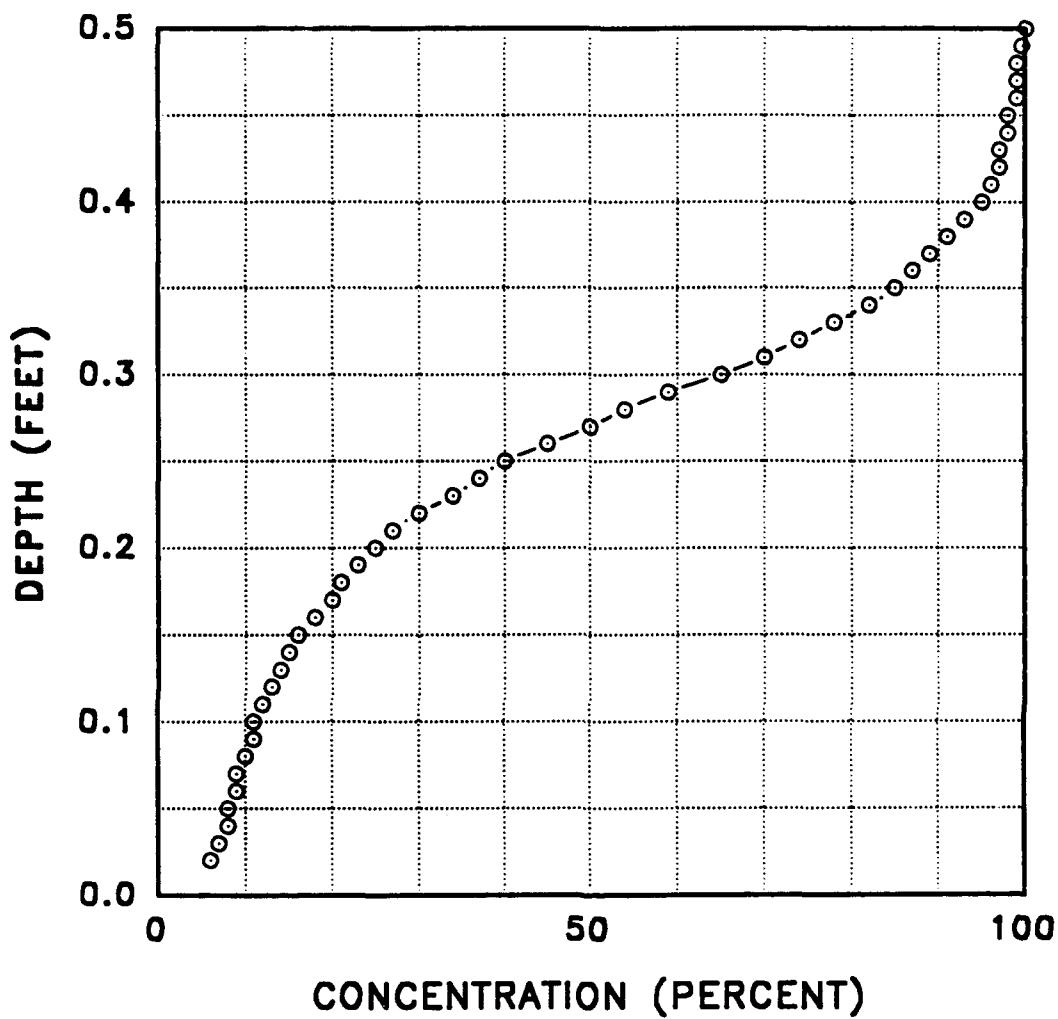
STRAUB AND ANDERSON 35, 30 DEGREE SLOPE

TEST DISCHARGE	1 2.2 CFS DEPTH	CONC.	2 3.2 CFS DEPTH	CONC.	3 4.2 CFS DEPTH	CONC.	4 5.2 CFS DEPTH	CONC.	5 6.4 CFS DEPTH	CONC.	6 7.2 CFS DEPTH	CONC.	7 8.2 CFS DEPTH	CONC.	8 9.6 CFS DEPTH	CONC.	9 11.2 CFS DEPTH	CONC.	10 12.1 CFS DEPTH	CONC.	11 12.6 CFS DEPTH	CONC.
	0.02	0.15	0.02	0.15	0.02	0.14	0.02	0.15	0.02	0.12	0.02	0.12	0.02	0.1	0.02	0.08	0.02	0.06	0.02	0.05	0.02	0.08
	0.03	0.17	0.03	0.16	0.03	0.15	0.03	0.16	0.04	0.13	0.03	0.13	0.03	0.1	0.03	0.08	0.03	0.06	0.03	0.06	0.04	0.08
	0.04	0.19	0.04	0.17	0.04	0.16	0.04	0.18	0.06	0.13	0.04	0.13	0.04	0.11	0.04	0.08	0.04	0.06	0.04	0.06	0.06	0.08
	0.05	0.23	0.05	0.18	0.05	0.17	0.05	0.17	0.08	0.14	0.05	0.14	0.05	0.12	0.05	0.1	0.06	0.08	0.05	0.06	0.08	0.1
	0.06	0.28	0.06	0.21	0.06	0.19	0.06	0.19	0.1	0.15	0.06	0.15	0.06	0.13	0.07	0.1	0.07	0.08	0.07	0.07	0.1	0.11
	0.07	0.38	0.07	0.24	0.07	0.21	0.07	0.2	0.12	0.16	0.07	0.16	0.07	0.13	0.08	0.11	0.08	0.08	0.08	0.07	0.12	0.13
	0.08	0.47	0.08	0.29	0.08	0.24	0.08	0.22	0.14	0.17	0.08	0.17	0.08	0.14	0.09	0.12	0.09	0.08	0.09	0.08	0.14	0.15
	0.09	0.58	0.09	0.35	0.09	0.28	0.09	0.24	0.16	0.18	0.09	0.18	0.09	0.16	0.1	0.13	0.1	0.09	0.1	0.08	0.16	0.17
	0.1	0.71	0.1	0.43	0.1	0.33	0.1	0.28	0.18	0.2	0.1	0.2	0.1	0.17	0.11	0.14	0.11	0.1	0.11	0.1	0.2	0.2
	0.11	0.8	0.11	0.5	0.11	0.4	0.11	0.3	0.2	0.22	0.11	0.21	0.11	0.19	0.12	0.16	0.12	0.11	0.12	0.11	0.24	0.24
	0.12	0.88	0.12	0.6	0.12	0.48	0.12	0.35	0.22	0.23	0.12	0.23	0.12	0.21	0.13	0.17	0.13	0.12	0.13	0.12	0.26	0.36
	0.13	0.92	0.13	0.69	0.13	0.54	0.13	0.41	0.24	0.25	0.13	0.25	0.13	0.23	0.14	0.18	0.14	0.13	0.14	0.13	0.28	0.44
	0.14	0.95	0.14	0.78	0.14	0.63	0.14	0.48	0.26	0.28	0.14	0.28	0.14	0.25	0.16	0.19	0.15	0.14	0.15	0.14	0.28	0.54
	0.15	0.98	0.15	0.85	0.15	0.7	0.15	0.53	0.28	0.3	0.15	0.33	0.15	0.29	0.17	0.2	0.16	0.15	0.16	0.15	0.3	0.65
	0.16	0.98	0.16	0.89	0.16	0.77	0.16	0.61	0.3	0.32	0.16	0.4	0.16	0.33	0.18	0.22	0.17	0.16	0.17	0.16	0.32	0.74
	0.17	1	0.17	0.83	0.17	0.84	0.17	0.67	0.32	0.44	0.17	0.44	0.17	0.31	0.2	0.24	0.18	0.17				
	0.18	0.95	0.18	0.84	0.18	0.74	0.18	1	0.16	0.39	0.18	0.39	0.18	0.28	0.22	0.28	0.36	0.38				
	0.19	0.97	0.19	0.92	0.19	0.8	0.19	0.55	0.18	0.35	0.19	0.35	0.25	0.15	0.23	0.44						
	0.2	0.98	0.2	0.95	0.2	0.84	0.2	0.61	0.2	0.41	0.2	0.41	0.17	0.2	0.42							
	0.21	0.995	0.21	0.97	0.21	0.87	0.21	0.69	0.21	0.47	0.21	0.2										
	0.22	1	0.22	0.99	0.22	0.9	0.22	0.73	0.22	0.52	0.22	0.23										
	0.23	0.94	0.23	0.94	0.23	0.79	0.23	0.71	0.23	0.44	0.23	0.44										
	0.24	0.98	0.24	0.87	0.24	0.6	0.24	0.76	0.24	0.35	0.24	0.48										
	0.25	1	0.25	0.9	0.25	0.9	0.25	0.69	0.25	0.41												
	0.26	0.95	0.26	0.93	0.26	0.84	0.26	0.75	0.26	0.49												
	0.27	0.97	0.27	0.9	0.27	0.88	0.27	0.8	0.27													
	0.28	0.98	0.28	0.92	0.28	0.84	0.28	0.72														
	0.29	0.995	0.29	0.94	0.29	0.87	0.29	0.77														
	0.3	0.98	0.3	0.97	0.3	0.9	0.3	0.8														
	0.31	0.98	0.31	0.98	0.31	0.93	0.31	0.85														
	0.32	0.995	0.32	0.99	0.32	0.95	0.32	0.67														
	0.33	1	0.33	0.98	0.33	0.9	0.33	0.81														
	0.34	0.97	0.34	0.98	0.34	0.92	0.34	0.84														
	0.35	0.98	0.35	0.98	0.35	0.94	0.35	0.86														
	0.36	0.98	0.36	0.995	0.36	0.98	0.36	0.89														
	0.37	0.99	0.37	0.94	0.37	0.92																
	0.38	0.995	0.38	0.95																		
	0.39	1	0.39	0.98																		
	0.4		0.4	0.98																		
	0.41		0.41	0.99																		
	0.42		0.42																			
	0.43																					
	0.44	0.995																				

TEST DISCHARGE	1 2.2 CFS DEPTH	CONC.	2 3.2 CFS DEPTH	CONC.	3 4.2 CFS DEPTH	CONC.	4 5.2 CFS DEPTH	CONC.	5 6.4 CFS DEPTH	CONC.	6 7.2 CFS DEPTH	CONC.	7 8.2 CFS DEPTH	CONC.	8 9.6 CFS DEPTH	CONC.	9 11.2 CFS DEPTH	CONC.	10 12.8 CFS DEPTH	CONC.	11 15.0 CFS DEPTH	CONC.
	0.02	0.43	0.02	0.48	0.02	0.48	0.02	0.44	0.02	0.45	0.02	0.44	0.02	0.41	0.02	0.35	0.02	0.31	0.02	0.26	0.02	0.17	0.02	0.08
	0.03	0.48	0.03	0.49	0.03	0.49	0.03	0.48	0.03	0.47	0.03	0.48	0.03	0.42	0.03	0.37	0.03	0.33	0.03	0.27	0.03	0.18	0.03	0.07
	0.04	0.5	0.04	0.5	0.04	0.51	0.04	0.49	0.04	0.49	0.04	0.48	0.04	0.44	0.04	0.38	0.04	0.34	0.04	0.28	0.04	0.2	0.04	0.08
	0.05	0.53	0.05	0.53	0.05	0.53	0.05	0.5	0.05	0.5	0.05	0.5	0.05	0.43	0.05	0.39	0.05	0.34	0.05	0.29	0.05	0.22	0.05	0.08
	0.06	0.56	0.06	0.55	0.06	0.55	0.06	0.52	0.06	0.52	0.06	0.5	0.06	0.44	0.06	0.4	0.06	0.37	0.06	0.29	0.06	0.23	0.06	0.08
	0.07	0.61	0.07	0.57	0.07	0.57	0.07	0.53	0.07	0.53	0.07	0.51	0.07	0.44	0.07	0.41	0.07	0.37	0.07	0.3	0.07	0.24	0.07	0.09
	0.08	0.67	0.08	0.6	0.08	0.6	0.08	0.55	0.08	0.54	0.08	0.52	0.08	0.46	0.08	0.42	0.08	0.38	0.08	0.32	0.08	0.25	0.08	0.09
	0.09	0.72	0.09	0.62	0.09	0.62	0.09	0.57	0.09	0.55	0.09	0.53	0.09	0.46	0.09	0.43	0.09	0.38	0.09	0.34	0.09	0.25	0.09	0.1
	0.1	0.77	0.1	0.65	0.1	0.65	0.1	0.59	0.1	0.58	0.1	0.54	0.1	0.48	0.1	0.43	0.1	0.4	0.1	0.35	0.1	0.26	0.1	0.11
	0.11	0.82	0.11	0.68	0.11	0.68	0.11	0.62	0.11	0.6	0.11	0.55	0.11	0.5	0.11	0.44	0.11	0.41	0.11	0.37	0.11	0.27	0.11	0.11
	0.12	0.85	0.12	0.73	0.12	0.73	0.12	0.64	0.12	0.62	0.12	0.57	0.12	0.52	0.12	0.46	0.12	0.42	0.12	0.37	0.12	0.28	0.12	0.12
	0.13	0.88	0.13	0.77	0.13	0.77	0.13	0.67	0.13	0.62	0.13	0.58	0.13	0.53	0.13	0.48	0.13	0.43	0.13	0.38	0.13	0.28	0.13	0.13
	0.14	0.92	0.14	0.81	0.14	0.81	0.14	0.71	0.14	0.64	0.14	0.59	0.14	0.55	0.14	0.48	0.14	0.44	0.14	0.38	0.14	0.29	0.14	0.14
	0.15	0.95	0.15	0.84	0.15	0.84	0.15	0.74	0.15	0.66	0.15	0.61	0.15	0.56	0.15	0.5	0.15	0.45	0.15	0.4	0.15	0.31	0.15	0.15
	0.16	0.96	0.16	0.87	0.16	0.87	0.16	0.77	0.16	0.69	0.16	0.63	0.16	0.57	0.16	0.51	0.16	0.46	0.16	0.41	0.16	0.32	0.16	0.16
	0.17	0.98	0.17	0.89	0.17	0.89	0.17	0.8	0.17	0.7	0.17	0.65	0.17	0.54	0.17	0.52	0.17	0.46	0.17	0.43	0.17	0.34	0.17	0.18
	0.18	0.98	0.18	0.92	0.18	0.92	0.18	0.83	0.18	0.73	0.18	0.67	0.18	0.6	0.18	0.53	0.18	0.48	0.18	0.45	0.18	0.36	0.18	0.18
	0.19	0.99	0.19	0.94	0.19	0.94	0.19	0.86	0.19	0.76	0.19	0.7	0.19	0.63	0.19	0.54	0.19	0.5	0.19	0.47	0.19	0.38	0.19	0.18
	0.2	0.995	0.2	0.95	0.2	0.95	0.2	0.88	0.2	0.79	0.2	0.72	0.2	0.65	0.2	0.57	0.2	0.52	0.2	0.48	0.2	0.4	0.2	0.2
	0.21		0.21	0.96	0.21	0.96	0.21	0.9	0.21	0.81	0.21	0.72	0.21	0.66	0.21	0.59	0.21	0.54	0.21	0.49	0.21	0.42	0.21	0.21
	0.22	0.96	0.22	0.97	0.22	0.97	0.22	0.91	0.22	0.84	0.22	0.75	0.22	0.68	0.22	0.59	0.22	0.57	0.22	0.53	0.22	0.3	0.22	0.23
	0.23	0.98	0.23	0.97	0.23	0.97	0.23	0.93	0.23	0.86	0.23	0.77	0.23	0.71	0.23	0.6	0.23	0.6	0.23	0.55	0.23	0.34	0.23	0.25
	0.24	0.98	0.24	0.97	0.24	0.97	0.24	0.94	0.24	0.9	0.24	0.8	0.24	0.73	0.24	0.64	0.24	0.63	0.24	0.54	0.24	0.4	0.24	0.37
	0.25	0.995	0.25	0.97	0.25	0.97	0.25	0.96	0.25	0.92	0.25	0.8	0.25	0.76	0.25	0.66	0.25	0.65	0.25	0.59	0.25	0.45		
	0.26		0.26	0.98	0.26	0.98	0.26	0.96	0.26	0.93	0.26	0.82	0.26	0.77	0.26	0.66	0.26	0.65	0.26	0.65				
	0.27	0.98	0.27	0.98	0.27	0.98	0.27	0.97	0.27	0.94	0.27	0.83	0.27	0.8	0.27	0.69	0.27	0.66	0.27	0.7				
	0.28	0.98	0.28	0.98	0.28	0.98	0.28	0.97	0.28	0.96	0.28	0.84	0.28	0.81	0.28	0.71	0.28	0.72						
	0.29	0.99	0.29	0.98	0.29	0.98	0.29	0.92	0.29	0.96	0.29	0.85	0.29	0.83	0.29	0.73	0.28	0.74						
	0.3	0.995	0.3	0.99	0.3	0.99	0.3	0.93	0.3	0.96	0.3	0.85	0.3	0.85	0.3	0.77	0.3	0.76						
	0.31		0.31	0.98	0.31	0.98	0.31	0.94	0.31	0.98	0.31	0.87	0.31	0.85	0.31	0.8	0.31	0.74						
	0.32	0.98	0.32	0.98	0.32	0.98	0.32	0.95	0.32	0.98	0.32	0.88	0.32	0.83	0.32	0.77								
	0.33	0.98	0.33	0.99	0.33	0.99	0.33	0.94	0.33	0.9	0.33	0.89	0.33	0.85	0.33	0.81								
	0.34	0.99	0.34	0.98	0.34	0.98	0.34	0.96	0.34	0.92	0.34	0.89	0.34	0.87	0.34	0.83								
	0.35		0.35	0.98	0.35	0.98	0.35	0.97	0.35	0.93	0.35	0.91	0.35	0.89	0.35	0.85								
	0.36		0.36	0.98	0.36	0.98	0.36	0.97	0.36	0.93	0.36	0.91	0.36	0.89	0.36	0.87								
	0.37	0.995	0.37	0.98	0.37	0.98	0.37	0.97	0.37	0.94	0.37	0.93	0.37	0.91	0.37	0.91								
	0.38		0.38	0.98	0.38	0.98	0.38	0.98	0.38	0.95	0.38	0.94	0.38	0.93	0.38	0.93								
	0.39	0.995	0.39	0.99	0.39	0.99	0.39	0.97	0.39	0.96	0.39	0.95	0.39	0.94										
	0.4		0.4	0.99	0.4	0.99	0.4	0.97	0.4	0.96	0.4	0.97	0.4	0.95										
	0.41	0.995	0.41	0.99	0.41	0.99	0.41	0.97	0.41	0.96	0.41	0.98												
	0.42		0.42	0.99	0.42	0.99	0.42	0.97	0.42	0.97														
	0.43		0.43	0.99	0.43	0.99	0.43	0.98	0.43	0.98														
	0.44	0.995	0.44	0.99	0.44	0.99	0.44	0.98	0.44	0.98														
	0.45		0.45	0.99	0.45	0.995	0.45	0.98	0.45	0.99														
	0.46		0.46	0.99	0.46	0.99	0.46	0.99																
	0.47		0.47	0.99	0.47	0.99																		
	0.48		0.48	0.99	0.48	0.99																		
	0.49		0.49	0.995																				
	0.5		0.5																					

Appendix F   Unpublished Measurements of Self-Aerated Flow, Tabular Form

13. ABSTRACT *(Maximum 200 words)*

Air entrainment in free-surface spillway flows is described with two concepts: "entrained air," which is air being transported by the flow as bubbles, and "entrapped air," which is the air transported with the flow in the roughness of the water surface. Results from flume experiments are used to develop a mathematical description of entrained and entrapped air for flow along a spillway face. Observations from a full-scale spillway validate the procedure. The theory of gas transfer shows how entrained air affects gas transfer with large increases in the interfacial area. A bubble-size distribution, based on photographic analyses, was used to estimate the surface area in self-aerated flow. Previous experimental work defined the minimum air concentration to prevent cavitation damage at approximately 8 percent. The location along the spillway now can be estimated where entrained air at the spillway surface reaches this concentration.